2021

# CHARACTERIZING THE PHYSIOLOGY AND GENETICS OF CONTACT DEPENDENT GROWTH INHIBITON SYSTEMS IN *BURKHOLDERIA* SPECIES

Alice Elizabeth Oates
*University of Kentucky*, oates.aelizabeth@gmail.com
Digital Object Identifier: https://doi.org/10.13023/etd.2021.451

STUDENT AGREEMENT:

I represent that my thesis or dissertation and abstract are my original work. Proper attribution has been given to all outside sources. I understand that I am solely responsible for obtaining any needed copyright permissions. I have obtained needed written permission statement(s) from the owner(s) of each third-party copyrighted matter to be included in my work, allowing electronic distribution (if such use is not permitted by the fair use doctrine) which will be submitted to UKnowledge as Additional File.

I hereby grant to The University of Kentucky and its agents the irrevocable, non-exclusive, and royalty-free license to archive and make accessible my work in whole or in part in all forms of media, now or hereafter known. I agree that the document mentioned above may be made available immediately for worldwide access unless an embargo applies.

I retain all other ownership rights to the copyright of my work. I also retain the right to use in future works (such as articles or books) all or part of my work. I understand that I am free to register the copyright to my work.

REVIEW, APPROVAL AND ACCEPTANCE

The document mentioned above has been reviewed and accepted by the student's advisor, on behalf of the advisory committee, and by the Director of Graduate Studies (DGS), on behalf of the program; we verify that this is the final, approved version of the student's thesis including all changes required by the advisory committee. The undersigned agree to abide by the statements above.

Alice Elizabeth Oates, Student

Dr. Erin C. Garcia, Major Professor

Dr. Carol Pickett, Director of Graduate Studies

# CHARACTERIZING THE PHYSIOLOGY AND GENETICS OF CONTACT DEPENDENT GROWTH INHIBITON SYSTEMS IN *BURKHOLDERIA* SPECIES

---

DISSERTATION

---

A dissertation submitted in partial fulfillment of the

requirements for the degree of Doctor of Philosophy in the

College of Medicine at the University of Kentucky

By: Alice Elizabeth Oates
Director: Dr. Erin C. Garcia, Committee chair and Assistant Professor
Department of Microbiology, Immunology, and Molecular Genetics
College of Medicine
Lexington, Kentucky
2021

ABSTRACT OF DISSERTATION
CHARACTERIZING THE PYSIOLOGY AND GENETICS OF CONTACT DEPENDENT GROWTH INHIBITON SYSTEMS IN *BURKHOLDERIA* SPECIES

Contact-dependent growth inhibition (CDI) systems mediate interbacterial competition. The genes encoding these systems are widespread among Gram-negative bacteria, including *Burkholderia* pathogens. CDI systems of *Burkholderia* species are composed of two-partner secretion pathway proteins and function to deliver the toxic C-terminus of a polymorphic surface-exposed exoprotein BcpA (*Burkholderia* CDI protein A) to the cytoplasm of neighboring recipient bacteria upon cell-cell contact. Specific outer and inner membrane proteins facilitate BcpA translocation both out of the donor bacterium and into the recipient cell cytoplasm. Most *Burkholderia* species-specific CDI translocation factors in recipient cells are unknown. BcpA intoxication functions as a mechanism by which 'non-kin' and 'kin' bacteria are differentiated. Survival of 'kin bacteria' is, in part, dependent on the presence of a small cognate immunity protein, BcpI, in the recipient bacterium. BcpI acts in an allele-specific manner to protect against BcpA from a particular CDI encoding locus.

Through this body of work, key components of both the donor and recipient bacteria are identified, adding further insight into the function of *Burkholderia* species-specific CDI mechanisms. Findings are broken into three overarching results. Utilizing *Burkholderia dolosa* as the primary model, comparisons of distinct CDI systems observed minimal differences in intoxication efficiency and secondary functions associated with CDI system proteins such as biofilm formation and motility. The pre-toxin region within the BcpA protein is demonstrated to be required for CDI of recipient cells. The final experiments identified proteins required in *Burkholderia dolosa* recipient cells for maximum intoxication by donor bacteria. Using transposon mutagenesis and whole genome sequencing approaches, CDI sensitivity candidate genes in quorum sensing regulation, stress response, metabolism, and lipopolysaccharide (LPS) structure and production genes were identified. Mutations in both the quorum sensing regulator and the LPS biosynthesis associated genes conferred resistance against both *Burkholderia dolosa* CDI system-1 and system-2. The other identified CDI candidates conferred partial protection against specific BcpA intoxication. All together this dissertation adds key information to the field, building a more robust understanding of the uniqueness of the *Burkholderia* CDI components and donor-recipient interactions. The spectrum of sensitivity each of the identified factors contributes to recipient susceptibility adds further insight into the complexity of the CDI mediated competition.

KEYWORDS:
*Burkholderia* species, Contact-dependent growth inhibition, kin-discrimination, interbacterial competition, translocation factors.

Alice Elizabeth Oates

10/29/2021

# CHARACTERIZING THE PHYSIOLOGY AND GENETICS OF CONTACT DEPENDENT GROWTH INHIBITON SYSTEMS IN *BURKHOLDERIA* SPECIES

By
Alice Elizabeth Oates

Dr. Erin C. Garcia
Director of Dissertation

Dr. Carol Pickett
Director of Graduate Studies

10/29/2021
Date

DEDICATION

To my family, both blood and built. Without the support and love, I never would have known what I was capable of.

Special appreciation for a girl's best friend, my cat Hermes 🐾 (2015-2020).

**ACKNOWLEDGMENTS**

"No one has ever completed a PhD alone". This is certainly true for me, and if I were to thank each person that has helped me get to this point, the list would be longer that my dissertation. However, there are specific individuals that without their support, I would not be where I am now.

First and foremost, I must thank my advisor Dr. Erin Garcia. Thank you for taking the leap of faith as your first graduate student, a challenge I do not envy. As a mentor, you have inspired me through your passion for science and personal strength. I have always felt supported with the freedom to make my own path, and my own mistakes. You have never made me feel less than even during the bumps both in and out of the lab. A good mentor helps you meet your potential; a great mentor pushes you to succeed far beyond, a statement certainly true of Erin.

I also owe a huge thank you to my lab mates, Tanya Morelas-Myers and Zaria Elery. To be in a laboratory of all strong and brilliant woman is rare and truly an honor. Tanya, your friendship, and advice has helped me push through the frustrations of failed experiments and all that graduate school throws. Zaria, thank you for your friendship, even when sassy. You will do amazing things!

I would also like to thank my advisory committee, Dr. Brian Stevenson, Dr. Ken Fields, Dr. Carrie Shaffer, Dr. Michael Freid, and outside examiner Dr. Donna Wilcock. Each of my committee members have gone beyond guidance on my project and helped me grow both as a scientist and a person. Ken and Brian have gone beyond the role of committee members, always having an open door for my questions, and made me feel like an additional member of their labs.

The community of the Microbiology, Immunology, and Molecular Genetics Department made a supportive and fun environment to ‘grow up in’. Almost every person apart of MIMG has helped me either through advice, lending reagents and equipment, or just a supportive cheer. Within the MIMG department, Dr. Beth Garvy, Melissa Hollifield and Robert Haymon have helped me every step of the way. Special thanks for Dr. Beth Garvy, going above and beyond. Although I know you would always do what you can to help each student, I would not have the job I started, the network I’ve built, nor the policy and communication experience I have gained. The endorsement of your high opinion is a gift I can never appreciate enough. Melissa Hollifield, you are simply the best, and we would all be lost without you. Thank you so much for your help, your friendship, and your Marry Poppins-zombie-apocalypse bag of wonders. Robert, you are a computer wizard and the number of times you saved my computer from being thrown out a window is endless. Whether at BFB, the racetrack or just hanging out, it is always a good time. Also, thank you to my friends Dr. Brian Higgins and Dr. Zach Porterfield. You both are wonderful cheerleaders, always willing to help and motivate me. Thank you for the, often unwarranted, advice – it was sometimes useful.

And to my fellow graduate students throughout the biomedical program, thank you for helping in any way you could, through being a cheerleader for other’s success, sharing old exams, or just making sure every student can feel supported.

Thank you to my Kentucky family. Tanner DuCote, Reni Scaringello, and Colleen Bodnar, thank you for your friendship and love. Each of you has helped me get through some of the toughest times and with only a little judgment. My lunch crew/fellow bourbon club members, Dr. Brooke Ahern, Dr-ish Ryan Cloyd, Dr-ish Brandon Farmer and work

wife Ben Shaw; I love each and every one of you. Brooke and Ben, from day one, have had my back. I have fallen so many times and could not have gotten back up without your help. Being a part of my 'Kentucky family' and watching as each of us are reaching the next step in our careers, is bitter-sweet. I wish you all the best with your growing families, next steps in your careers, and all that life has to offer. Although we are moving apart, I know each of you will always be there with just a call.

To my significant others, Dr. Gabby Keb and Charles Seaks, I love you both more than you will ever know. Gabby, you are my partner in crime and best friend. There was nothing I couldn't tell you or help you wouldn't give. Together we goth into and through so much trouble and strife. You helped me work to be a better person, and understood my faults and fears to grow so much over the past 5 years. You were always there when I needed you and I know that won't change. Charles, you knew what you were getting and thank you for being all in. Together we have made a family with our fur-babies Arke, Iris, and Ody, and are going into the unknown future hand in hand. Together we have gone through losses, stressors, and a pandemic- and still going strong. Thank you for keeping me grounded and supporting me through the, often self-induced, stress over the past 3 years. I am excited for what our future holds.

Finally, I would like to thank my family; Mom, Dad, Tommy and Nikki. You have been my biggest cheerleaders, and I am so lucky to have you. I would not be where I am today without you believing in me. If I were to list all you have done, I would never stop writing. So here is a blanket thank you for everything. I love you.

# TABLE OF CONTENTS

**ACKNOWLEDGMENTS** **i**

**Table of Contents** **iv**

**Table of Figures** **ix**

**List of Tables** **xi**

**Chapter 1: Introduction** **1**

1.1. Burkholderia Species ..... 1

1.1.1. Burkholderia cepacia complex 1

1.1.2. Bcc associated with cystic fibrosis infections. 2

1.1.3. Bcc member - *Burkholderia dolosa* 3

1.1.4. *Burkholderia pseudomallei* complex 4

1.2. Toxin-antitoxin systems ..... 5

1.3. Bacterial Competition ..... 6

1.3.1. Direct bacterial competition 7

1.3.2. Non-kin discrimination competition 7

1.3.3. Bacteriocins 8

1.3.4. Contact-mediated competition 10

1.4. Contact-Dependent Growth Inhibition ..... 14

1.4.1. CDI Classification 14

1.4.2. CDI System Mechanism 15

1.4.3. Function of mobile orphan domains 16

1.4.4. Recipient susceptibility factors 17

1.4.5. Kin discrimination mediated by CDI. 19

1.4.6. Genomic island mobility 20

1.4.7. CDI systems in other bacterial species 20

1.5. Bacterial cooperation and kin signaling ..... 22

1.5.1. Kin communication by diffusible signals 22

1.5.2. Community outcomes 23

1.6. Overall Hypothesis ..... 25

**Chapter 2: Methods** **30**

2.1. Bacterial strains and culture conditions ..... 30

2.2. Genetic manipulations ..... 30

2.3. Interbacterial competition assay ..... 32

2.4. Motility assay ..... 33

2.5. Crystal-Violet staining assay ..... 33

2.6. Microscopy ..... 34

2.7. Immunoblotting ..... 34

2.8. Dot Blots ..... 35

2.9. Transposon mutagenesis selection ..... 35

2.10. Arbitrary PCR ..... 36

2.11. Growth curves ..... 37

2.12. Auxotrophic growth cultures ..... 37

2.13. Whole genome re-sequencing ..... 37

2.14. LPS extraction and analysis ..... 38

2.15. β-galactosidase assays ..... 39

2.16. β-galactosidase co-cultures assay ..... 40

2.17. Bioinformatics and statistics ..... 40

**Chapter 3: Optimization of assays to compare *B. dolosa* CDI system function. 42**

3.1. Summary ..... 42

3.2. Introduction ..... 43

3.3. Results ..... 45

3.3.1. *B. dolosa* CDI systems function similar to CDI systems of other *Burkholderia* species. 45

3.3.2. Growth in antibiotic cultures prior to input competitions alter the competitive index. 47

3.3.3. Expression of a singular BcpA protein does not alter motility or biofilm formation. 49

3.4. Discussion ..... 61

**Chapter 4: Functional BcpA requires the pre-toxin region. 68**

4.1. Summary ..... 68

4.2. Introduction ..... 69

4.3. Results ..... 72

4.3.1. Deletion of the pre-toxin region is toxic in *B. thailandensis.* 72

4.3.2. Antibodies against E264 BcpA C-terminal toxin cross react with the C-terminal toxin of AU0158. 73

4.3.3. Deletion of the pre-toxin region is not lethal in *B. dolosa* BcpA-1. 73

4.3.4. Deletion of the pre-toxin region inhibits CDI but not BcpA production. 74

4.3.5. There are differential banding patterns associated with BcpA pre-toxin subdomain deletions compared to wild-type BcpA. 76

4.4. Discussion ..... 87

**Chapter 5: Transposon mutagenesis used to identify genes associated with CDI susceptibility. 90**

5.1. Summary ..... 90

5.2. Introduction ..... 90

5.3. Results ..... 92

5.3.1. Selection of *Burkholderia dolosa* mutants resistant to CDI system-1 or CDI system-2. 92

5.3.2. Deletion of candidate genes does not alter *B. dolosa* growth. 94

5.3.3. Quorum sensing regulator CepR influences CDI efficiency. 94

5.3.4. Genes *cspD* and *hisD* have a minor contribution to recipient cell CDI susceptibility. 97

5.3.5. Intracellular membrane associated proteins encoded by BDAG_00967 and BDAG_00966 do not alter CDI susceptibility. 99

5.3.6. Whole Genome Sequencing identified additional unique mutations in the chromosomes of resistant transposon mutants. 102

5.3.7. Alteration in LPS regulation locus correlates with resistance to CDI indiscriminately. 103

5.4. Discussion ..... 128

**Chapter 6: Discussion and Future Directions 133**

**References 143**

**Appendix A: Acronyms 189**

**Appendix B: Strains used in this body of work. 194**

**Appendix C: Plasmids used in this body of work. 202**

**Appendix D: Experimental replicates of *B. thailandensis* and *B. dolosa* BcpA banding patterns. 206**

**Appendix E: Variations[a] in *B. dolosa* Δ*bcpAIOB-1* Δ*bcpAIOB-2* mutant identified by whole genome re-sequencing. 208**

**Appendix F: Influence of *B. thailandensis* BcpA/BcpI complex on SOS response. 209**

**Appendix G: Polymicrobial biofilm formation of *B. dolosa* CDI mutants. 216**

**Appendix H: Contributions 218**

**Vita 219**

**Table of Figures**

**Figure 1.1.**Major, unweighted, grouping of *Burkholderia* species. ..... **26**

**Figure 1.2.** Model of contact-dependent system encoding loci and basic components donor and recipient cell components. ..... **28**

**Figure 3.1.** Determine differences of environmental limitations between class I and class II CDI systems. ..... **53**

**Figure 3.2.** Bacterial competitions co-cultured for 24h and 48h**. ..... 55**

**Figure 3.3.** Influence of antibiotic supplemented input cultures on competitive index outcomes. ..... **56**

**Figure 3.4.** Motility assay for swimming and swarming**. ..... 58**

**Figure 3.5.** Influence of CDI-systems on *B. dolosa* biofilm formation. ..... **59**

**Figure 3.6.** Influence of CDI-systems on *B. dolosa* biofilm architecture. ..... **60**

**Figure 4.1.**Model for BcpA topology and toxin translocation. ..... **79**

**Figure 4.2.** E264 αBcpA C-terminus antibody is cross reactive with AU0158 BcpA-1. **82**

**Figure 4.3.** Deletion of pre-toxin subdomains inhibit BcpA-1 intoxication but are translated. ..... **83**

**Figure 4.4.** Banding patterns between pre-toxin region deletions mutants vary from wild-type BcpA-1. ..... **85**

**Figure 5.1.** Selection of CDI-resistant *B. dolosa* transposon mutants. ..... **106**

**Figure 5.2.** Diagram of identified transposon disruptions. ..... **109**

**Figure 5.3.** Susceptibility of identified transposon mutants to BcpAIOB-1 and BcpAIOB-2..... **110**

**Figure 5.4.** Liquid culture bacterial growth of deletion of regulatory, stress response or quorum sensing genes. ..... **112**

**Figure 5.5.** Recipient cell susceptibility tested at different growth phases. ..... **113**

**Figure 5.6.** Susceptibility to CDI tested for the transposon candidate quorum sensing regulation gene, *cepR*. ..... **115**

**Figure 5.7.** Susceptibility to CDI tested for the transposon candidate genes, *cspD* and *hisD*. ..... **117**

**Figure 5.8.** Growth of *B. dolosa* Δ*hisD* mutant in minimal medium. ..... **119**

**Figure 5.9.** Deletion and complementation of transposon identified inner membrane susceptibility factors encoded in BDAG_00967 and BDAG_00966 locus. ..... **120**

**Figure 5.10.** Influence of BDAG_00967 on *B. dolosa* biofilm formation tested. ..... **123**

**Figure 5.11.** LPS structure and CDI susceptibility for BDAG_01005 and BDAG_01005 mutants. ..... **126**

**Appendix Figure 1.** Banding patterns between pre-toxin region deletions mutants vary from wild-type BcpA-1. ..... **206**

**Appendix Figure 2.** Measuring DNA damage in *B. thailandensis* E264 bacteria. ..... **214**

**Appendix Figure 3.** Confocal co-culture B. dolosa CDI mutant biofilms**.** ..... **216**

**List of Tables**

**Table 4.1.** Deletion of the pre-toxin region is lethal in E264 wild-type bcpA. ..... 81

**Table 5.1.** Chromosomal insertion sites of CDI-resistanta *B. dolosa* miniTn5 mutants. ..... 108

**Table 5.2.** Unique variations[a] in *B. dolosa* transposon mutants identified by whole genome re-sequencing. ..... 125

# Chapter 1: Introduction

## 1.1. Burkholderia Species

The genus *Burkholderia* belongs to the Betaproteobacteria class within the phylum of the Proteobacteria (1). Originally, *Burkholderia* strains were classified under the Pseudomonas genus (2, 3). The *Burkholderia* genus was identified and separated on the basis of 16S rRNA sequencing, DNA-DNA sequence homology, cellular lipid and fatty acid composition, and phenotypic characteristics (4, 5). The genus *Burkholderia* is diverse and consists of two clades, and further divided into multiple sub-clades (Figure 1.1) (6). The genus of *Burkholderia, originally* consisting of only seven species, now encompasses over 120 species *(*http://www.bacterio.net/*Burkholderia*.html*)* (4). Members of the *Burkholderia* genus include both pathogenic and non-pathogenic Gram-negative, non-spore forming bacilli that are commonly found in soil but can occupy a diverse range of ecological niches (2, 3). *Burkholderia* species distribution is strongly affected by soil pH, allowing them a competitive advantage in microbial diverse acidic soils (7, 8).

### 1.1.1. Burkholderia cepacia complex

The *Burkholderia cepacia* complex (Bcc) is a sub-clade that consists of 20 closely related but genetically distinct species that include opportunistic human and phytopathogens (Figure 1.1) (9). While the Bcc was initially recognized as an onion pathogen causing ‘sour skin onion rot’, Bcc members have also been associated with ecologically beneficial interactions with plants (10). Bcc species have also been found to degrade man-made and natural pollutants such as trichloroethylene (11–13).

Bcc species are clinically significant pathogens due to the multidrug resistance exhibited in patients with compromised immune systems like those with cystic fibrosis (CF) and chronic granulomatous disease (CGD) (14–17).

### 1.1.2. Bcc associated with cystic fibrosis infections.

Cystic fibrosis (CF) is often the result of a mutation in the cystic fibrosis transmembrane conductance regulator (*CFTR*) gene and is found in approximately 1/2,500 births in the United States. In the United States, CF occurs in 1/3,200 White Americans, 1/1,000 Hispanic Americans, 1/10,500 Native Americans, 1/15,000 Black Americans, and 1/3,000 Asian Americans. Mutation in the *CFTR* gene results in improper balance of the chloride ions in the liquid surface of many tissues. This chloride imbalance results in accumulation of dehydrated mucus, most often seen in the lungs and gastrointestinal tract (18). The mucus is high in nutrients and patients with CF have difficulty clearing the mucus, resulting in patients having chronically infected airways starting at an early age. The most common chronic bacterial infections for CF patients are *Pseudomonas aeruginosa*, *Staphylococcus aureus*, and *Haemophilus influenzae* (19). These chronic infections result in patients with CF experiencing bouts of lung function decline followed by prolonged courses of antibiotic treatments (18).

Bcc members can also cause chronic infections in patients with CF, although less frequently than the above-mentioned bacteria. Bcc bacteria act as opportunistic pathogens often associated with infections in patients with CF, increasing morbidity and mortality (20, 21). Bcc infections vary between patients with CF, similar to other CF associated pathogens, with some patients presenting with asymptomatic and others with chronic

infections (22, 23). Approximately 3% of patients with CF will have a Bcc infection, prevalence increasing with age (23, 24) and 20% of those patients will have chronic infections resulting in rapid health deterioration, primarily driven by necrotizing pneumonia and septicemia (14, 25).

Bcc organisms interact with epithelial cells through adherence and invasion, allowing them to evade host macrophages (26, 27). Many Bcc bacteria are capable of biofilm formation *in vitro* (28). Biofilms allow organisms to be protected from host defenses, heat, desiccation, and antibiotics (29). Member bacteria of Bcc have been shown to evade the actions of multiple antibiotic classes, partially responsible for the severity of CF infections (30–32). *Burkholderia* species have atypical lipopolysaccharide (LPS) structure, specifically in the lipid A domain, altering outer membrane permeability and play a role in antibiotic resistance (33). Other mechanisms utilized by Bcc members in antibiotic resistance includes efflux pumps and additional intrinsic resistance (34, 35). Persistent infections are maintained using additional virulence factors such as catalase, superoxide dismutase (36), quorum sensing (37, 38), siderophores (39, 40), and a type III secretion system (T3SS) (41).

### 1.1.3. Bcc member - *Burkholderia dolosa*

*Burkholderia dolosa* was identified as a member of Bcc in 2001 and named in 2004 after genotyping methods improved. The newly described *B. dolosa* was responsible for infection incidences that were originally attributed to *B. multivorans* (42, 43). Although *B. dolosa* characterization did not occur until later, *B. dolosa* had been causing infections, most notably in an outbreak in Boston Children's Hospital in 1998 (44, 45). *B. dolosa* is

not prevalent amongst the Bcc infections, representing less than 5% of Bcc isolates from 606 patients with CF across the US (23). However, patients with CF that were infected with *B. dolosa* had accelerated decrease in lung function and reduced survival compared to other Bcc infections (45). The exact reason that *B. dolosa* leads to rapid decline of patients with CF compared to other Bcc members remains unknown. *B. dolosa* was found *in vitro* to be comparable to opportunistic strains *B. multivorans* and *B. cenocepacia* in both invasion and biofilm formation (46).

### 1.1.4. *Burkholderia pseudomallei* complex

One of the other major phylogenetic group and sub-clade is the *Burkholderia pseudomallei* complex (BPC). BPC consists of *Burkholderia pseudomallei* and closely related phylogenetic relatives, such as *Burkholderia mallei* and *Burkholderia thailandensis* (Figure 1.1) (47). *B. pseudomallei* is the causative agent of the disease melioidosis and is considered a tier 1 select agent for bioterrorism by the U.S. Center for Disease Control and Prevention (CDC) (48). Melioidosis was first recognized in 1911, presenting with sepsis and can also include pneumonia and localized abscesses (49, 50). These symptoms are associated with acute melioidosis, making up about 85% of melioidosis cases (51). However, due to the nonspecific signs and symptoms, diagnosing melioidosis is challenging. Chronic melioidosis infections are comparatively rare but defined by the symptoms of melioidosis persisting for over 2 months (51). *B. pseudomallei* can infect healthy individuals in endemic areas such as Australia and countries in southeast Asia, in part due to repeated exposure (52). One major risk factor for chronic infection is diabetes

mellitus, with 23-60% of patients with *B. pseudomallei* infections having the preexisting condition (51).

*B. thailandensis* are soil bacteria that are typically avirulent (53, 54). Over 85% of genes are conserved between *B. pseudomallei* and *B. thailandensis*. Most of the differences between the species are restricted to specific genomic islands (55). Unlike *B. Pseudomallei*, *B. thailandensis* is not a Bio-safety level (BSL)-3 pathogen, and, as a BSL-2 microbe, is often used as a model to study homologous genes to the pathogenic *B. pseudomallei* (56). Similar to *B. pseudomallei*, *B. thailandensis* can be found in the soil of tropical and subtropical regions (54).

*B. mallei* causes the zoonotic infectious disease glanders, which primarily afflicts equines but can also infect humans. Unlike *B. pseudomallei* and *B. thailandensis*, *B. mallei* is a host-restricted pathogen and does not have an environmental reservoir (57). *B. mallei* has a genome that is approximately 20% smaller than that of *B. pseudomallei* but the genes retained have high sequence identity (57, 58). The genes that were lost are hypothesized to be critical for environmental survival while still retaining the *B. pseudomallei* gene orthologs necessary for host survival (58, 59).

### 1.2. Toxin-antitoxin systems

Bacteria encode 'addiction' genetic elements called toxin-antitoxin (TA) modules in which a secreted toxin inhibits cell growth, and a cognate antitoxin counteracts the toxin activity (60, 61). TA modules are abundant in bacterial genomes, often found on plasmids or other mobile genomic elements associated with horizontal transfer (62). The high number of TA modules results in high variability of the number and composition of

chromosomal TA loci (63). There are three major biological functions maintaining TA modules: post-segregational killing (64), abortive infection (65), and antibiotic resistance (66). TA modules are inherently kin discriminatory (67, 68). Maintaining TA modules are frequently called 'addiction mechanisms' because loss or mutation within the TA systems leads to incompatibility of merged colonies and results in a 'winner' and a 'loser' (69, 70). Additionally, in many TA modules, both the toxin and the antitoxin can be toxic to the cell resulting in an "all or nothing" phenotype (71). The number of TA loci often coincides with adaptation to hostile or dynamic environments in which horizonal gene transfer could happen at a higher rate (72, 73). Therefore, due to the diverse environments that *Burkholderia* spp. inhabit, there is little surprise that there is a myriad of TA modules found within this genus.

### 1.3. Bacterial Competition

Bacteria are natively found in polymicrobial environments with limited nutrients and resources. Bacterial populations with similar nutrient requirements must compete for dominance in the environment. However, with continuous growth of a large singular population, depletion of nutrients becomes problematic. Competition and nutrient depletion give rise to mutations that allow a new population to adapt to a particular niche, maintained by negative frequency-dependent selection (74). Adaptations can result in variants specific to the environment. One example is the *Pseudomonas fluorescens* variant that over-produces extracellular polysaccharides (EPS) to form biofilms, allowing the biofilm to float on the air-liquid interface to improve access to oxygen (75, 76). Mutations can also contribute to the evolution of competitive networks (74, 77). These competition

mechanisms are often strain-specific. However, they can have detrimental influence on other bacteria inhabiting the same environmental niches (78).

### 1.3.1. Direct bacterial competition

Bacteria have multiple mechanisms to compete with other microbes within their environment. This competition can either be direct or indirect (79–81). Indirect, such as exploitation competition, involves rapid utilization of limited resources without direct interaction between the competitors (80, 82). Direct competition, as in contest competition, involves direct antagonistic interactions between competitors resulting in a "winner" and a "loser" for appropriating resources (82). Bacteria are constantly at war with various competitors and require 'weapons' for both direct and indirect competition to survive, thrive, and conquer new territory. These competitions are often beneficial for kin bacteria.

### 1.3.2. Non-kin discrimination competition

Theoretically, kin discrimination traits are due, in part, to kin selection (83, 84). Kin recognition, in the simplest of terms, is the means by which individuals identify others that are closely related in order to form a cooperative group (85, 86). Kin cooperation will be further discussed below (see section 1.5 of Introduction). The ability to discriminate kin from non-kin via competitive mechanisms results in the elimination of non-kin bacteria that would otherwise compete for the same environmental resources, resulting in a more isogenic population (87). The benefit of killing or inhibiting similar bacteria is the elimination of competition for the same nutrients and environmental resources (88, 89). The selection through kin discrimination can happen both broadly and narrowly at the

strain-specific level (90). Kin discrimination is often associated with greenbeard alleles (84, 91). Greenbeard genes allow phenotypic matching through three-part effects. The three components were first theorized by Dawkins and include: (i) a visible signal, (ii) the ability to recognize the signal in others, and (iii) the ability to direct altruistic behaviors to those expressing the signal (92, 93). Greenbeard genes can also allow for phenotypic matching of non-kin bacteria if the non-kin bacteria express similar greenbeard alleles as the antagonist bacterium (84, 94, 95). However, greenbeard cooperation will more effectively target bacteria with higher similarities in alleles, excluding those of phenotype matching alone (95, 96). The specific community-level distributions of kin-bacteria play major roles in polymicrobial infections and virulence of pathogens (97). Thus, bacteria have evolved numerous competition mechanisms to ensure kin will survive and thrive.

### 1.3.3. Bacteriocins

Bacteriocins are a diverse family of antimicrobial proteins defined by their relatively narrow spectrum of killing, specific to closely related bacteria. The most extensively studied bacteriocins are specific to *Escherichia coli*, known as colicins (98, 99) Bacteria can release bacteriocins through either transport systems or cell lysis (100–102). Once released into the environment, bacteriocins bind to specific cell surface receptors on target cells and kill through various mechanisms (71). Binding to the outer membrane receptor is one of the means of specificity for target cell killing (103). Producer cells and kin are resistant to their own bacteriocins because of cognate immunity proteins they produce. Bacteriocins have a wide range of intoxication mechanisms, including pore formation in recipient cells, which leads to membrane permeabilization. Examples of pore-

forming bacteriocins can be found in *Lactococcus lactis* (105) and *Lactobacillus sakei* (106), which produce the bacteriocins Nisin and Sakacin, respectively. *Enterobacteriaceae* species produce nuclease bacteriocins with a wide range of substrate specificity including DNA, 16S rRNA, and tRNA to digest nucleotides in recipient bacteria (99, 104). Bacteriocins that act against Gram-positive bacteria can inhibit peptidoglycan production, such as the klebicins produced by various *Klebsiella* species (107). Orthologs to bacteriocins are diverse and associated with bacterial delivery systems including type VI secretion and contact-dependent growth inhibition (discussed below).

The mechanisms of import for bacteriocins into recipient cells can vary almost as much as the toxic activities. Bacteriocins require an outer membrane receptor on recipient cells for recognition, transport, and toxicity. Nisin, from *Latococcus lactis,* utilizes Lipid II as a receptor (105), sakacins are shown to use Mannose permease (108), and Gassericin A, produced by *Lactobaccilus gasseri,* uses ABC transporters as receptors (109). Many *Enterobacteriaceae* colicins and *Pseudomonas aeruginosa* pyocin utilize lipopolysaccharides (LPS) (110–112).

Bacteriocin systems are relatively simple and provide an effective means for dominating an environmental niche. *Pseudomonas* species are prolific producers with nearly all clinical and environmental *P. aeruginosa* samples producing bacteriocin-like toxins. Less is understood about the role of bacteriocins in *Burkholderia* species (113). Unlike other proteobacteria, very few bacteriocins have been identified and characterized in *Burkholderia* species (114–117). Bacteriocin systems are simplistic, yet the spectrum of susceptible bacteria can be narrow or broad, depending on the bacteriocin, leading to the

potential to develop alternatives to clinical antibiotics currently in use (118, 119). To date the use of bacteriocins, often nisins, are restricted to plants and veterinarian settings (118).

### 1.3.4. Contact-mediated competition

Bacteria physically interact in high density populations (120). These direct interactions can be beneficial; facilitating the transfer of genetic information through plasmid exchange via conjunction (121, 120, 122). At the same time, high-density soil microbial environments often induce stress and competition mechanisms (121, 123, 124). Contact-mediated competition in bacteria utilizes membrane and cell envelope-embedded mechanisms to interact with competitors and ultimately alter the surrounding microbial environments (125).

Gram-negative bacteria have been observed to use their own membrane to deliver insoluble toxins. Outer membrane exchange (OME) is contact dependent, requiring cells to share membrane components such as phospholipids and lipoproteins (126). OME has been primarily studied in *Myxobacteria* species. The only known components required for OME are found within the protein complex TraAB. TraAB proteins must be produced both in the donor and the recipient cells in order to facilitate successful OME (127). The mechanism for exchange involves transient outer membrane fusion catalyzed by the TraA receptor and an associated protein, TraB. The TraAB complex is located in the outer membrane and has a polymorphic domain that determines the selectivity of the target cells (128). Due to the narrow range of target bacteria, it is not surprising that OME is associated with kin discrimination (129). Kin-discrimination can either allow for cooperative or antagonistic behaviors dependent on how closely related the bacteria are. For

*Myxobacteria,* the SitAI complex acts as a toxin-antitoxin in OME kin verification (129). Homologs of these proteins have not been found in *Burkholderia* species. *Burkholderia spp.* and other Gram-negative bacteria have been observed to use outer membrane vesicles (OMV), like OME, to exchange genetic information, communicate, and immunomodulate. However, OMV is not cell-cell contact dependent. Additionally, OMV is also associated with bacterial pathogenicity (130). *B. pseudomallei* vaccines target OMV to inhibit lethal sepsis and glanders in various animal models (131, 132).

Gram-negative bacteria in close proximity can utilize contact-dependent transport proteins via the type VI secretion system (T6SS) apparatus (133–135). The T6SS uses a contractile apparatus comprised of 13 core components that assemble in the membrane to facilitate the delivery of effectors through the penetration of the recipient cellular membrane (136–138). The structure of T6SS shares homology with bacteriophages. In both, effector proteins are shuttled through a syringe-like mechanism (138–141). There are two main complexes that make up the T6SS module: the membrane complex that anchors the module in the periplasm of the donor cell, and the tail complex that harbors a needle-like apparatus encircled by the sheath structure. In the native state, the T6SS system is extended into the donor cell cytoplasm anchored by the periplasmic membrane. Upon receiving an unknown extracellular signal, the sheath that surrounds the tail complex will contract, resulting in the ejection of the needle-like complex across the target cell membrane, thereby delivering the effector proteins into the cell (138, 139, 141, 142). The disassembling of the sheath enables the reassembly of the T6SS module back into the native, extended state, after release of subunits (138).

Initially, the T6SS was thought to function directly in an anti-eukaryotic manner via delivery of effector proteins into the eukaryotic cells of a host organism (143). *Burkholderia* species utilize the T6SS, named T6SS-5 or cluster-1 T6SS, during bacterial-host interactions *in vivo* (144, 145). The T6SS has been additionally established in inter-bacterial competition (133, 135, 146). Further studies demonstrate the T6SS function is extended to competitive actions against microbial fungi (143, 147). While the 13 core components of T6SS are conserved amongst protobacteria, the divergent functions of T6SS can be split into six sub-families, with much of the variability residing in the function of the effectors (148–150). Many of the effectors function in the periplasm of the target cell and act as a toxin through targeting the peptidoglycan cell wall, acting as a lipase/phospholipase, or forming pores in the membrane. The target of effector molecules limits the toxicity of T6SS to Gram-negative bacteria (148, 151–153). However, there are effectors which act in the cytoplasm as nucleases or degrade essential cytoplasmic cofactors (154, 155)**.**

The antibacterial nature of T6SS toxicity requires bacteria to encode a means of inhibiting self-intoxication (156, 157). Immunity proteins are as variable as the effectors themselves and are encoded adjacent to the gene encoding the cognate effector (150, 158). The immunity proteins reside in the compartment of the cell that is targeted by the effector and normally binds tightly to the effector to physically prevent toxicity (156). In general, the T6SS effector-immunity pairs are acquired via horizontal gene transfer as a means of bacterial 'arms-race' (159, 160). For specialized effectors, homologous recombination facilitates the exchange of the C-terminal effector domains and the downstream cognate

immunity encoding gene (161). These recombinant domains result in highly variable loci resulting in strain specific kin discrimination (162–164).

T6SS is also associated with virulence and host interactions. Some of the most dramatic virulence phenotypes are associated with *Burkholderia* strains that contain T6SS (165–167, 56). In *B. mallei,* the T6SS is shown to be critical for virulence, intracellular growth, actin polymerization, and formation of multinucleated giant cells *in vitro* (167, 144, 168). These results were further mimicked in members of Bcc, as *B. cenocepacia* T6SS is associated both with virulence in chronic lung infection in mouse models as well as bacterial-bacterial competition (169, 170).

Additional secretion systems also act as specialized antibacterial mechanisms, including the type IV, type Vb, and type VII secretion systems (T4SS, T5SSb, and T7SS, respectively). Similar to T6SS, T4SS and T5SSb are widespread throughout Gram negative bacteria (171). However, T4SS-mediated interbacterial competition currently is characterized only in the *Xanthomonas citri* species (172, 173). The role of T4SS is better known for the movement of DNA either through conjunction, transformation, or effector translocation, which also can include delivery of additional substrates (174, 175). The T7SS carries out interbacterial competition in Gram-positive bacteria (176–178). T7SS secrete bacterial antagonists and toxic effectors into a competing bacterium. The full understanding of the T7SS mechanism is still underway as there are challenges in regulation and activation of the system under laboratory conditions (179). Of the contact-dependent interbacterial secretion systems, T5SSb (also referred to as contact-dependent growth inhibition, or CDI) and the T6SS are the most well characterized (180).

## 1.4. Contact-Dependent Growth Inhibition

Contact-dependent growth inhibition (CDI) systems consist of two-partner secretion (TPS) proteins (also called T5SSb proteins) employed by proteobacteria in interbacterial competition (181). TPS systems are characterized by a 'TpsA' exoprotein and a 'TpsB' partner transporter. The C-terminus of the 'TpsA' CDI associated exoprotein is delivered into a neighboring bacterium upon cell-to-cell contact (181, 182).

CDI was first discovered in *Escherichia coli* isolate EC93, as EC93 outcompeted another *E. coli* strain (K12) upon cell-cell contact (181). Further investigations revealed genes predicted to encode CDI systems are widespread in proteobacteria and a key component of these systems are immunity proteins, which protect against CDI toxins (183, 184).

### 1.4.1. CDI Classification

CDI systems fall into two broad classes: the *E. coli*-type systems and the *Burkholderia*-type systems. *E. coli*-type systems are usually seen in α-, β-, γ-proteobacteria, whereas *Burkholderia*-type systems are limited to *Burkholderia* genus and closely related species (183, 184). Both CDI locus types are thought to be co-transcribed and expressed (181, 185). Classification between the two types is primarily dependent on the CDI locus arrangement. *E. coli*-type systems are encoded by *cdiBAI* loci (181), and *Burkholderia*-type systems are encoded by *bcpAIOB* loci (185). The genes are homologs with the exception *bcpO*. The *bcpO* genes are unique to the *Burkholderia*-type CDI system, although not all contain a *bcpO* in CDI-encoding loci (185, 187). Currently, the role of BcpO is still unknown. However, within the *Burkholderia*-type CDI systems can be further

divided into two classes, in part due to different amino acid sequences of BcpO. Within class I, the BcpO proteins are predicted to be membrane-bound lipoproteins (185, 187). Class II BcpO may either not exist or encode an unknown, variable open reading frame (ORF). In both *B. thailandensis* and *B. dolosa,* class I BcpO has been implicated in CDI efficiency (Figure 1.2AB) (185, 188).

### 1.4.2. CDI System Mechanism

Despite their different loci organization, both *E. coli*-type and *Burkholderia*-type CDI systems function similarly. The transporter protein CdiB/BcpB forms a β-barrel in the outer membrane to allow to the translocation of the CdiA/BcpA exoprotein. CdiA/BcpA are large filamentous proteins that extend past the cell surface. The size of these proteins varies between ~180kDa (*Moraxella* species) to ~ 630kDa (*Pseudomonas* species) (Figure 1.2C) (181, 189). Much of the CdiA/BcpA proteins are conserved as the N-terminus is made primarily of the structural filamentous hemagglutinin motif domains and repeats. The functional toxin domain is restricted to the C-terminus. The variation of the C-terminus follows a conserved amino acid motif, which also is differentially associated between *E. coli*-type (VENN motif) and *Burkholderia*-type (Nx(E/Q)LYN motif) (Figure 1.2AB). The diversity of the catalytic toxin domain in the C-terminus varies between genus and to distinct CDI systems within the same bacteria strain (183, 185). The function of the C-terminal toxins is primarily predicted to function as nucleases, degrading either DNA or tRNA in the recipient cell (190). Although, one *E. coli* (EC93) CdiA toxin forms pores to disrupt the recipient cell proton gradient (191).

Immunity proteins CdiI/BcpI function to block autointoxication and protect kin bacteria from CDI-associated killing from their own kind. Due to the high level of variability in the C-terminus of CdiA/BcpA toxins, the immunities co-vary in an allele-specific manner (Figure 1.2). The cognate CdiA-I/BcpA-I proteins form polymorphic toxin-antitoxin pairs (183, 185). Chimeric CDI systems have been created by replacing both the variable CdiA/BcpA C-terminus region and the cognate CdiI/BcpI. The chimeric mutants still have functional CDI, the recipient cell susceptibility is dependent on the presence of the cognate CdiI/BcpI (183, 192, 193). Functional chimeric CdiA/I (or BcpA/I) mutants can be created by fusing the modular C-terminal CdiA/CdiI following the conserved pre-toxin motif (either VENN, or N(Q/E)LYN) (183, 184, 187, 192, 193). Limitations to creating these chimeras include creating chimeric BcpA toxins between classes and, even further for *Burkholderia spp*., between sub-classes (183, 187, 193, 194).

Little is known about the regulation of CDI-encoding loci. *E. coli* strain EC93 is the first identified CDI system natively expressed under laboratory conditions (171, 184). *Erwinia chrysanthemi* EC16 strains express *cdi* genes specifically during plant-host colonization. The study focused on regulation of *virA* which is part of the predicted homologous CDI encoding loci (185). Regulation of *B. thailandensis* E264 strain was shown to regulate expression so that 1:1,000 bacteria express CDI systems in at high levels when under laboratory conditions (175). In *B. thailandensis* quorum sensing system is associated with regulating expression of the CDI *bcpAIOB* operon (195).

### 1.4.3. Function of mobile orphan domains

CDI loci often reside in mobile genomic islands, and genomic analyses suggest that *cdiA-I/bcpA-I* elements can be exchanged between different bacterial CDI systems (184). Regardless of the CDI locus type (*E. coli* vs *Burkholderia*), many contain open reading frames (ORFs). These ORFs are distinctly different from the *Burkholderia*-type class I hypothetical lipoprotein encoding *bcpO* orphan regions, containing two short ORFs that resemble C-terminal *cdiA* and cognate *cdiI* (in *Burkholderia bcpA/bcpI*) (185, 187). Predicted C-terminal toxin-immunity ORFs have been found by bioinformatics across CDI encoding species such *as E. coli, Yersinia pseudotuberulosis, Burkholderia* spp., and *Neisseria meningitidis* (184, 185, 187, 196).

### 1.4.4. Recipient susceptibility factors

Toxicity from BcpA is dependent on a variety of susceptibility factors in the recipient cell. The current model for translocation of the CDI toxin, using *E. coli* CDI system proteins, involves the toxin interacting with specific outer membrane receptors (OMR) on the recipient cell surface. To date, three *E. coli* OMR are identified, BamA, OmpC/OmpF complex, and Tsx (197–199). Genetic transposon mutagenesis was used to select mutants resistant to CDI of interest to identify these receptors.

In addition to identifying OMR specific to *E. coli*, receptor studies illustrate the restrictive nature of CDI systems. Identification of *E. coli* EC93 CdiA- BamA binding site revealed a high level of sequence variability in the BamA domain compared to other CDI encoding *E. coli.* The variability in the amino acids sequence for the BamA binding site corelates with inability for EC93 CDI of other *E. coli* strains, restricting EC93 to intraspecies CDI (183, 199, 200). Similar restrictions were identified with OmpC/OmpF

complex and *E. coli* EC536 CdiA intoxication (198, 199). These data suggest the use of CDI systems in distinguishing 'self' from 'non-self' to promote kin interactions. OMR have yet to be identified for any bacterial species other than *E.* coli, including *Burkholderia* species' CDI systems.

Following binding to the OMR, BcpA is understood to then translocate through the periplasm and inner membrane. Using similar genetic screens as OMR, several inner membrane components have been identified in *E.coli* (191, 197, 198, 201). Data from *E. coli* show that membrane receptors can vary from strain to strain, adding an additional level of specificity in recipient cell susceptibility to individual CdiA/BcpA toxins. CdiA/BcpA translocation is not necessarily dependent on the function of translocation factors (197).

Less is known about *Burkholderia* susceptibility factors and translocation of BcpA. *B. pseudomallei* 1026b is shown to require specific LPS structures and proteins encoded by BTH_I0359 and BTH_II0599 genes for BcpA translocation in *B. thailandensis* E264 model bacteria (202). The functional relationship between LPS, BTH_I0359 and BTH_II0599 encoded proteins, and BcpA is still undetermined. Recent studies show the recipient cells for *B. multivorans,* CGD2M, require the cytoplasmic membrane proteins GltJK for entry of BcpA-2 into recipient cells (203). Similar to *E. coli* factors, sensitivity to CDI protein intoxication differs significantly between closely related species.

In addition to membrane specific proteins, some *E. coli* CDI systems can require cytoplasmic factors for recipient cell susceptibility. Identified factors include O-acetylserine sulfhydrylase A (CysK), Elongation Factor Thermo-Unstable (EF-Tu), and the Elongation Factor Thermo-Stable (EF-Ts). CysK and EF-Tu/EF-Ts are associated with CdiA C-terminus tRNase activity (198, 204–206). Function of the outer membrane

receptors are not always necessary (197), however functional activity is thought to be required for cytoplasmic factors. The necessity of each intracellular factor is variable between *E. coli* strains, although the use of EF-Tu has been established between CdiA toxins with little similarity (205, 206). Currently, there are no identified cytoplasmic factors required for *Burkholderia* CDI systems. As many proteobacteria possess CDI systems with high variability between them, identification of additional recipient cell factors is anticipated. With each additional identified component, our understanding of the restrictive and targeted nature of CDI systems increases.

### 1.4.5. Kin discrimination mediated by CDI.

As part of their functions, CDI systems kill 'non-kin' bacteria, lacking the respective immunity protein. This results in 'kin' bacteria survival. One proposed benefit of killing non-kin, beyond nutrient competition, is to pre-establish self-segregation prior to biofilm formation and other beneficial community behaviors (187, 192). Mathematical modeling showed that in two mutually exclusive CDI expressing species, extinction of one of the species is always the result. In contrast, depending on the spatial separation of two different CDI expressing species, competing species can co-exist in species specific segregation patterns (207). Separation patterns are additionally affected by potency of the CDI loci encoded toxin, additional beneficial systems such as T6SS, and environmental advantages. Kin discrimination via solitary CDI *in silico* is dependent on contact time, effect of the toxin, and cost of CDI system expression. Further, donor cells do not have to kill the recipient, but require a reduction in the recipient growth to gain the kin-specific spatial environment (208). These studies demonstrate specific CDI toxin–immunity protein

control “self”/“non-self” discrimination in mixed bacterial populations. Kin recognition and segregation of outsiders through competition can then lead to single species community behavior, like biofilms (192, 209, 210).

### 1.4.6. Genomic island mobility

*B. thailandensis* E264 has been shown to utilize the CDI system both as a means of competition and as a means of intercellular interaction. E264 required the BcpAIOB proteins when mediating biofilm formation and is associated with additional phenotypes including pigmentation and Congo-Red binding. These community behaviors were dependent on the function of BcpA. Inactivation of BcpA C-terminal toxin via an amino acid mutation (E3064A to K3066A substitution - EKA) was defective in the associated cooperative behaviors (209, 210). CDI induced biofilm formation in E264 is independent of cell lysis and interbacterial killing for extracellular DNA (209). Instead, BcpAIOB induces global gene expression changes in recipient cells. RNA sequencing identified expression changes in genes encoding extracellular polysaccharide synthesis machinery and pilus proteins, both have been associated with structure and biofilm formation. This CDI system-mediated intercellular communication was termed contact-dependent signaling (CDS) (210). However, follow-up studies show that the CDS phenotype seen in *B. thailandensis* is due to large mobile genetic elements termed ‘mega circle’ that contain the *bcpAIOB* locus of *B. thailandensis* (196). Similar mechanisms have not been observed for other *Burkholderia* CDI systems (188, 193).

### 1.4.7. CDI systems in other bacterial species

Over a hundred *Pseudomonas* species are predicted to have CDI encoding loci. Conserved CdiA pre-C-terminus motifs for *Pseudomonas* species vary and fall into five subclasses, one of which includes the *E. coli*-type VENN motif (211, 212). CDI competition is speculated to have an important role in shaping the population through competition and the variability of the C-terminal toxin sequences. In addition to interbacterial competition functions, the *Pseudomonas* CDI system is associated with virulence in cell culture, mouse models, and in acute and chronic infection models (213, 214). Similar to *B. thailandensis*, *Pseudomonas aeruginosa* PA01, has been shown to utilize the CDI system in adhesion and biofilm formation (212), although not to bronchial epithelial cells (214).

The bacterial symbiont, *Xenorhabdus doucetiae*, includes an additional gene, *cdiC,* in its *E. coli*-like CDI encoding locus. The *cdiC* gene is co-transcribed with the other CDI genes (*cdiBCAI*) (215). The gene encodes for CdiC, the function of which is unknown, but has partial identity to *E. coli* HlyC, an acyltransferase (215, 216).

In addition to bacterial competition, CDI systems have been associated with aggregation and bacterial virulence in *Erwinia chrysanthemi* EC16 (217), *Xylella fastidiosa* (218), and *Xanthomonas axonopodis* (219). In *Neisseria meningitidis*, *hrpA* mutants (*cdiA* homolog) were attenuated for intracellular survival in HeLa cells (220). Multiple *Acinetobacter* species have been found to contain functional CDI systems (194, 221–223). *A. baylyi* ADPI found no correlation in biofilm or adhesion (222), however *A. baumanni* DSM30011 one of the CDI systems were associated with repression of biofilm formation and host cell adhesion (194).

## 1.5. Bacterial cooperation and kin signaling

Kin cell-to-cell recognition can set the foundation for beneficial interactions separate from others in a mixed microbial environment. Kin recognition and non-kin discrimination share many characteristics and often end with the same result of segregation or species overtaking the environmental niche. For this work, kin recognition will be centered on systems that exclude non-kin inadvertently.

### 1.5.1. Kin communication by diffusible signals

In addition to contact-dependent means of recognition, the use of quorum sensing is widespread in the microbial world as a means of communication through a diffusible signal. Quorum sensing allows bacteria to recognize both kin species and population density within their environment. Quorum sensing utilizes diffusible signals as autoinducers to regulate cooperative behaviors, such as bioluminescence, competence, virulence, motility, and biofilm formation (224–226).

A major class of quorum sensing systems in Gram-negative bacteria utilize acylated homoserine lactones (AHLs) as a signaling molecule. In comparison, Gram-positive bacteria frequently use oligopeptides as signaling molecules (224). Specificity in Gram-negative quorum sensing is derived from the molecule receptor, where quorum sensing receptors bind cognate signaling molecule determined by various factors. In the case of AHLs, chemical structures vary depending on substitutions, saturation, and overall length of the acyl chains. These structural differences allow bacteria to recognize kin at the sub-species level (224, 227).

Members of the *Burkholderia* genus often encode AHL-associated quorum sensing systems with homology to the LuxI/LuxR systems (39). The LuxI/LuxR quorum sensing system was first characterized in *Vibrio fischeri* to regulate bioluminescence (228). The *Burkholderia* LuxI/LuxR homologs are CepI/CepR in which CepI synthase regulates the production of the signaling molecule *N*-octanoyl homoserine lactone (C8-HSL). CepR is the transcriptional regulator that interacts with C8-HSL to modulate quorum sensing associated genes. Similar to other LuxI/LuxR quorum sensing systems, *cepR* regulates expression of various genes including *cepI* and itself (39). Various *Burkholderia* strains encode multiple CepI/CepR systems which are associated with different and specific AHL molecules (39, 195, 229, 230). Quorum sensing regulation is associated with global gene expression changes. In *B. thailandensis* the CepR/CepI system homolog activates the expression of the CDI *bcpAIOB* operon, although it is unknow if the regulation is direct (195).

### 1.5.2. Community outcomes

Bacteria have been shown to interact in highly diverse communities, including formation of biofilms between different species and different Gram classes (231–233). Biofilms are commonly used as an indicator of community behaviors even though diversity of the makeup can include both inter- and intra-bacterial species. Perfect cooperation in biofilms is predicted when they contain a single strain with high genetic relatedness (234).

Biofilms are defined as a 3D structure assembled by bacteria embedded in an extracellular matrix. Due to the 3D structure and lifestyle required for a biofilm, the assembled bacteria exist in a heterogeneous environment and bacteria in different regions

of a biofilm have different functions. The various groups within a biofilm present different traits (235, 236). Internal subpopulations of the assembled structure are protected from environmental stresses and are thought to be, in part, the reason biofilm infections are difficult to cure by antibiotic treatment (236–238). In fact, biofilm formation is hypothesized to play a role in Bcc multi-drug resistance and persistence of infection in patients with CF (239, 240).

## 1.6. Overall Hypothesis

Primarily using the pathogenic bacteria species, *B. dolosa*, experiments will test the hypothesis that *Burkholderia*-type CDI requires; 1) BcpA functional regions for translocation from the donor cell to the recipient cell, and 2) CDI system-specific recipient cell susceptibility factors.

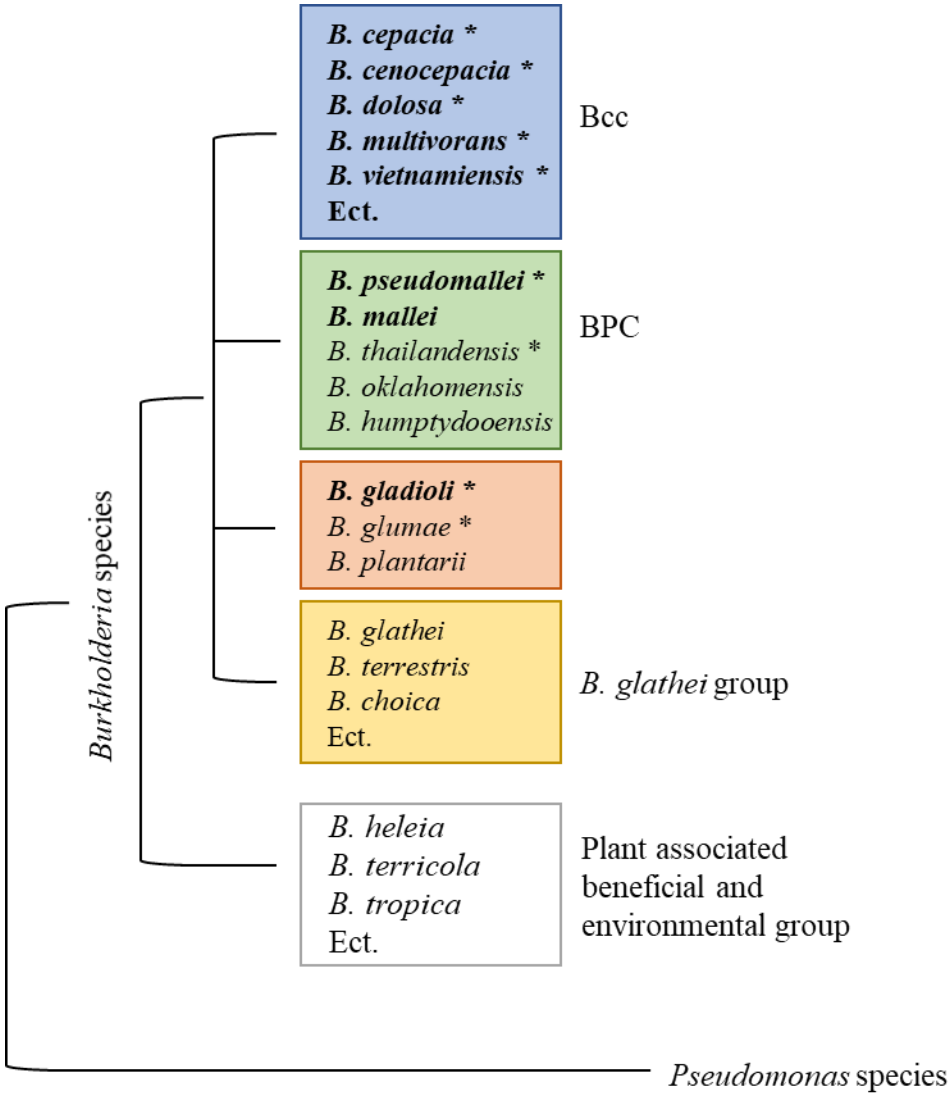


**Figure 1.1.Major, unweighted, grouping of *Burkholderia* species.**

**Figure 1.1. Major, unweighted, grouping of *Burkholderia* species.**

Groups are organized based on the 16S rRNA-based phylogenetic tree. The species grouping is unweighted. Species most commonly associated with human infections are in bold. Bacterial species that contain CDI encoding strains referenced in this body of work are denoted with an asterisk (*). Acronyms used are *Burkholderia cepacia* complex members (Bcc), and *Burkholderia pseudomallei* complex members (BPC). The groupings are non-exhaustive lists. (193, 241, 242)

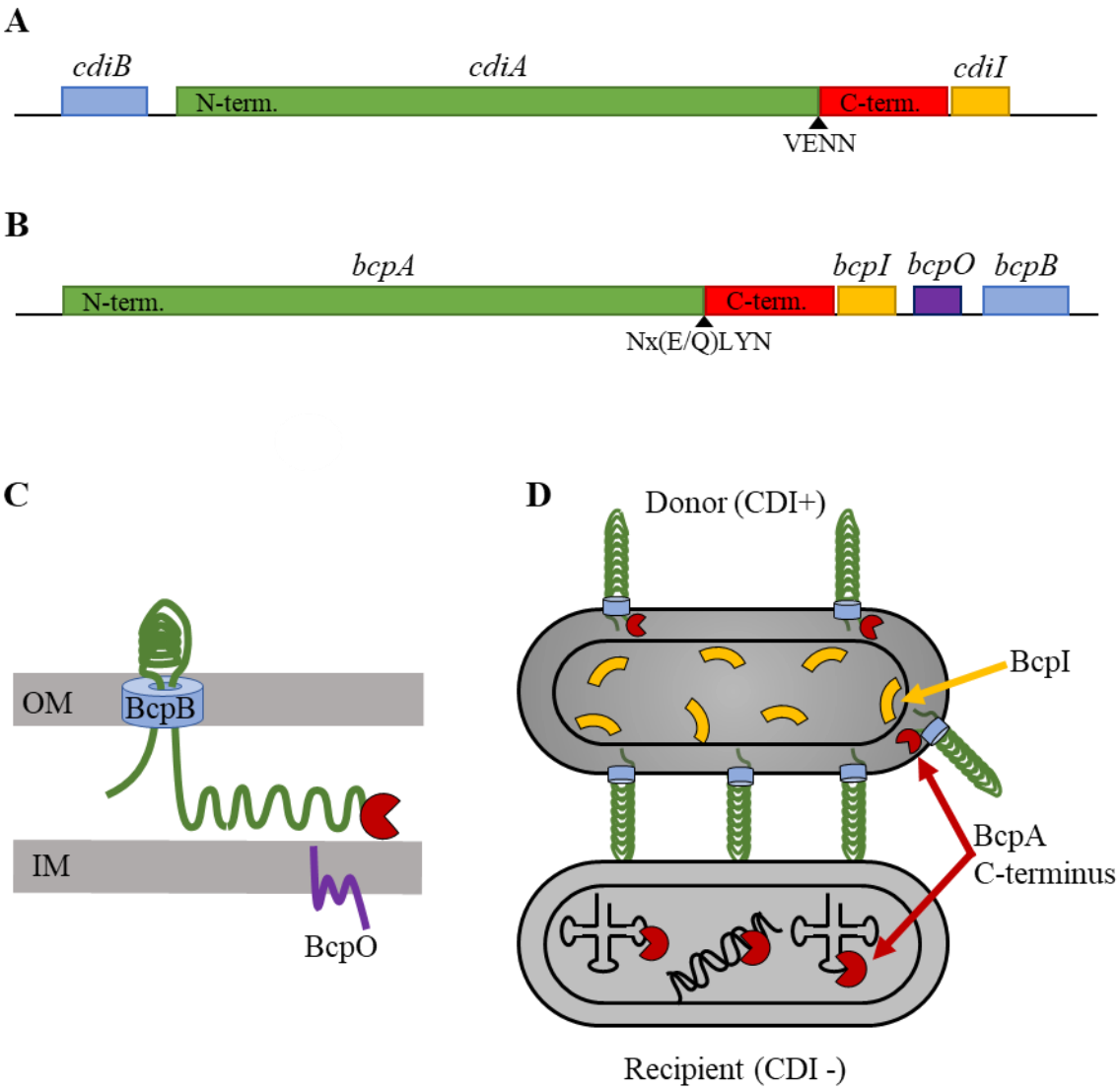


**Figure 1.2. Model of contact-dependent system encoding loci and basic components donor and recipient cell components.**

**Figure 1.2: Model of contact-dependent system encoding loci and basic components donor and recipient cell components.**

**A)** The organization of *E. coli*-type and **B)** *Burkholderia*-type contact-dependent growth inhibition (CDI) encoding loci. Corresponding homologues genes are color-coordinated for comparison of locus organization between the two locus-types. The exoprotein toxin (*cdiA/cpA*) is divided into the filamentous N-terminal region (green) and the catalytically active, ~300aa, C-terminal domain (red). N -terminus and C-terminus are distinguished by the corresponding conserved amino acid sequences (*E. coli*-type, VENN; and *Burkholderia*-type, Nx(E/Q)LYN). **C)** The $CDI^+$ donor cell native protein localization of the CDI two-partner secretion system (TPS). Proteins and specific domains are color coordinated with the corresponding *Burkholderia*-type genes. Outer membrane (OM) and inner membrane (IM) of the donor bacterium are in grey. **D)** The basic model for CDI. The C-terminus of an exoprotein toxin (BcpA/CdiA) of $CDI^+$ donor bacteria is delivered into the cytoplasm of recipient/neighboring bacterium to then, typically, nuclease activities such as degrading DNA, tRNA, or RNA. Kin-bacteria produce an immunity protein (BcpI/CdiAI) that if present, will protect against BcpA-mediated growth inhibition. Adapted from Aoki et al., 2010; Anderson et al., 2012; Nikolakakis et al., 2012; Ruhe et al., 2018 (183, 185, 187, 190).

# Chapter 2: Methods

## 2.1. Bacterial strains and culture conditions

*Burkholderia* strains and *E. coli* strains used in this body of work are listed in appendix B and were cultured in low-salt (0.5% NaCl) Luria-Bertani medium (LSLB). Plasmids were maintained in *Escherichia coli* DH5α and delivered to *B. dolosa* using conjugation donor strain *E. coli* RHO3, a 2,6-diaminopimelic acid (DAP) auxotroph (243).

For selection of *Burkholderia* strains, LSLB was supplemented with 250-500 μg/ml kanamycin, 50-125 μg/ml tetracycline, or 20 μg/ml chloramphenicol (Cm). *E. coli* strains were cultured in LSLB supplemented, where appropriate, with 100 μg/ml ampicillin, 50 μg/ml kanamycin, 25 μg/ml tetracycline, or 200 μg/ml DAP (185, 188, 193).

M63 minimal medium (110 mM KH2PO4, 200 mM K2HPO4, 75 mM (NH4)2SO4, 16nM FeSO4) was supplemented with 1 mM MgSO4 and 0.2% glucose when noted (185, 188, 193).

## 2.2. Genetic manipulations

Plasmids used are listed in Appendix C. Plasmids were verified by DNA sequencing (Eurofins Genomics or ACGT, Inc.) and bacterial mutant strains verified by PCR.

In-frame deletion mutations were constructed by allelic exchange using plasmid pEXKm5 (243). PCR amplification of two fragments: one fragment ~500bp 5' to the ORF (including the first three codons) and another ~500bp 3' to the ORF (including the last three codons). Plasmids were constructed by either restriction-ligation or using Gibson

assembly (Appendix C). For plasmids constructed using restriction-ligation, fragments were joined by overlap PCR and cloned into pEXKm5 by restriction digestion. For plasmids constructed using Gibson assembly, Gibson assembly kit (Gibson Assembly® HiFi 1 Step Kit, Synthetic Genomics Inc.) was used to join the two fragments with linearized pEXKm5. Assembly was completed using Gibson Assembly® HiFi 1 Step Kit, Synthetic Genomics Inc. reagents, according to the manufacturer's instructions. Plasmids were used for allelic exchange in either E264 strains or AU0158, as described (243).

Gene disruption mutants were made by cloning 1Kb of the ORF into pEXKM5 plasmid (243). Plasmids were mated in to integrate within the gene of interest. Gene disruptions were confirmed by DNA sequencing.

Bacterial mutants were marked with antibiotic resistance cassettes by delivering pUC18Tmini-Tn-Kan (244) or pUCTet (185) to an *att*Tn7 site within genome of either E264 or AU0158. Markers were delivered via triparental mating of E. coli RH03 with helper plasmid pTNS3 (245), as previously described. Successful delivery to an attTn7 site associated with BDAG_00405 (*glmS-1*) or BDAG_04221 (*glmS-3*) for AU0158 or BTH_I0288 (*glmS-1*) or BTH_II0348 (*glmS-2*) for E264 was confirmed by PCR (185, 188, 246).

To complement deletion or transposon mutants, the gene of interest was PCR-amplified and cloned into an *att*Tn7 site delivery plasmid. ORFs were cloned by restriction digestion into pUCS12 (185), 3' to the strong, constitutive promoter, $P_{S12}$ (*Burkholderia thailandensis*, E264, *rpsL* gene promoter), or into pUC (244).

For complementation of kanamycin-resistant miniTn5 mutants, BDAG_00967, BDAG_00966, and a fragment containing both BDAG_00966 and BDAG_00967 in their

native orientation were PCR-amplified and cloned 3' to pUCS12 in the tetracycline-resistant backbone, pUCTet (185). All genes for complementation were delivered to *att*Tn7 sites in the genome of either E264 or AU0158 via triparental mating with helper plasmid pTNS3 as described (244, 245).

### 2.3. Interbacterial competition assay

Interbacterial competition assays were performed as previously described (185, 187, 188) with modifications. *Burkholderia* strains carrying antibiotic resistance cassettes at *att*Tn7 sites were cultured overnight without antibiotics and resuspended in sterile PBS to $OD_{600}$ 0.2 for *B. thailandensis* E264 strains or $OD_{600}$ = 2 for *B. dolosa* AU0158 strains. Bacteria were mixed at a 1:1 ratio, 20 µl of the mixture was plated on LSLB agar without antibiotic selection, and plates were incubated at 37°C for 24–26 h, unless otherwise indicated. The input ratio (donor:recipient) was determined by plating the co-culture inoculum on antibiotic plates. Bacteria were collected from co-cultures with a sterile loop, diluted in sterile PBS, and plated on LSLB with antibiotic selection to quantify each strain. The competitive index (CI) was calculated as the ratio of the donor strain to the recipient strain at 24 h divided by the input (donor:recipient) ratio.

For bacterial competitions between tetracycline-resistant donor strains and recipient strains resistant to both kanamycin and tetracycline, donor strain CFUs were calculated by subtracting the recipient (kanamycin-resistant) CFUs from the total (tetracycline-resistant) CFUs prior to CI calculation. Two to three independent experiments with 3 biological replicates.

For competitions in liquid cultures, bacteria were cultured overnight, washed with PBS, and diluted to $OD_{600}$ = 2 in fresh LSLB medium. Strains were mixed at a 1:1 ratio (final volume of 2 ml) without antibiotic selection and cultured for 24 h at 37°C. Aliquots were taken at 0 h and 24 h, diluted in PBS, and plated on LSLB with antibiotic selection to determine the CFU per ml of each strain in the competition. At least two independent experiments were performed in triplicate.

### 2.4. Motility assay

Motility was separated into swimming (mimicking movement through liquid-like environments) and swarming (mimicking movement over surfaces, determined by the percent agar in the culture plates). Swimming motility was measured on 0.3% agar plates, and swarming motility was measured on 0.6% agar plates. Pipetted 20µL of overnight cultures at $0.2OD_{600}$ in the center of low-density TSB with 1% glucose.

Growth from the confluent area of a freshly cultured plate was inoculated into the center of the swimming motility agar plates. Motility plates were then incubated at room temperature for 24h and 48h. The diameter of the colonial growth from the initial inoculation site was measured at 24h and 48h.

### 2.5. Crystal-Violet staining assay

Overnight cultures were diluted in TSB with 1% glucose and pipetted into wells of a 96-well PVC plate. Plates were incubated 48 hours at 37°C, in humid container. Unattached bacteria were washed with DI water. Biofilms were stained with 0.5% crystal

violet (CV) and excess stain was washed away and let to air dry. CV stain was solubilized with 33% acetic acid. The solution was transferred to a flat bottom plate, and then solubilized staining was quantified by measuring $OD_{540}$ (247).

### 2.6. Microscopy

Static biofilms were setup with overnight cultures diluted into TSB with 1% glucose to have 0.02 $OD_{600}$. Pipetted 400µL of diluted cultures into 4 wells of a 4-well glass chamber slide (Lab-Tek) and incubated for 48h at 37°C. At 24h spent media was removed and 400µL of fresh TSB with 1% glucose was added to each chamber. After 48h, non-adherent bacteria were removed by three washes with PBS. Following the washes, the biofilms were overlaid with 400µl PBS. Static biofilm for confocal imagining adapted from Schaefers et al., 2017 (247). Confocal laser scanning microscopy with a Leica SP8 using a 20x objective lens was used to image slides. Collected Z stacks were processed with and quantified with COMSTAT program (248).

### 2.7. Immunoblotting

Bacteria were cultured overnight in LSLB, pelleted, and resuspended in 2× SDS PAGE loading buffer to $OD_{600}$ = 50. For full length BcpA Western blots, samples were boiled and 10µl were loaded in the wells of a 5% SDS PAGE gel. 5% SDS-PAGE gels were run at 100V for 6 h. For BcpA banding comparison Western blot, 10µl of samples were loaded into the wells of 10-20% SDS-PAGE Tris-glycine gels (Invitrogen, TM.) 10-20% SDS-PAGE gels were run for 1.5 h at 100V. Samples were then transferred to nitrocellulose and probed with Rabbit polyclonal αBcpA-CT (*B. thailandensis* E264 BcpA

C-terminal toxin) antibody at 4:25,000 and fluorescent secondary goat-αrabbit IgG at 1:15,000. Images were acquired on a Li-Cor (Odyssey) with software Odyssey v3.0. or Bio-Rad ChemiDoc imaging system.

### 2.8. Dot Blots

Overnight cultures were washed in PBS and duplicate samples were resuspended to an $OD_{600}$ of 4.0. One set of samples was boiled for 5m (lysate). Five microlitres of each sample (whole cells and lysate) were pipetted onto nitrocellulose and air-dried. Membranes were processed as described above, probed with αBcpA-CT (E264 BcpA C-terminal toxin) at 1:1000 followed by secondary αRabbit antibody and detection as described with on a Li-Cor (Odyssey) with software Odyssey v3.0 (209).

### 2.9. Transposon mutagenesis selection

Random transposon mutagenesis of AU0158 Δ*bcp-1* Δ*bcp-2* double mutant was made by delivering pUT-miniTn5-Kn by conjugation (203, 249). The mating was collected, serially diluted in PBS, and plated on LSLB with 250 µg/ml kanamycin to select for transposon insertion mutants. Isolated colonies were pooled in LSLB with 15% glycerol for storage of the transposon mutant library at -80°C.

For selection of CDI resistant mutants, sequential interbacterial competition assays were used (203). In brief, 20 µL of the transposon pool was inoculated into 25 ml LSLB with 250 µg/ml kanamycin and cultured overnight. Tetracycline-resistant donor strains Δ*bcp*-1 or Δ*bcp*-2 were cultured overnight in 2 ml LSLB with 50 µg/ml tetracycline. Cultures were pelleted via centrifugation at 15,000 × g for 5 min and resuspended in sterile

PBS to $OD_{600}$=2. Inter-bacterial competition assays were performed as described below with the transposon pool (recipients) mixed 1:1 with either donor strain. Input ratios were determined by serially diluting the initial mixture and plating dilutions on antibiotic plates. For competitions, 20 µl of the mixture was spotted on LSLB agar (without antibiotics) in triplicate, air dried, and incubated at 37°C for 48 h. Co-cultures were collected with a sterile loop, serially diluted in sterile PBS and plated on antibiotic plates to determine the output competition ratios. Kanamycin-resistant recipient colonies were collected from output plates and pooled from all replicates in LSLB with 15% glycerol for storage. This output pool of transposon mutants was used to inoculate fresh LSLB (25 ml) and was re-competed against the appropriate donor strain in the next round of selection. In total, three rounds of competition selection were performed.

### 2.10. Arbitrary PCR

Transposon insertion sites of CDI-resistant mutants were determined using arbitrary PCR, as described (203, 250). Genomic DNA was extracted from transposon mutants and wild-type AU0158 strain (as a control) using the Wizard® Genomic DNA Purification system (Promega) according to the manufacturer's protocol. Nested arbitrary-primed PCR was performed using this genomic DNA as template with primers Arb1 (arbitrary primer) and Tn3out (first round primer annealing to the 3' end of the transposon). PCR products were treated with ExoSAP-IT™ PCR Product Cleanup Reagent (Applied Biosystems) and used as templates for the second, nested PCR reaction with primers Arb2 and Tn3in. Second-round PCR products from transposon mutants were compared to the wild-type AU0158 negative control by agarose gel electrophoresis and treated with

ExoSAP-IT™. The transposon-chromosome junctions in the second-round PCR products were sequenced with primer Tn3seq and transposon-disrupted genes identified by BLAST analysis.

### 2.11. Growth curves

Overnight cultures were pelleted via centrifugation at 15,000 × *g* for 5 min and resuspended in sterile PBS. LSLB (25 ml) was inoculated to $OD_{600}$ = 0.025. Cultures were grown at 37°C on a shaker for 24 h with periodic $OD_{600}$ measurements. Two independent experiments were performed in duplicate.

### 2.12. Auxotrophic growth cultures

Bacterial cultures were grown overnight in LSLB at 37°C. Cultures were then washed in PBS and resuspended to an $OD_{600}$= 2. Resuspended cultures then inoculated 2ml of M63 for $OD_{600}$= 0.002. Selected cultures were then supplemented with L-histidine to = 0.1mM. Cells were grown for an additional 24 h at 37°C and then imaged. Histidine auxotrophic growth assay adapted from Price, et al., 2018 (251). Two independent experiments were performed in duplicate.

### 2.13. Whole genome re-sequencing

Genomic DNA was extracted from transposon mutants and AU0158 Δ*bcp*-1 Δ*bcp*-2 (as a control) using the Wizard® Genomic DNA Purification system (Promega) according to the manufacturer's protocol. Whole genome sequencing was done using

services from two different companies, ACGT,Inc., and Microbial Genome Sequencing Center LLC (MiGS, LLC). In brief, DNA sequencing libraries were constructed as per manufacturer's instructions (Illumina, Inc). The libraries were bar-coded with index tags. Libraries were sequenced using NextSeq™ 200 systems (Illumina, Inc) for MiGS, LLC and NextSeq™ 500 systems (Illumina, Inc) for ACGT, Inc. to generate reads. Reads were mapped against the National Center for Biotechnology Information (NCBI) genome database for *Burkholderia dolosa* AU0158 genomic chromosomes to identify unique mutations.

Sequencing results are compiled in Appendix E.

Whole Genome Sequencing performed at ACGT, Inc., 35 Waltz Drive, Wheeling, IL 60090 USA.

Whole Genome Sequencing performed at Microbial Genome Sequencing Center LLC, 355 Fifth Avenue, Suite 810, Pittsburg, PA 15222 USA.

### 2.14. LPS extraction and analysis

Cells were cultured overnight in LSLB medium, and lipopolysaccharides (LPS) were extracted from pellets equivalent to $OD_{600}$ of 2.0 per manufacturer's instructions using an LPS Extraction Kit (iNtRON Biotechnology). Extracted LPS was resuspended in sodium dodecyl sulfate-polyacrylamide gel electrophoresis (SDS-PAGE) sample buffer and equal amounts of LPS (equivalent to that extracted from $OD_{600}$ of 0.5) were analyzed by SDS-PAGE on Novex 10-20% Tricine Gels (Invitrogen™). The LPS was visualized using Molecular Probes' proprietary Pro-Q™ Emerald 300 LPS Gel Stain Kit (Invitrogen™), per manufactures instructions, on a Gel Doc EZ Imager (Bio-Rad).

## 2.15. β-galactosidase assays

Mitomycin C (MMC) induced DNA damage assay - Reporter strains were grown overnight in LSLB at 37°C. Inoculate 2ml LSLB cultures with 20$\mu$l of overnight cultures and incubate at 37°C for 4h. To the MMC treated samples add 20 $\mu$l of 5$\mu$g/ml MMC, then incubate at 37°C for an additional 2h. Dilute cultures into 1:10 Z+ buffer (15ml Z buffer (6mM $Na_2HPO_4$, 4mM $NaH_2PO_4$, 1mM KCl, 0.1mM $MgSO_4$) + 40.5µlβ-mercaptoethanol (β-ME)). MMC DNA damage assay adapted from Ulrich R. L., et al., 2013 (252).

BcpA induced DNA damage assay - From an overnight culture, spot 20$\mu$l of reporter strains onto LSLB plate, air dry, and incubate at 37°C overnight. Harvest sports and resuspend in 1:10 Z+buffer (15ml Z buffer (6mM $Na_2HPO_4$, 4mM $NaH_2PO_4$, 1mM KCl, 0.1mM $MgSO_4$) + 40.5µl β-mercaptoethanol (β-ME)).

Once reporter strains are diluted into Z+ buffer, 250µl of each culture were pipetted into a 96-well plate. The remaining 750µl of culture was treated with 10µl of 0.1%SDS+50µl chloroform to permeabilize the cells. 250µl of diluted permeabilized cells (50:150 Z+ buffer) was then pipetted into remaining well in the 96-well plate. Using Molecular Devices SpectraMax 5M plate reader and SoftMax Pro software, endpoint of 600λ was read on the non-permeabilized cell wells to determine the $OD_{600}$. 50µl of ortho-Nit (50µl of ortho-Nitrophenyl-β-galactoside (ONPG)) was then added to each of the permeabilized cell wells. β-galactosidase activity was determined by measuring colorimetric substrate production at 420λ 5m every 30s by SpectraMax plate reader. Miller units were then calculated using the reads from SoftMax software output data.

$$\text{Miller Units} = \frac{OD_{420}}{(T)(OD_{600})(\text{ml of Cells})}$$

T= time in min. Pick a time point from $OD_{420}$ run, that would be within linear range of $OD_{420}$ vs. Time well was measured

β-galactosidase assay controls include promoterless *lacZ* in the pUC backbone (promoterless-*lacZ*) and overexpression under the S12 constitutive promoter in pUCS12 backbone (*lacZ*$^{ON}$) (210). β-galactosidase assay protocol adapted from Garcia, E. C., et al., 2016 (210)

### 2.16. β-galactosidase co-cultures assay

Reporter strains were cultured overnight in LSLB at 37°C, washed in PBS, and then resuspended to a 0.2$OD_{600}$. For co-cultures between donor and recipients (marked with *lacZ*) were mixed at a 1:1 ratio and 20µl were spotted onto M63-Xgal plates. Plates were air-dried and incubated 24 h at 37°C, followed by an additional two days at room temperature and then imaged (210).

### 2.17. Bioinformatics and statistics

*Burkholderia* BcpA amino acid sequences are from the National Center for Biotechnology Information (NCBI) genome database. Amino acid sequencing either was of the BcpA proteins or BcpA through the BcpI protein sequences. Alignments were curated using the ClustalW alignment function in Geneious (v.6.1.8) (253). Protein

structure predictions were conducted using the Phyre2 online server (254). Native promoters were identified using Softberry BPROM Operon and Gene Finding in Bacteria 2016 (255). *Burkholderia* homologs were identified using the NCBI BLASTP suite and the *Burkholderia* Genome Database (256). One-way ANOVA with Tukey tests were performed on all data sets. All statistics were performed with GraphPad Prism (v.6) (257).

# Chapter 3: Optimization of assays to compare *B. dolosa* CDI system function.

## 3.1. Summary

*B. dolosa* expresses two CDI system-encoding loci under laboratory conditions (188). I hypothesized that each CDI system would have distinct differences in the ability to outcompete one another and to form biofilms. *B. dolosa* BcpA-1 is associated with a stronger CDI dependent killing against a CDI-sensitive mutants during independent studies. However, when Bcp-1 and Bcp-2 were in competition against one another, they remained near a 1:1 ratio indicating that neither were strong enough to outcompete the other. Competition outcomes between Bcp-1 and Bcp-2 could be affected by growing cultures in antibiotics prior to setting up competitions. Similar to other *Burkholderia,* AU0158 cannot perform CDI-dependent killing in liquid cultures. Furthermore, competitions restricted to solid media can continue for 24h to 48h with no significant change in the competitive index. There were no significant differences identified in biofilm formation between wild-type (WT) bacteria and the single mutants by either crystal violet staining or confocal imaging. The biofilm biomass calculated from confocal imaging identify that deletion of both *bcpAIOB*-1 (Δ*bcp-1*) and *bcpAIOB*-2 (Δ*bcp-2*) had a partial inhibition in biofilm formation compared to WT strains. Finally, constitutive production of either Bcp-1 or Bcp-2 resulted in significant inhibition in biofilm formation and swimming-associated motility.

## 3.2. Introduction

In addition to the two classes of CDI systems, *Burkholderia*-type and *E. coli*-type, each can be further broken down into sub-classes. Focusing on *Burkholderia*-type, the classes are separated into class I and class II. Class distinction is determined on three components; the amino acid sequence of BcpB, BcpO, and the conserved N-terminal region of BcpA. Within class I, the BcpO proteins contain a conserved C-terminus region with a variable region in the N-terminal signal sequence, typically ~20aa long (185, 187, 192). The variable N-terminal signal sequence of BcpO correlates with the allele specific variability of BcpA C-terminus and BcpI (185, 192). These findings indicate that the class I BcpO proteins are most likely functionally identical. The *bcpO* genes in class II CDI-systems have little to no similarity across the different alleles (185, 192).

*B. thailandensis* and *B. pseudomallei* class I CDI systems of are the most well characterized for *Burkholderia*-type. Functional CDI system chimera was created by exchanging *B. pseudomallei* BcpA C-terminus and associated BcpI with the corresponding genes in *B. thailandensis;* the chimeric system could still kill competing bacteria in a CDI dependent manner (185, 192). Similar studies have found that functional chimeric CdiA/I (or BcpA/I) mutants can be created by fusing the modular C-terminal CdiA/CdiI following the conserved pre-toxin motif (either VENN, or N(Q/E)LYN) (183, 184, 187, 192, 193). Functional chimeras seem to be restricted to BcpA C-terminus/BcpI from the same class (187, 193, 194).

*B. dolosa* AU0158 contains three CDI system encoding loci, *bcpAIOB-1* (*bcp-1*), *bcpAIOB*-2 (*bcp-2*), *bcpAIOB*-3 (*bcp-3*). The Bcp-1 system is a member of class I, and the variability regions have high amino acid identity to *B. thailandensis* E264 CDI proteins.

AU0158 Bcp-2 and Bcp-3 are both designated under class II. As expected from the definition for each class, the conserved regions of BcpA-2 and BcpA-3 are highly similar sharing an overall identity of 79.9%, while the variable C-termini share 19.9% identity. All three BcpA C-terminal toxins are predicted to be nucleases. Although the Bcp-3 CDI system can kill competing bacteria in a CDI-dependent manner, under laboratory conditions, this locus is not expressed. BcpA-1 was hypothesized to be more toxic than BcpA-2, determined by the competitive index measured for each donor strain when competed against a CDI-sensitive recipient. Although direct comparisons were not made (188).

Many bacteria utilize CDI systems to aid in biofilm formation either directly or indirectly. Bacteria can utilize CDI to kill non-kin bacteria and then signal for community behaviors such as biofilm formation (192, 209, 210). *B. thailandensis* and *Pseudomonas aeruginosa* PA01, (209, 210, 212). In *Acintobacter bamannii* DSM30011 two identified CDI systems were found to (194). Clinical isolates of *in vitro* (247). The goal of this research was to determine if Bcp-1 or Bcp-2 play a role in *B. dolosa* AU0158 biofilm formation.

Due to the lack of expression of *bcp-3* under laboratory conditions, comparisons were focused on the CDI-systems expressed by *bcp-1 and bcp-2*. As only one study has focused on *B. dolosa* CDI systems, further characterization Bcp-1 and Bcp-2 would be benificial to the understanding of these systems. Mathematical modeling of CDI systems predicted that one system will outcompete another and result in kin selection (207). I hypothesized that the competitive indices, motility, and biofilm formation will differ between *B. dolosa* AU0158 Bcp-1 and Bcp-2 systems.

## 3.3. Results

### 3.3.1. *B. dolosa* CDI systems function similar to CDI systems of other *Burkholderia* species.

CDI systems in *Burkholderia* species function similar to their *E. coli* homologs (181, 185, 187). However, differences in the mechanisms of the CDI systems distinguish the bacterial species from one another. *E. coli* CDI can be carried out in liquid cultures and on solid media (185, 197). *B. thailandensis* (E264) had no growth inhibition in liquid cultures; competition was observed after 6h on solid media (192). Data for this observation were not shown (185, 192). As E264 BcpA and AU0158 BcpA-1 share 83.0% amino acid identity, it is likely similar environmental competition limitation would be seen. *B. dolosa* AU0158 produces two highly variable CDI systems. The N-terminus is conserved throughout *Burkholderia* species and yet BcpA-1 and BcpA-2 N-termini only share 38.7% amino acid identity (Figure 3.1A). The current model based on *E. coli* proposes the N-terminus contains a domain that determines the strength of BcpA/CdiA and recipient cell receptor binding (190). To determine if Bcp CDI systems can intoxicate recipient cells in liquid and solid media, competitions with WT donor cells were competed against either Δ*bcp*-1 or Δ*bcp*-2 recipients with and without cognate *bcpI*. Bacterial competitions were conducted in triplicate with initial input ratios of 1:1 donor/recipient. Competitions were harvested, and the competitive index is calculated by antibiotically differentiating donor and recipient colony forming units (CFUs).

In both competitions done in liquid cultures with WT bacteria co-cultured with either Δ*bcp*-1 or Δ*bcp*-2 recipients, no competition was observed with donor and recipient cells remaining at 1:1 ratio (Figure 3.1BC). On solid media WT strains outcompeted Δ*bcp*-

1 recipient by an average of 4.7 logs. Similar results were observed with WT bacteria outcompeting Δ*bcp*-2 recipients by an average of 3.2 logs (Figure 3.1BC). WT bacteria remained near a 1:1 ratio with recipient cells expressing cognate immunity genes on solid media, as expected. These data indicate that AU0158 cannot carry out CDI competitions in liquid cultures for either Bcp-1 or Bcp-2 systems.

In previous studies *Burkholderia* competition assay protocols differ in the amount of time input co-cultures were incubated for prior to the competition harvest. Initial co-culture incubation times range from 6h to 48h and with most incubating for 24h (185, 187, 188, 192). To determine if *B. dolosa* AU0158 required 48h to carry out comparable competition outcomes, sets of input competition plates were incubated for 24h and 48h before harvest. Competitions using either Δ*bcp*-1 or Δ*bcp*-2 as donors were competed against WT, Δ*bcp*-1, Δ*bcp*-2, Δ*bcp*-1Δ*bcp*-2, and Δ*bcp*-1Δ*bcp*-2 expressing *gfp* (Δ*bcp*-1Δ*bcp*-2+*gfp*) strains. The competitive index for both Δ*bcp*-1 and Δ*bcp*-2 donor competitions trends were similar (Figure 3.2AB). WT donor cells outcompeted both Δ*bcp*-1 and Δ*bcp*-2 average of 2.7 logs and 1.7 logs respectively. There was no significant difference in competition output when left to incubate for 24h or 48h. The Δ*bcp*-1 donor outcompeted Δ*bcp*-1Δ*bcp*-2, and Δ*bcp*-1Δ*bcp*-2+*gfp* by an average of 2.6 and 2.7 logs respectively. As with WT bacteria, there was no significant difference in the competitive index when left for 24h or 48h. Furthermore, expression of *gfp* in bacteria has been shown to alter growth and can result in a different phenotype than bacteria expressing an empty antibiotic-tagged vector alone (258). Our data suggests that in competition against BcpA-1 toxins, the production of GFP in the recipient cell does not alter sensitivity (Figure 3.2A). Similar results were seen with BcpA-2 donor cells outcompeting Δ*bcp*-1Δ*bcp*-2 mutants

by 2.7 logs regardless of presence of GFP or being harvested at 24h or 48h (Figure 3.2B). These data support that AU0158 CDI occurs within 24h and additional incubation extending up to 48h does not change the competitive index for either BcpA-1 and BcpA-2. Additionally, production of GFP in recipient cells does not seem to alter sensitivity to BcpA-1 or BcpA-2.

### 3.3.2. Growth in antibiotic cultures prior to input competitions alter the competitive index.

To compare the extent to which individual a *bcp* locus can carry out CDI, WT donor cells were competed against Δ*bcp*-1, Δ*bcp*-2, and Δ*bcp*-1Δ*bcp*-2 mutants. WT bacteria produce both Bcp-1 and Bcp-2 CDI systems. Competing WT cells against individual locus deletion mutants indicate the competitive strength of each locus because the recipient single mutants will be producing one of the CDI systems including the protective cognate immunity and only be susceptible to CDI from the other BcpA toxin. There was no significant difference between the single mutants and their susceptibility, with WT bacteria outcompeting the Δ*bcp*-1 mutant by 2.9 logs and Δ*bcp*-2 mutant by 2.7 logs. When WT strain was competed against the double deletion mutant, Δ*bcp*-1Δ*bcp*-2, the WT strain outcompeted by an average of 4 logs. Taken together this data indicates that an individual BcpA is no stronger than the other in *B. dolosa*. Additionally, expression of both *bcpI*-1 and *bcp*-2 CDI loci produce an additive phenotype nearly doubling the competitive index when competed against Δ*bcp*-1Δ*bcp*-2 (Figure 3.3A).

Competition mathematical modeling of CDI indicate that one system will outcompete another and result in kin selection (207). Following this model, one of the CDI

systems should be more toxic than the other when competed against one another. Competitions were set up with single mutants competed against themselves, the other single mutant, Δ*bcp*-1Δ*bcp*-2, and Δ*bcp*-1Δ*bcp*-2 expressing either *bcpI*-1 or *bcpI*-2. As expected, when Δ*bcp*-1 was competed against itself or Δ*bcp*-1Δ*bcp*-2 expressing *bcpI-2*, mutants remained at a near 1:1 ratio. When Δ*bcp*-1 was competed against Δ*bcp*-1Δ*bcp*-2, Δ*bcp*-1 outcompeted by an average of 2.3 logs. A small but significant increase in the competitive index was observed by Δ*bcp*-1 out competing Δ*bcp*-1Δ*bcp*-2+*bcpI*-2 by an average of 2.8 logs (Figure 3.3B). These results are similar to what was observed when WT bacteria competed against Δ*bcp*-2, indicating that the experimental setup is comparable to one another (Figure 3.3AB). Interestingly, when Δ*bcp*-1 was competed against Δ*bcp*-2, Δ*bcp*-1 had a competitive index of 1.2 logs, indicating that BcpA-2 is the stronger toxin. However, when Δ*bcp*-2 became the donor, BcpA-1 outcompeted BcpA-2 by 2.6 logs (Figure 3.3C). These data were conflicting because the only difference between competitions were the antibiotic markers to identify donor from recipient. These results were further confirmed in a similar study Δ*bcp*-1 against Δ*bcp*-2 in conjunction with one another. Competitions were done in which the donor bacteria were tagged with tetracycline and recipients with kanamycin. In both cases tetracycline resistant donors Δ*bcp*-1 and Δ*bcp*-2 outcompeted the kanamycin recipients by 1.9 logs and 2.1 logs, respectively. There was no significant difference between Δ*bcp*-1 marked with tetracycline competed against kanamycin marked Δ*bcp*-2 from that of the reversed antibiotic resistance marked donor/recipient (Figure 3.3D). I hypothesized that the antibiotics the bacteria were grown overnight in, prior to competition input, effected the competitive index results.

To determine the extent to which supplementing overnight cultures with antibiotics influence the competitive index output, a similar experiment as described for Figure 3.3D was setup. Modification to the previous experiment included having one set of overnight cultures supplemented with antibiotics and the other set of cultures without antibiotics. As seen in the previous experiment, there were no significant difference between Δ*bcp*-1 and Δ*bcp*-2 tetracycline donors against the opposite with kanamycin (Figure 3.3E-*left panel*). There was a significant difference between competitions setup in antibiotics and competitions setup without antibiotics in the overnight cultures. When Δ*bcp*-1 (tetracycline) was competed against Δ*bcp*-1 (kanamycin) from overnight cultures with antibiotics, Δ*bcp*-1 (tetracycline) outcompeted Δ*bcp*-1 (kanamycin) by an average of 0.91 logs. However, when the same competition was setup without antibiotics in the overnight cultures Δ*bcp*-1 (tetracycline) was outcompeted by Δ*bcp*-1 (kanamycin) by an average of 0.25 logs ($p<0.001$). Similar results are seen with the antibiotic markers swapped. When Δ*bcp*-2 (tetracycline) was competed against Δ*bcp*-1 (kanamycin), from antibiotic supplemented cultures Δ*bcp*-2 outcompeted Δ*bcp*-1 by 0.95 logs and without antibiotics by 0.11 logs ($p=0.0006$) (Figure 3.3E). Taken together these data suggest that when donor cells resistant to tetracycline are grown in antibiotic media prior to competition, they are given a competitive advantage and that these results are specific to BcpA-1 against BcpA-2 CDI competitions.

### 3.3.3. Expression of a singular BcpA protein does not alter motility or biofilm formation.

Gram-negative bacteria utilize CDI systems as means of kin cooperation in addition to direct non-kin killing. In many cases biofilm formation and motility regulation are inversely related (194, 207–209, 212). Motility can be broken down into swimming and swarming phenotypes. Swimming is associated with an individual bacterium in response to receiving a chemical signal, chemotaxis. Swarming is characterized by a social motility of bacteria to migrate above solid substrates in groups of tightly bound cells (259, 260). To determine the role of BcpA in *B. dolosa*, swimming and swarming assays were performed on Bcp mutants and diameter of the bacteria growth measured after 24h and 48h. Swimming plates of 0.3% of agar allow for bacteria to move freely from the initial position. Swarming is identified by the ability to move on 0.6% agar plates requiring the bacteria to adapt locomotion machinery to achieve a specialized form of flagellum-driven and surface-adhering motility. Results found that neither presence nor absence of BcpA production under native expression altered swimming or swarming phenotypes, while overexpression of BcpA-1 diminished swimming phenotype. At 24h overexpression of BcpA resulted in a diameter less than half, at an average of 7.5mm compared to the average of native expressing *bcp* loci of 22.6mm in diameter (Figure 3.4A). BcpO in competition has shown to aid in BcpA CDI efficiency. However, BcpO does not play a role in altering motility as shown by Δ*bcpO* mutants having no significant difference in ability to swim than the BcpA differentially regulated mutants. Swarming was unaffected by differential expression of either BcpA-1, BcpA-2, or presence of BcpO both at 24h and 48h (Figure 3.4B).

Biofilm formation often is inversely associated with swimming because biofilms require bacteria to adhere to a surface to develop the biofilm matrix. To determine if BcpA overexpression would inhibit biofilm formation as hypothesized, strains were grown to

allow for static biofilm formation. Using crystal violet staining to determine biomass, absorbance of crystal violet (at λ540) was measured and normalized to the inoculated free media blank. There were no significant differences in crystal violet absorbance comparing WT, Δ*bcp*-1, Δ*bcp*-2, and Δ*bcp*-1Δ*bcp*-2 strains (Figure 3.5). These results are consistent with the swimming assay trends as CDI systems did not seem to influence either ability (Figure 3.4A). However, overexpression of either *bcp*-1 or *bcp*-2 were recorded with an absorbance significantly lower than seen with WT bacteria. Absorbance associated with biomass average for WT strains were 2.12nm, Δ*bcp*-$1^{ON}$ mutants were 1.53nm, and Δ*bcp*-$2^{ON}$ mutants were 1.18nm. There was no significant difference in absorbance measured between Δ*bcp*-1 and Δ*bcp*-2 strains under their native promoters (Figure 3.5). These data suggest that overexpression of either BcpA-1 or BcpA-2 inhibits both swimming motility and biofilm formation. Expression under native promoters or deletions for both BcpA-1 and BcpA-2 did not alter biofilm formation or swimming motility.

The previous experiments found no significant differences between BcpA-1 and BcpA-2 for motility or biofilm formation. Next, we asked if there would be architectural differences in the biofilms between the different CDI-system mutants. Using confocal microscopy to visualize the *gfp*-expressing mutants, Z-stacks of biofilms from WT, Δ*bcp*-1, Δ*bcp*-2, and Δ*bcp*-1Δ*bcp*-2 bacteria were compiled. The structure of the *B. dolosa* biofilms were unique in comparison to the architecture of other *Burkholderia* species biofilms (192, 209, 239, 240, 261). A literature search found a study on *B. dolosa* biofilm formation and oxygen-sensing two component systems which included *B. dolosa* confocal biofilm images (247). Confocal microscopy of the *B. dolosa* biofilms in the reported study are consistent with the structures seen in our microscopy images. In the confocal Z-stack

images, there is a monolayer of cells that adhered to the slide which then would grow to form a mushroom-like biofilm. The biofilms have a small stalk connecting the monolayer to a larger cluster of cells forming at the 'top of the mushroom' (Figure 3.6A). Analysis software used to determine differences in structure had high variability between Z-stack of the same mutant and was not consistent between experiments (data not shown). Due to this limitation, quantitative structural differences in the biofilm formation of WT, Δ*bcp*-1, Δ*bcp*-2, and Δ*bcp*-1Δ*bcp*-2 strains could not be confidently determined. However, the software was able to quantify biomass from the confocal Z-stacks. WT, Δ*bcp*-1 and Δ*bcp*-2 strains did not have any significant differences in biomass, measuring at an average of 40.55 $mm^3$, 31.16 $mm^3$, and 28.28 $mm^3$, respectively. I was able to determine that Δ*bcp*-1Δ*bcp*-2 is partially inhibited in biofilm formation in comparison to WT bacteria with biomass averaging 19.46 $mm^3$ (Figure 3.6B). As confocal microscopy is more sensitive, small differences in biomass can be identified clearer than in crystal violet staining assays (262, 263). Taken together, these data suggest that biofilm formation is partially inhibited in the absence of both BcpA-1 and BcpA-2. Expression of at least one *bcpAIOB* encoding system is sufficient for equivalent WT levels of biofilm formation.

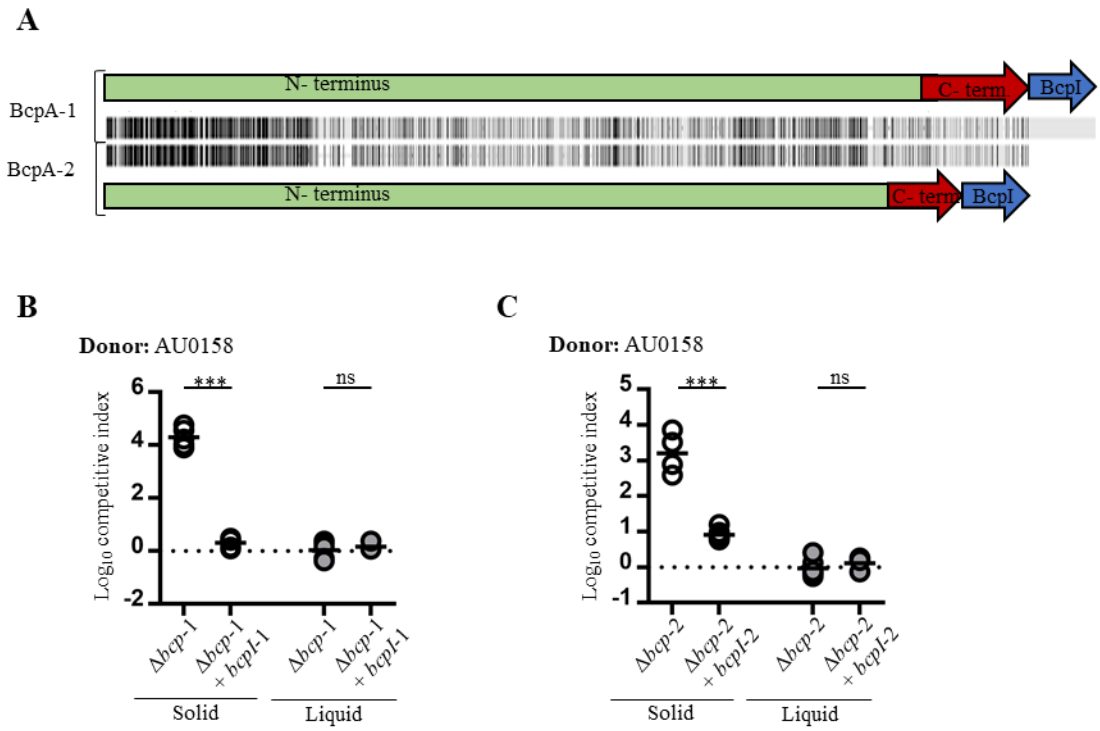


**Figure 3.1. Determine differences of environmental limitations between class I and class II CDI systems.**

**Figure 3.1. Determine differences of environmental limitations between class I and class II CDI systems.**

**A)** Alignment of *B. dolosa* AU0158 CDI systems toxin, BcpA, and immunity, BcpI, amino acid sequences. **Top)** BcpA-BcpI from locus 1. **Bottom)** BcpA-BcpI from locus 2. Interbacterial competition assays between **B)** Δ*bcp-1* and with cognate *bcpI* or **C)** Δ*bcp-2* and with cognate *bcpI* recipient bacteria. Symbols represent competitive index values from multiple (2) biological replicate and bars show the mean (*n*=5-6). Dashed line shows competitive index = 0 (1:1 ratio of donor to recipient). The competitive indices were calculated as (output donor CFU/recipient CFU) divided by (input donor CFU/recipient CFU). The open symbols represent competitions performed in liquid overnight co-cultures and the grey symbols represent competitions with co-cultures plated on solid media low salt-LB. A one-way ANOVA was used to report significance (ns; not significant, *; $p<0.05$, **; $p<0.005$, and ***; $p<0.0005$).

**A)** Adapted from Perault and Cotter, 2018 (188)

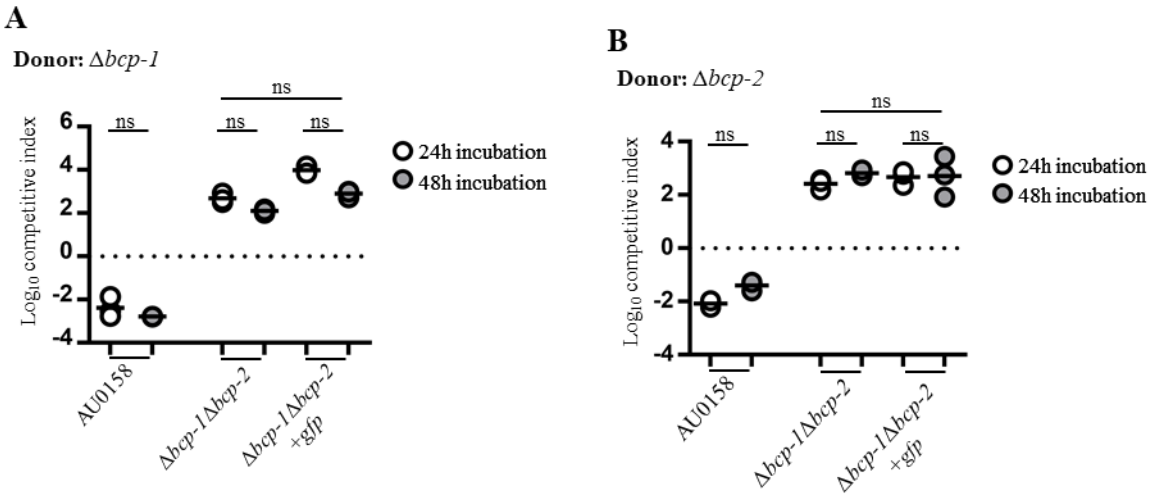


**Figure 3.2. Bacterial competitions co-cultured for 24h and 48h.**

Interbacterial competition assays between **A)** Δ*bcp-1* or **B)** Δ*bcp-2* donor bacteria and the indicated recipient bacteria; WT/AU0158, Δ*bcp-1* Δ*bcp-2*, and Δ*bcp-1* Δ*bcp*-2 expressing *gfp*-plasmid. Symbols represent competitive index values from experiment and bars show the mean ($n$=3). Experimental recipient mutants are colored to indicate the length of time co-culture competitions were incubated (24h are colored light grey and 48h are dark grey). Dashed line shows competitive index = 0 (1:1 ratio of donor to recipient). The competitive indices were calculated as described in Figure 1. A one-way ANOVA was used to report significance (ns; not significant, *; $p$<0.05, **; $p$<0.005, and ***; $p$<0.0005).

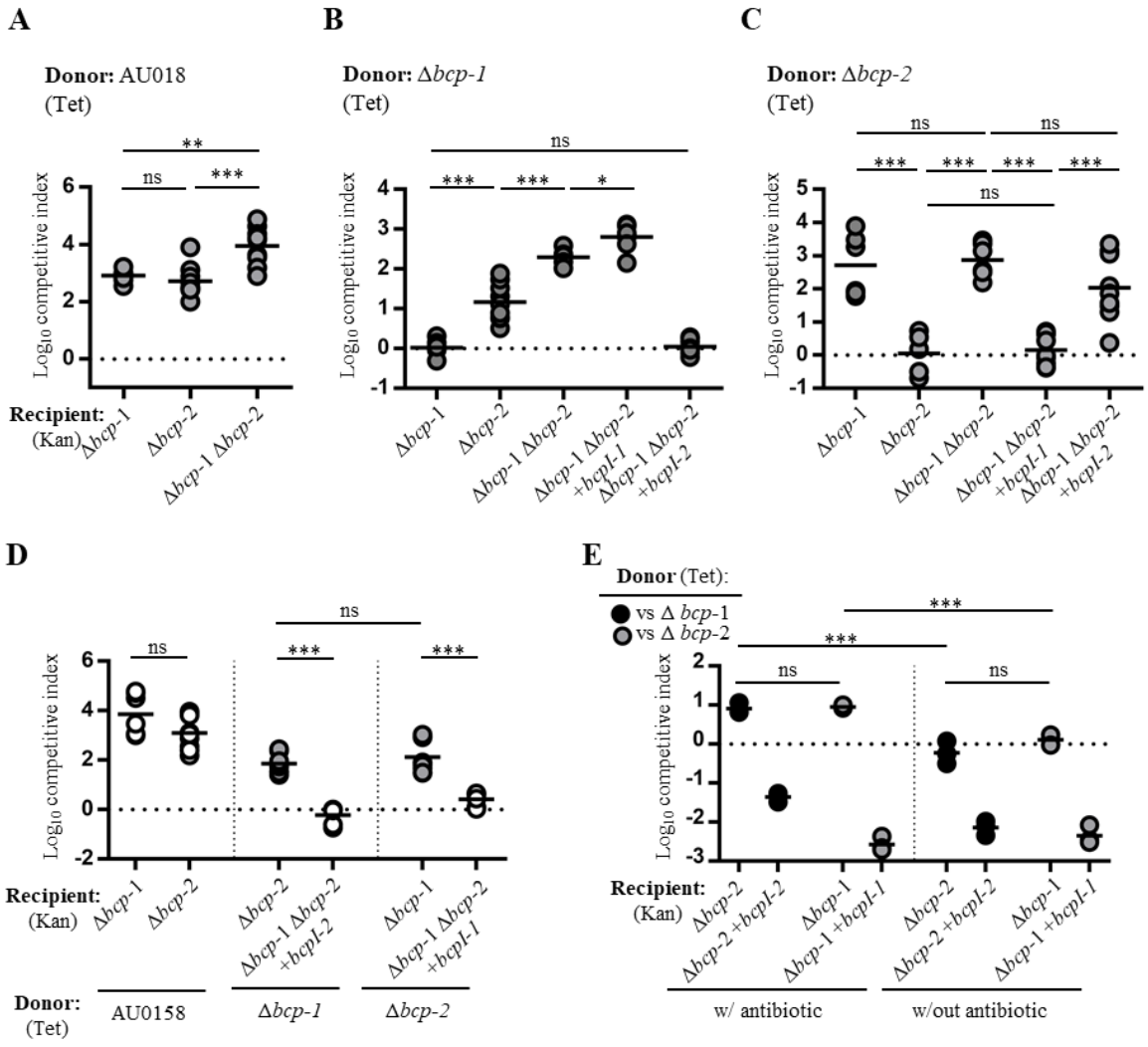


**Figure 3.3.Influence of antibiotic supplemented input cultures on competitive index outcomes.**

**Figure 3.3. Influence of antibiotic supplemented input cultures on competitive index outcomes.**

Interbacterial competition assays between **A)** WT/AU0158, **B)** Δ*bcp-1*, or **C)** Δ*bcp-2* donor bacteria and the indicated recipient bacteria; single locus deletions Δ*bcp-1*, Δ*bcp-2*, and Δ*bcp-1* Δ*bcp*-2. **B, C)** Recipient mutants additionally include Δ*bcp-1* Δ*bcp*-2 expressing either cognate immunity genes, *bcpI-1*, or *bcpI-2*. Symbols represent competitive index values from multiple (2) biological replicate and bars show the mean (*n*=6). **D)** Interbacterial competition assays with each donor; WT/AU0158, Δ*bcp-1*, or Δ*bcp-2* competed against recipient strains. Competitions using all three donor bacteria were carried simultaneously in each biological replicate. Symbols represent competitive index values from multiple (2) biological replicate and bars show the mean (*n*=6). Grey symbols represent the same co-culture with the donor, Tet, and recipient, Kan, strains reversed. **E)** Interbacterial competition assays with each donor; Δ*bcp-1*, or Δ*bcp-2* competed against recipient single CDI-system mutants with cognate immunity, Δ*bcp-1*, Δ*bcp-2*, Δ*bcp-1+bcpI-1*, or Δ*bcp-2+bcpI-2*. Experimental recipient mutants are colored to indicate the donor competed against (Δ*bcp-1* are colored black and Δ*bcp-2* are grey). Symbols represent competitive index values from one biological experiment and bars show the mean (*n*=3). **Left)** input cultures were supplemented with antibiotics, **Right)** input cultures did not have antibiotics**.** Dashed line shows competitive index = 0 (1:1 ratio of donor to recipient). The competitive indices were calculated as described in Figure 1. Input cultures were supplemented with 4µl of 125mg of Kan for recipient strains, and 2µl of 50mg of Tet antibiotics, unless otherwise stated. A one-way ANOVA was used to report significance (ns; not significant, *; $p<0.05$, **; $p<0.005$, and ***; $p<0.0005$).

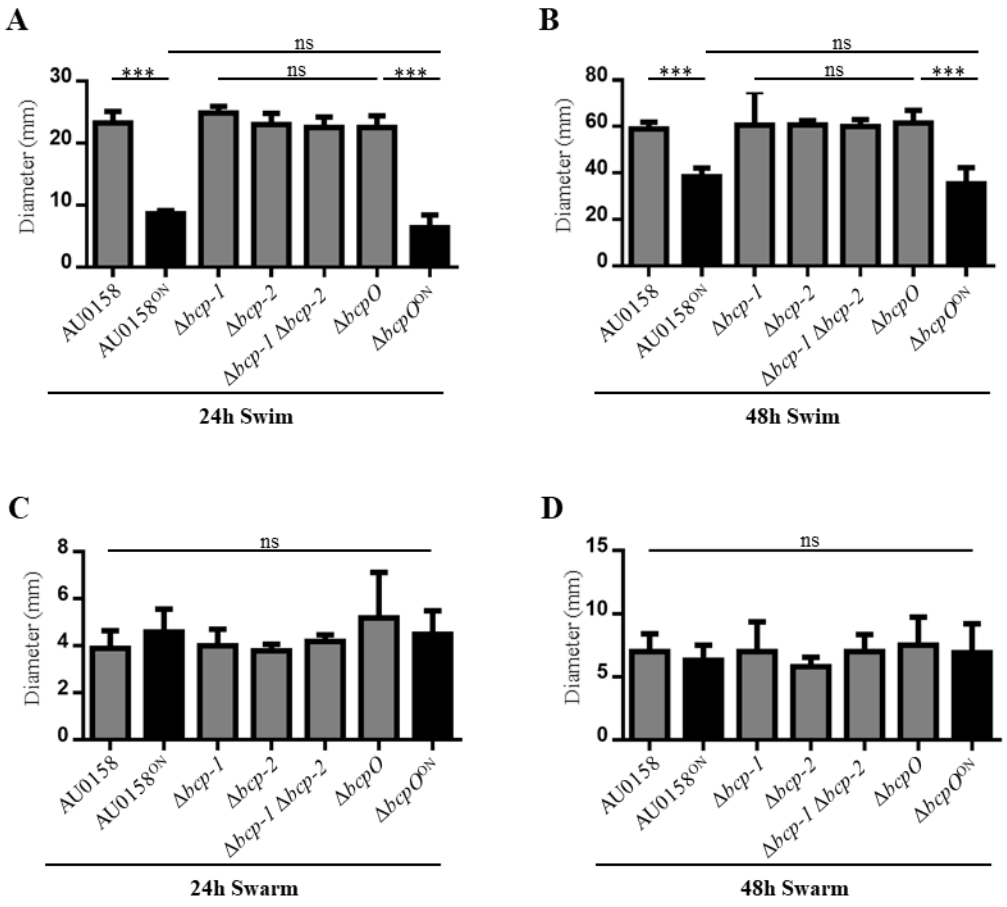


**Figure 3.4.Motility assay for swimming and swarming.**

Swimming motility measured the diameter of bacterial spread after A) 24 hours and, B) 48 hours. Swarming motility measured the diameter of bacterial spread after A) 24 hours and, B) 48 hours. Each strain started from 20µl spot on the center of plate at 0hours. Data is of two biological replicates and bars show the mean ($n$=4). Overexpression via the S12 constitutive promoter of *bcp-1* locus is denoted as 'ON'. A one-way ANOVA was used to report significance (ns; not significant, *; $p$<0.05, **; $p$<0.005, and ***; $p$<0.0005).

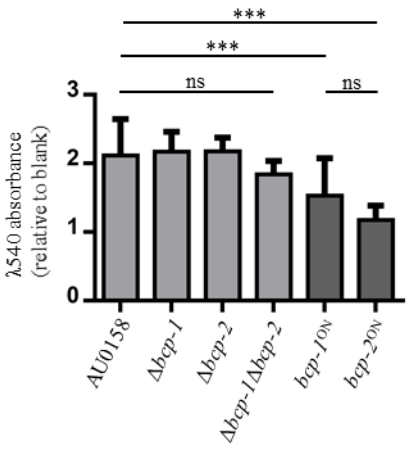


**Figure 3.5. Influence of CDI-systems on *B. dolosa* biofilm formation.**

Crystal violet staining assay of *B. dolosa* for 48 h in TSB+1% glucose supplemented microtiter plates. Graph shows $OD_{540\lambda}$ values of Crystal violet bound cells normalized to the average measurement for the blanks (media alone wells). Data is of two biological replicate and bars show the mean (*n*=8). Overexpression via the S12 constitutive promoter of either *bcp-1* or *bcp-2* locus is denoted as 'ON'. A one-way ANOVA was used to report significance (ns; not significant, *; $p<0.05$, **; $p<0.005$, and ***; $p<0.0005$).

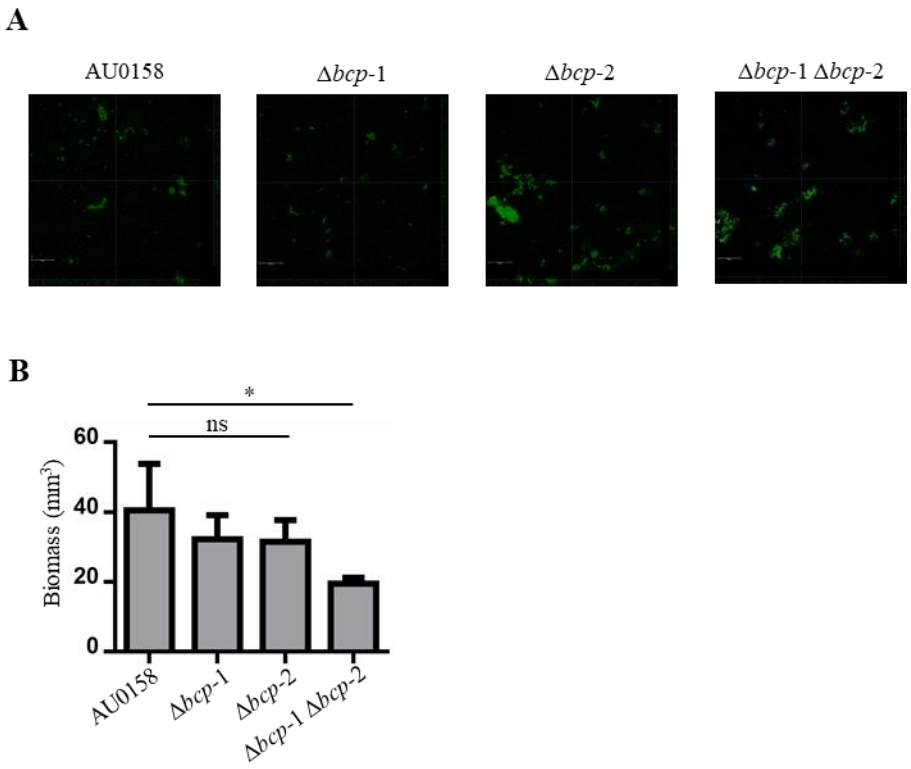


**Figure 3.6. Influence of CDI-systems on *B. dolosa* biofilm architecture.**

**A)** Confocal laser scanning microscopy of biofilm formation in chambered well by *gfp* constitutive expressed *B. dolosa* strains. Bacteria were grown for 48h in TSB+1% glucose cultures grown in three biological replicate and bars show the mean (*n*=2 from 2 experimental replicates). In Z stack renderings cross-sections through the plane parallel to the coverslip (shown by large center image). Scale bars represent 20 μm. Images are representative. **B)** For each of the strains in (A), total biofilm mass was calculates using COMSTAT analysis of Z stacks collected. A one-way ANOVA was used to report significance (ns; not significant, *; $p<0.05$, **; $p<0.005$, and ***; $p<0.0005$).

### 3.4. Discussion

Characterizing the similarities and differences in function of *Burkholderia* spp. CDI systems, particularly their role in bacterial motility and biofilm formation, allows us to identify and understand the influence *Burkholderia* spp. CDI systems. Much is unknown about CDI especially in *Burkholderia*-type systems. Most CDI findings are in *B. thailandensis* E264 or using chimeric C-terminal BcpA/BcpI of other *Burkholderia* species. The studies on characterizing CDI-systems in *Burkholderia* spp. are primarily focused on class I (185, 187, 209).

Like other *Burkholderia* CDI systems, *B. dolosa* cannot perform CDI-associated killing in liquid cultures. This environmental limitation could be due to various means; I speculate that this is caused by the loss of a specific region in *Burkholderia* CDI systems that are present in *E. coli* CDI systems. These results are consistent with the current CdiA translocation model for *E. coli.* In this model, the CdiA protein is separated into functional regions and mutations are made to identify and characterize the function of each. Within the N-terminus of CdiA, there is a predicted outer membrane binding region and following is a region enriched for tyrosine (Y) and proline (P) and named YP region. In the Ruhe 2018 model, the YP region is predicted to stabilize and strengthen the CdiA binding to the outer membrane receptor. When YP region was mutated, cell-to-cell interaction was low in liquid media, however when competition co-cultures were done on LB solid media, mutants were still able to carry out competitions (190). *Burkholderia*-type CDI systems lack the tyrosine-proline rich (YP) region relative to the predicted homologous domains between BcpA and CdiA. I suspect the absence of *E. coli* associated YP region is the reason *Burkholderia*-type CDI system competitions are restricted to solid media. An additional

possibility is that the sequence diversity of *E. coli* and *Burkholderia* result in a different BcpA translocation mechanism from that proposed for *E. coli* CdiA.

Competitions by BcpA-1 and BcpA-2 maintained similar competitive index at 24h and 48h. *B. thailandensis* CDI appear starting at 6h and the competitive index continue to increase through time point until 24h (163). In a published study of *B. dolosa* competitions, co-cultures were incubated at 37°C for 48h. The reasoning for the prolonged incubation was not stated (165). Taken together, these suggest that *B. dolosa* competitions reach a max competitive index and maintain the ratio for at least 48h. Future studies can be performed to determine the rate of which *B.* dolosa CDI phenotypes are observed by harvesting competitions at time points between 0h to 48h and calculating the competitive index. I hypothesize that similar results would be seen as *B. thailandensis* E264 with CDI competition phenotypes starting far earlier than 24h.

Further support for CDI competition phenotypes starting early on is that antibiotics alter the competitive index when Δ*bcp*-1 is competed against Δ*bcp*-2. Competitions with antibiotics were washed and resuspended to an $OD_{600}$ = 2, as standard with competition setups. This setup would eliminate the majority of the antibiotics in the original overnight culture resulting in both donor and recipients at the same initial input ratio at 0h. Bacteria resistant to tetracycline and grown in tet-supplemented overnight cultures outcompeted bacteria resistant to kanamycin and grown in kan-supplemented media. I propose that the antibiotics altered the growth rate, resulting in tetracycline-associated bacteria to start with an initial competition advantage. As the advantage is associated with the overnight culture, I would expect that the bacteria will adapt to the new environment of the antibiotic-free LSLB plate and reach stationary phase of growth by the time competitions are harvested. I

suspect the phenotype of antibiotic-associated advantage cause the recipient (kanamycin) and donor (tetracycline) to reach exponential phase at different rates and the ratio from that early on stage allows for the donor bacteria to be in higher abundance and utilizes CDI to maintain the ratio throughout the competition. Tetracycline resistance is a beneficial in clinical settings, often antibiotic resistance is a tradeoff associated with fitness disadvantage (264)**.** If growth rate is affected by antibiotics, growth curve could be performed, and differential rates measured.

Interestingly, the antibiotics-specific phenotype was most well exemplified when Δ*bcp*-1 is competed against Δ*bcp*-2. Recipient bacteria marked with kanamycin resistance and expressing *bcpI* cognate immunities remained at a 1:1 ratio with the donor bacteria regardless of the presence or absence of antibiotics in the overnight cultures. Similarly, competitions in antibiotics against in which donor is competing against itself also remain at a near 0 competitive index. Taken together these results can indicate that the antibiotic advantage observed is specific to CDI against non-kin bacteria. Tetracycline provided and advantage while kanamycin has minimal effect on bacterial competition outcomes (E. C. Garcia, data not shown).

Future experiments aimed at identifying the benefits of antibiotic cultures on CDI associated competitive index outcomes. Competitions started from antibiotic supplemented cultures and from antibiotic-free cultures are setup at different input ratios. Competitions are harvested and the competitive index is calculated. From our data, the antibiotic advantage in the donor results outcompeting recipient by 1 log. Starting antibiotic advantage donor to recipient at 1:10 ratio, I would expect the result to be a competitive index of 0. If the donor still outcompetes the recipient, could indicate that the antibiotics

are influencing the toxicity of BcpA and not growth rate. If the recipient outcompetes the antibiotic advantage donor, then the benefits are insufficient to alter the benefits of higher input ratio.

In competitions without antibiotics in culture media, Δ*bcp*-1 remained near 1:1 ratio to Δ*bcp*-2. Mathematical modeling proposes in two well-mixed mutually exclusive CDI expressing species, competition will always lead to a singular winner (207). However, these competiotions are not considered 'well mixed'. Additionally, the modeling does state that extinction is also altered by growth-inhibition trade offs and initial conditions. The model also takes into consideration generation of initial bacteria out to $10^4$, thus is more an evolutionary result instead of our snapshot (207). Bcc isolates have a doubling time ranging between 4.4 to 11h per generation (265). Assuming *B. dolosa* has a doubling time on the shorter period, our data would capture results from 5-6 generations during a 24h harvest. Although our data also suggest that ratios do not change significantly between 24h and 48h in *B. dolosa*, that still would encompass 10-12 generations. A caveat is that growth for any of the CDI mutants has not been measured in this study or in previous *B. dolosa* CDI literature. To determine the fittest Bcp, Δ*bcp*-1 and Δ*bcp*-2 competitions would require incubation from 1:1 input for closer to a week. The output could still have coexistence of Δ*bcp*-1 and Δ*bcp*-2 based on the variables including special differentiating and the tradeoff between inhibition strength and metabolic cost (207).

Biofilm formation often is inversely associated with swimming phenotypes. Our data suggests that overexpression of either CDI system inhibits both. The inverse correlation often associated with biofilm formation and swimming is due to swimming being associated with bacteria in planktonic phase and biofilms require bacteria to adhere

to a surface and then develop the biofilm matrix (194, 207–209, 212). As both functions are inhibited, I would hypothesize that the CDI systems are not altering the bacterial phase but instead alter the cell structure. Electron microscopy has been used to image the alterations to the cell surface and visualize CDI-system cell-to-cell interactions (190). I propose that electron microscopy can similarly be used in *B. dolosa* to identify if the cell surface is altered in overexpression of either CDI system. A potential alteration in overexpression of the CDI systems could occur in the production and structure of the lipopolysaccharides (LPS) or in exopolysaccharides. In *B. cenocepacia* isolate from patients, biofilm formation correlated with the amount of exopolysaccharide produced. O-antigen polysaccharide also were shown to contribute to variability in motility, although the motility observed was restricted to swarming (266). Visualization of polysaccharides can be observed with silver staining methods (267) and lipopolysaccharide staining kits following LPS extraction described in Chapter 2.13.

The structure of the *B. dolosa* biofilms are unique in comparison to confocal microscopy of other *Burkholderia* species biofilms (192, 209, 210). Previous research on *B. dolosa* biofilm formation and oxygen-sensing two component systems characterized similar biofilm structures as done in this study (247). *B. dolosa* biofilm formation in our study and characterized in the Schaefers et al., 2017 study observe dome-like structures in biofilms formed by WT bacteria (247). The similar bulbous biofilm structures are consistent in *bcp* deletion mutants and support that CDI systems do not alter biofilm structure in *B. dolosa*. *B. thailandensis* CDI systems can carry out CDI-dependent competition in biofilms. Biofilm formation in *B. thailandensis* is dependent on the functional toxicity of BcpA (209). As deletion of either *bcp*-1 or *bcp*-2 did not alter the

biomass calculated from confocal images, and double deletion for both *bcp*-1 and *bcp*-2 had a small defect in biomass, I can assume that the function of CDI is minimally necessary for *B. dolosa* biofilm formation. Confirming that CDI toxin activity is not required in *B. dolosa* biofilm formation, inactivating the functional C-terminal toxin domain of BcpA-1 and BcpA-2 and imaging biofilms with confocal microscopy will indicate if the biomass is altered in comparison to WT biomass.

*Burkholderia* CDI alters the spatial organization of biofilms in a kin-discriminatory manner. *B. thailandensis* E264 BcpA chimeras of *B. pseudomallei* C-terminal toxins where cocultured with WT *B. thailandensis* at 1:1 ratio and biofilms after 48hr remained at similar ratios. However, the biofilms resulted in independent patches of kin-CDI expressing species, indicating kin discrimination. When I co-cultured WT AU0158 strain with mutants producing a single Bcp system, I expected either similar kin-discrimination phenotype or WT bacteria outcompeting the single mutants. Neither predicted outcome occurred and as WT+*rfp* mutants seemed to remain at a similar ratio to the *gfp* expressing WT strains, and Δ*bcp*-1 or Δ*bcp*-2 mutants (Appendix H). These results could indicate that CDI is not functional in *B. dolosa* biofilms. An additional reason could be that protection against one of the BcpA toxins is sufficient for both WT bacterial CDI protection and for the mutant to be considered kin. Biofilm co-culture experiments should be further repeated and additional mixtures included. Co-culturing WT bacteria with Δ*bcp*-1Δ*bcp*-2 mutants would indicate if CDI occurs in *B. dolosa* biofilms. If CDI is functional in *B. dolosa* biofilms, I would expect to see more WT bacteria than Δ*bcp*-1Δ*bcp*-2. However, if *B. dolosa* CDI systems are not functional for competition but still play a role in kin-discrimination, I would expect to see patches of WT cells separate from Δ*bcp*-1Δ*bcp*-2 mutants. Our

competition on low salt LB indicate that neither BcpA-1 or BcpA-2 is sufficient to outcompete one another without an initial advantage. I would expect that ratios would remain similar in biofilms as observed after competition. As our data indicate that there is no significant difference in the biofilm formation associated with locus-1 or locus-2. If competitions remain with similar phenotypes in biofilms, I can also identify kin discrimination in *B. dolosa.* If kin-discrimination is occurring via CDI-system regulation, I would expect to see patchwork biofilms of Δ*bcp*-1 separate from the biofilms formed by Δ*bcp*-2.

In this chapter, I identified that *B. dolosa* BcpA-1 is associated with a stronger CDI dependent killing. However, the increased toxicity of Bcp-1 was insufficient to outcompete Bcp-2 mutants. Competition outcomes between BcpA-1 and BcpA-2 could be altered with antibiotic-advantage associated with growing donors in tetracycline prior to coculturing inputs for competitions. I determined that AU0158 cannot perform CDI-dependent killing in liquid cultures as predicted using the *E. coli* proposed function of the YP region that is absent in *Burkholderia* BcpA sequence. The competitive index for *B. dolosa* competitions is not affected by incubating competitions between 24 to 48h indicating that CDI results occur prior to 24h and remain consistent over long periods of time. Finally, I determined that CDI systems have a small effect on biofilm formation only seen in Δ*bcp*-1Δ*bcp*-2although overexpression of either CDI encoding locus inhibits swimming motility and biofilm formation, phenotypes that are often inversely related.

# Chapter 4: Functional BcpA requires the pre-toxin region.

## 4.1. Summary

BcpA proteins amongst the identified *Burkholderia* CDI systems follow similar domain architecture. In the BcpA protein is an uncharacterized domain upstream of the C-terminal toxin with the conserved sequence motif (Nx(E/Q)LYN) referred to as the pre-toxin region. The pre-toxin region, aside from the variable C-terminal toxin, has high variability between subclasses of *Burkholderia* spp. BcpA proteins within the same subclasses have well conserved pre-toxin region amino acid sequences. Following the same proposed model for *E. coli* CdiA translocation, in *Burkholderia* CDI, the pre-toxin region and the FHA-2 domain is associated with C-terminal toxin processing once inside the recipient cell. Our data indicated that deletion of the pre-toxin region is lethal in *B. thailandensis* E264, although the deletion is tolerated in the highly similar BcpA-1 produced in *B. dolosa* AU0158. Deletion of the pre-toxin region and subsequential smaller deletion mutants cannot carry out BcpA-1 mediated CDI. The inhibition of CDI is suspected to be due to the alteration in BcpA translocation as the protein is still made in the donor cell. Using αBcpA C-terminal toxin (αBcpA-CT), banding patterns of BcpA and pre-toxin region mutants can be compared. Multiple differences are observed in the BcpA-1 banding patterns between WT bacteria and the pre-toxin subdomain mutants. Although further identification and interpretation of the unique bands could not be done at this time, future experiments will be aimed at tracking BcpA in the donor cell and translocation into the recipient cells.

## 4.2. Introduction

The translocation of CdiA/BcpA is proposed to be a multi-step process that is dependent on domains of the toxin protein and required components produced by the recipient cells (190, 268). Although CdiA/BcpA proteins are heterogeneous, with size and sequence variability between genus and species, CdiA/BcpA proteins share the same general domain architecture (189).

CdiA/BcpA proteins are structurally broken into two large parts: the N-terminus and the C-terminus. The C-terminus refers to the catalytic toxin domain and is distinguished by succeeding the conserved sequence motif: Nx(E/Q)LYN in *Burkholderia*-type and VENN in *E. coli*-type (189). The conserved sequence motifs establish what is considered the N-terminus, upstream of the motif, and the C-terminus, downstream of the motif relative to the conserved sequence.

The BcpA N-terminus starts with two transport domains, the first is a signal sequence that directs BcpA to the Sec complex for secretion into the donor cell periplasm. Following the Sec-signal sequence is the conserved two-partner secretion (TPS) domain for toxin export across the outer membrane via the beta-barrel protein, CdiB/BcpB (Figure 4.1AB). The majority of the N-terminus is comprised of FHA-1 hemagglutinin repeat motifs. FHA was identified in *Bordetella* species as filamentous hemagglutinin (FHA) and associated with bacterial adhesion (269). The structure of FHA motifs is characterized by β-helices that can elongate during forced extension (270, 271). CdiA/BcpA includes an additional FHA-2 domain near the end of the N-terminus whose structure-function is unknown. Separating the two FHA-1 domains in CdiA is the predicted outer membrane receptor (OMR) binding region (OMR-BR) (Figure 4.1A). The OMR-BR has variability

between CdiA homologs, and the variability is associated with discerning receptor specificity. In *E. coli* three OMR have been identified and correlate to the three OMR-BR, BamA, OmpC/OmpF, and Tsx (197–199). The predicted OMR-BR in *Burkholderia* BcpA proteins have high variability, indicating OMRs may vary between different CDI-systems. Following the FHA-2 domain is an uncharacterized pre-toxin region. In *Burkholderia* species, the pre-toxin region contains variability between the class I and class II. However, pre-toxin regions are relatively conserved across CDI-systems within the same subclass (Figure 4.1A) (185, 187). The variability in toxin sequences and function are described extensively in Chapter 1.3. In brief the C-terminal toxins differ significantly from CDI system to system even within a single strain. C-terminal toxins typically function as nucleases, although there has been one identified CdiA associated with pore formation in recipient cells. Allele specific immunity proteins are produced to prevent self-inhibition and distinguish kin from non-kin bacteria (181, 185, 187).

In both *E. coli* and *Burkholderia*, CdiA/BcpA have been shown to be modular, i.e. the C-terminal toxin, with the associated cognate immunity, function independently and are interchangeable (183, 184, 187, 192). However, within *Burkholderia*, the modularity of BcpA C-termini is restricted to specific groups. Functioning chimeric BcpA proteins were restricted to within the same subclass, either class I or class II. Cross-class chimeric strains could not carry out CDI. The majority of the N-terminus, up to the LYN conserved sequence, are highly similar (192). As the pre-toxin domain similarities are also restricted to subclasses, we hypothesize that the pre-toxin region plays a role in the modular restrictions of BcpA C-terminal toxins.

The original proposed mechanism for CdiA/BcpA translocation was modeled as a "toxin-on-a-stick", referring to the filamentous N-terminus extending beyond the cell surface, exposing the C-terminal toxin extracellularly (272). The current model proposed by Ruhe et al., 2018, characterizes that the CdiA C-terminal toxin remains in the donor cell periplasm, while the filamentous regions expose the OMR binding region extracellularly. Upon binding to the OMR, FHA β-helices extend and trigger transfer of the toxin to the recipient cell. Once in the cell, the C-terminus is thought to be cleaved and transported into the cytoplasm using the recipient cell inner membrane receptor (IMR) (Figure 4.1B) (190).

The role of CdiA/BcpA pre-toxin region remains ambiguous, although the predicted location suggests it could play a role in release of the toxin from the donor cell during transport into the recipient bacteria. The current model predicts that the pre-toxin region remains in the periplasm with the FHA-2 and C-terminal toxin until transported into the recipient cell (Figure 4.1B). In *E. coli* CdiA, mutations in the FHA-2 domain and pre-toxin region inhibited the toxin delivery, but did not alter OMR triggered export. Additional data suggests that the pre-toxin region and the C-terminal toxin domain are both transferred into the recipient cell (190).

The proposed CdiA translocation mechanism was created using *E. coli* as the model system. Although many of the domains and architectural regions remain similar between CdiA and BcpA, the systems themselves have been shown to be unique in their function and mechanism (183, 185, 187). The pre-toxin region in *Burkholderia*-type class I contain high similarity, and thus likely use the domain in a similar mechanism. I hypothesize that the pre-toxin is involved in regulating BcpA release or processing. This study created pre-

toxin region mutants in AU0158 *Bd*-BcpA-1 to determine the function of the pre-toxin region.

## 4.3. Results

### 4.3.1. Deletion of the pre-toxin region is toxic in *B. thailandensis.*

To understand the function of the pre-toxin region in *Burkholderia* species, *B. thailandensis* E264 was used as it has the most well-defined CDI system. Initial experiments attempted to delete 300aa that began within the FHA-2 and spanned up to the conserved sequence motif, Nx(E/Q)LYN of BcpA. In-frame chromosomal deletions are made by creating plasmids that include 500bp upstream of the intended deletion sequence and fused with 500bp downstream of the area of interest. The plasmid is then reversibly integrated into the chromosome via homologous recombination. Using counter selection to induce allelic loop-outs, PCR screens were used to identify colonies with the desired region deleted. Frequency of incorporation of the deletion allele vs wild-type (WT) allele is 50:50.

This method of creating chromosomal deletions was attempted in WT E264. After screening 111 colonies from separate integration mutants, none were found to have lost the intended 300aa pre-toxin region, resulting in loop-outs reverting back to WT allele (Table 5.1). To determine if the deletion of the domain is only lethal if the protein is trafficked to the donor periplasm, the same 300aa deletion was then attempted in a *Bt*-BcpA mutant that did not contain the Sec-signal sequence, *Bt-bcpA*ΔSecSS. The Sec-signal sequence in *Burkholderia* BcpA is associated with trafficking the unfolded BcpA into the periplasm of the donor cell prior to toxin translocation. Screening colonies from one integration of the homology plasmid, 2 of the 3 had the deletion of the pre-toxin region (Table 4.1). These

results indicate that deletion of the BcpA pre-toxin region is lethal in *B. thailandensis* if trafficked to the donor periplasm. However, production of E264-BcpA in the *Bt-bcpA*ΔSecSS or *Bt-bcpA*ΔSecSSΔ300aa mutants was not confirmed.

### 4.3.2. Antibodies against E264 BcpA C-terminal toxin cross react with the C-terminal toxin of AU0158.

*B. thailandensis* BcpA E264 has 83.3% identity with the BcpA-1 of *B. dolosa* AU0158. The identity is similar enough that E264 BcpI has been shown to protect against BcpA-1 of AU0158 in CDI competitions (188). Although the BcpA toxins for each species are similar in sequence, would polyclonal antibodies raised against the E264 C-terminal toxin (αBcpA-CT) cross-react with AU0158 *Bd*-BcpA-1? Using whole cell lysate and Western blot techniques, αBcpA-CT antibodies were confirmed to be cross-reactive against *Bd*-BcpA C-terminal toxin (Figure 4.2 and Figure 4.3B). E264 with *Bt-bcpA* under a constitutive promoter, *Bt-bcpA* under its native promoter and in AU0158 with *Bd-bcp*-1 under a constitutive promoter, all three lanes have a band running above 250kD. The expected weight of BcpA in E264 is 314.6kD and for AU0158 is 374.96kD. Additionally, there are no bands observed in the *Bt*-Δ*bcp* lane. Furthermore, *Bt*-BcpA bands have higher intensity under the constitutive promoter, *Bt-bcp*$^{ON}$, compared to *Bt-bcp* under the native promoter (WT). Similar intensity in BcpA bands were seen with the AU0158 under the same constitutive promoter, *Bd-bcp-1*$^{ON}$ and the E264 *Bt-bcpA*$^{ON}$ (Figure 4.2).

### 4.3.3. Deletion of the pre-toxin region is not lethal in *B. dolosa* BcpA-1.

Due to the similarity, the truncation of the pre-toxin region in AU0158 *Bd*-BcpA would hypothetically be lethal as was seen in the WT *Bt*-BcpA (Figure 4.3A). Using the same method for in-frame chromosomal deletions, 2 of 5 colonies in AU0158 had 500aa deletion incompasing the pre-toxin subdomain region deleted in *Bd*-bcpA-1 (Table 1). These results suggest that the pre-toxin deletion alters the mutant's toxicity differently in donor *Burkholderia*. As the size of the deletion are different for *B. thialandensis* and *B. dolosa*, 500aa and 300aa respectivly, this could be associated with the difference in survival of the mutants. Another possibility is that the periplasmic trafficking within a donor cell is different between *B. dolosa* BcpA-1 and *B. thailandensis* BcpA. The lethality of the deletion could be due to *B. thailandensis* E264 being more sensitive to periplasmic stress.

### 4.3.4. Deletion of the pre-toxin region inhibits CDI but not BcpA production.

To test that the tolerance of the 500aa region deletion (*Bd*-BcpAΔsubdomain1) (Figure 4.3A) was not due to lack of protein production, the presence of the truncated *Bd*-BcpA protein was confirmed via Western blot assays. Using whole cell lysate and antibodies against the *Bt*-BcpA C-terminus, a band was observed for *Bd*-Bcp-1 at about 200kD and for the *Bd*-BcpAΔsubdomain1 just below 150kD. Although the expected molecular weight of *Bd*-BcpA-1 is predicted to be 374.96kD and *Bd*-BcpAΔsubdomain1 at 318.13kD, the size difference of 57kD does correlate with the distance between the bands on the blot. Further support that the bands are *Bd*-BcpA is that no band near that size is seen in the negative control lysate from *Bd*-Δ*bcp*-1 (Figure 4.3B).

*Burkholderia* have been shown to express *bcpAIOB* loci differently throughout the growth phase, with higher expression during stationary phase. CDI can only be carried out

on solid media (185, 187, 192). To compare the expression of BcpA from bacteria grown and collected in different environments, liquid cultures and from plates, bacteria for both environments were collected and brought to the same $OD_{600}$ before cell lysis and loading the wells. There was a faint band in the *Bd*-BcpA well from the liquid cultures at the 200kD, same size as *Bd*-BcpA grown on solid media. However, the intensity of the bands is significantly higher when bacteria were collected from plates instead of cultures. There was no band observed in the *Bd*-BcpAΔsubdomain1 liquid culture lane. These results indicate that there is a higher production of BcpA-1 when bacteria are grown on solid media compared to liquid cultures (Figure 4.3B). These results are intriguing as in both cases wild-type *Bd-bcp-1* locus and the locus containing the *Bd-bcpA*Δsubdomain-1 loci were under a constitutive promoter, although transcription and translation do not always correlate.

The 500aa deletion, *bcpA*Δsubdomain-1, removes both the pre-toxin region and a portion of the FHA-2 domain. Comparing our results to the *E. coli* model indicate that the FHA-2 and pre-toxin region are both required for translocation into the recipient cell but not in donor cell trafficking (190). To specifically understand the function of the pre-toxin region, three sequential deletions were attempted. *Bd-bcpA*Δsubdomain-2 deletion spans only the 100aa pre-toxin domain, *Bd-bcpA*Δsubdomain-3 deletion spans the first half of the pre-toxin region and *Bd-bcpA*Δsubdomain-4 deletion spans the latter half (Figure 4.3A). The plasmid required for homologous recombination to delete *Bd-bcpA*Δsubdomain-4 could not be constructed thus this mutant was not made.

Next the pre-toxin subdomain deletion mutants were tested for CDI function through bacterial competition assays. The *Bd*-BcpA subdomain deletion mutants and WT

BcpA producing bacteria were competed against susceptible *Bd*-Δ*bcp*-1. As described in previous chapters, bacterial competitions are conducted in triplicate with initial input ratios of 1:1 donor/recipient. Competitions are harvested, and the competitive index is calculated by differentiating donor and recipient CFUs via antibiotic resistance. In competitions WT BcpA outcompetes *Bd*-Δ*bcp*-1 by an average of 1. 75 logs. Deletion of any of the pre-toxin subdomains result in the competitive index remaining near zero, indicating that the domain deletion mutants are incapable of carrying out CDI using BcpA-1 (Figure 4.3C). The subdomain deletions were made in WT AU0158 background. As the interplay between the two CDI systems produced by *B. dolosa* are not fully understood, the function for *Bd*-Bcp-2 CDI system was tested. *B. dolosa,* competitions were setup with the subdomain donors competed against *Bd*-Δ*bcp*-1Δ*bcpA*-2 mutants. The *Bd*-Δ*bcp*-1Δ*bcpA*-2 mutants are susceptible to both intoxication by *Bd*-BcpA-1 and *Bd*-BcpA-2. There was no significant difference in the competitive index of any of the donor strains containing the subdomain deletions from WT Bcpa-2 producing bacteria (Figure 4.3D). This indicates that BcpA-2 remains functionable even though BcpA-1 is not.

### 4.3.5. There are differential banding patterns associated with BcpA pre-toxin subdomain deletions compared to wild-type BcpA.

The banding patterns of BcpA were compared between the subdomain mutants and WT BcpA as to suggest where in the BcpA translocation process the pre-toxin region mutants disrupt. Using Western blot assays, whole cell lysate was collected from each strain and blotted against BcpA C-terminus. As CDI for both E264 and AU0158 cannot occur in liquid media, those lanes were used as controls for BcpA translocation, all other

strains were grown on solid media. The caveat is BcpA bands in this assay cannot be distinguished between BcpA in donor cells from that of recipient. The whole cell lysate was probed for the BcpA C-terminus (Figure 4.4A). Using ImageJ software, each lane was analyzed, and banding patterns were plotted with X-axis referring to the length of the gel and Y-axis referring to intensity of the bands (Figure 4.4B).

In all wells with lysate from BcpA producing bacteria, a band >250kD was observed (Figure 4.4A, B- lane 1-4). That top band is consistent with full length BcpA, respective to each BcpA truncation mutants. Furthermore, the top band in the well for *Bd*-ΔSubdomain-1 was shifted down, which would be consistent with the deletion of 500aa *Bd*-BcpA (Figure 4.4A, B- lane 4&6). As observed in figure 4.3, the intensity of BcpA is stronger in the lanes that the bacteria were collected from plates instead of liquid cultures (Figure 4.4A, B- lane 1-4). Using lane 5, *Bd*-Δ*bcp*-1, as a BcpA-1 negative control, three bands were identified and consistently seen in all loaded wells, indicating that these are cross reactive bands. As these bands are not associated with BcpA, they can be used as internal loading control (Figure 4.4A, B).

The banding pattern analysis of the BcpAΔsubdomain-1 (blue), BcpAΔsubdomain-2 (orange), and BcpAΔsubdomain-3 (green) mutants were overlayed on WT *bd*-BcpA analysis (Black). Compared to WT *Bd*-BcpA, all of the subdomain mutants had loss of a band at ~37kD and ~75kD. Additionally, WT *Bd*-BcpA has a band at 100kD which seems to be shifted to 90kD in the subdomain mutants (Figure 4.4A,C). Additional replicates experimental Western blots using the same protocol can be found in Appendix D Taken together the only definitive statement from these data is that the banding patterns associated

with BcpA differ from E264 BcpA and AU0158 BcpA-1, as well as AU0158 BcpA-1 bands differ from the subdomain mutants.

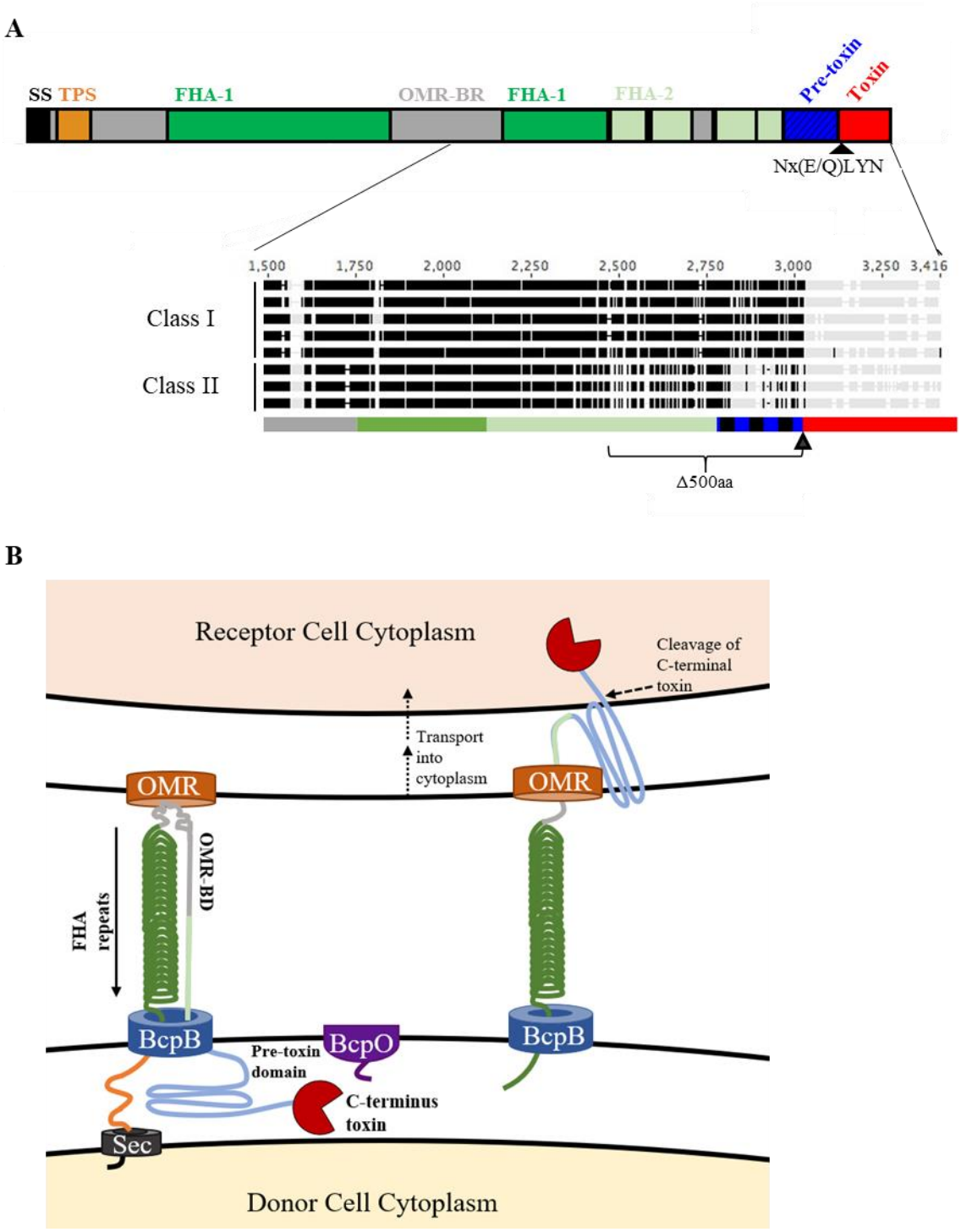


**Figure 4.1.Model for BcpA topology and toxin translocation.**

**Figure 4.1. Model for BcpA topology and toxin translocation.**

**(A)** The architecture of *Burkholderia* spp. BcpA protein. SS (black) refers to Sec-signal sequence. TPS (orange) refers to two-partner secretion signal. FHA-1 and 2 (green) refer to filamentous domains. Pre-Toxin (blue) refers to uncharacterized region before the C-terminal toxin. Toxin (red) refers to the catalytic C-terminal variable toxin. **(B)** Model of BcpA surface topology. Receptor recognition triggers translocation of the C-terminal half of BcpA. Once transferred into the target-cell periplasm, the BcpA C-terminal toxin is cleaved and trafficked to the recipient cell cytoplasm.

Figure adapted from Ruhe, Z. C. et al., 2018 (190).

**Table 4.1. Deletion of the pre-toxin region is lethal in E264 wild-type *bcpA*.**

In-frame chromosomal deletions efficiency of homologous recombination loop out of deletions containing the BcpA pre-toxin region.

| ***Burkholderia* strain** | **Δpre-toxin region BcpA colonies / total colonies** | |
|---|---|---|
| Loop out expectancy | 50% | |
| *B. thailandensis* (E264) | 0/111 colonies | 0% |
| *B. thailandensis* (E264) ΔSec-signal sequence | 2/3 colonies | 66.7% |
| *B. dolosa* (AU0158) | 2/5 colonies | 40% |

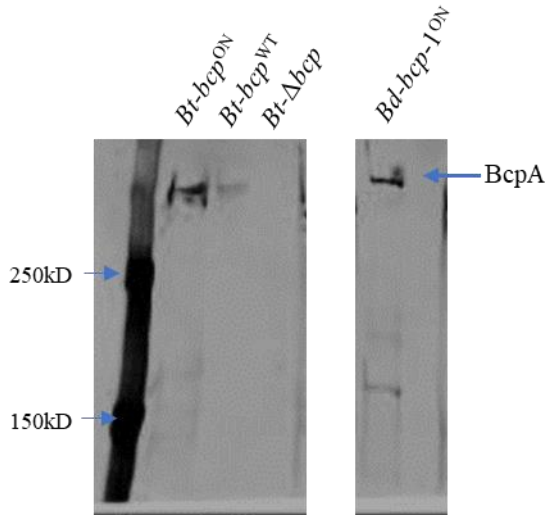


**Figure 4.2. E264 αBcpA C-terminus antibody is cross reactive with AU0158 BcpA-1.**

Western blot of whole cell lysate of *B. thailandensis* E264 and *B. dolosa* AU0158. Constitutively (ON) expressing E264 *bcpAIOB* (*Bt-bcp*$^{ON}$) and AUO *bcpAIOB* locus 1 (*Bd-bcp-1*$^{ON}$). E264 expressing the *bcpAIOB* locus under the naive promoter is denoted as *Bt-bcp*$^{WT}$, and deletion of the E264 *bcpAIOB* locus is denoted as *Bt*-Δ*bcp*. Prior to cell lysis, cultures were standardized to the same $OD_{600}$. Membrane probed with αBcpA C-terminal primary antibodies and fluorescent αRabbit secondary antibodies.

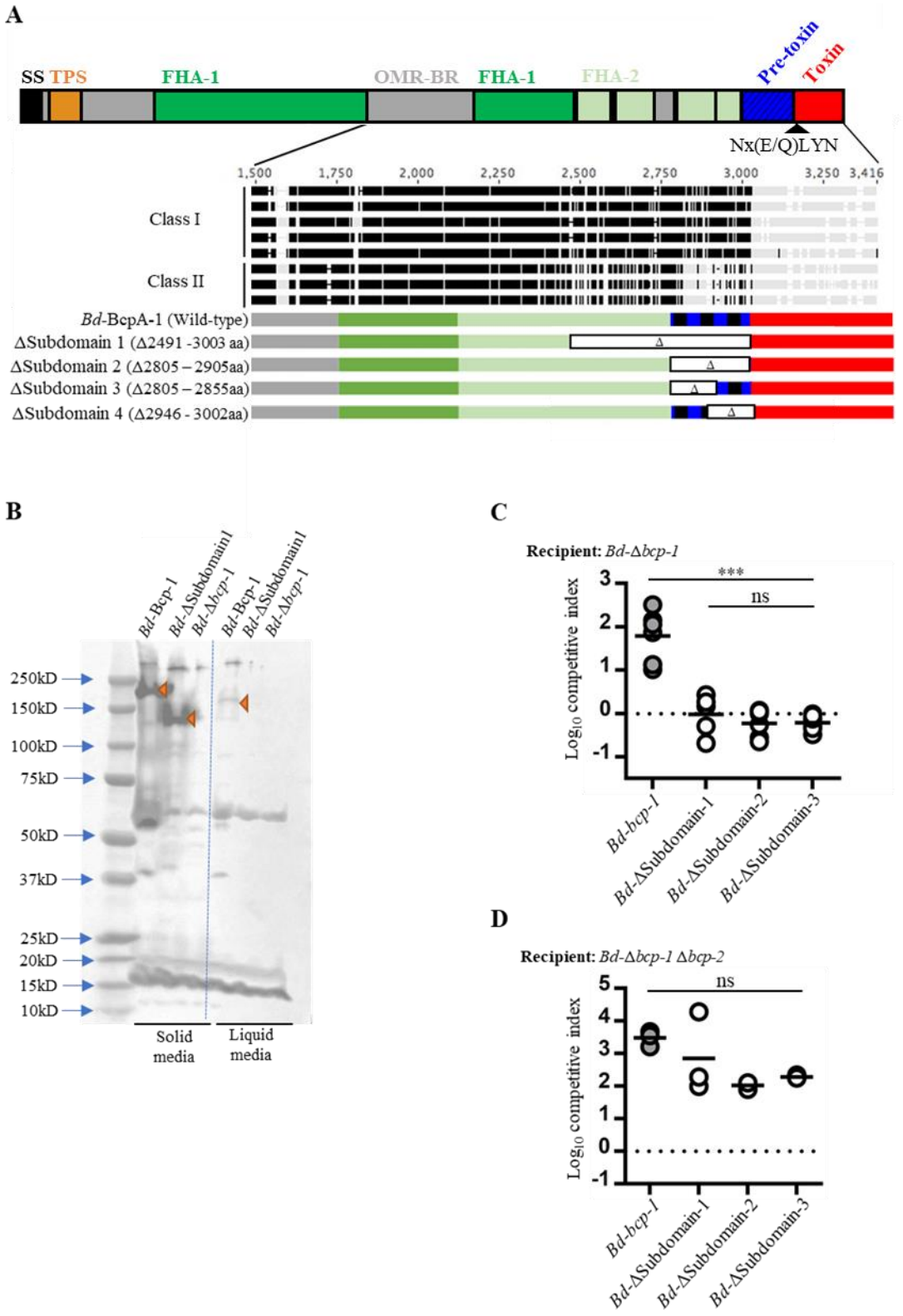


**Figure 4.3. Deletion of pre-toxin subdomains inhibit BcpA-1 intoxication but are translated.**

**Figure 4.3. Deletion of pre-toxin subdomains inhibit BcpA-1 intoxication but are translated.**

**(A)** The location of the subdomain deletions within *Burkholderia dolosa* BcpA protein. The 3 subdomain deletions within the Pre-toxin region (blue) refers to in frame deletions within the uncharacterized domain before the C-terminal toxin. Toxin (red) refers to the catalytic C-terminal variable toxin. **(B)** Western blot of whole cell lysate of *B. dolosa* (AU0158) strains, all mutants were constitutively expressing *Bd-bcpAIOB* locus 1 with wild-type BcpA-1, the BcpAsubdomain-1 domain deletion, or deletion of the locus *bcpAIOB*-1. Prior to cell lysis, cultures were standardized to the same $OD_{600}$. Membrane probed with α*Bt*-BcpA C-terminal (αBcpA-CT) primary antibodies and fluorescent αRabbit secondary antibodies. Orange triangles indicate full length BcpA bands. **(C)** CDI mediated competition assay of AU0158 strains. *Bd*-Δ*bcp*-1 (recipient) co-cultured at 1:1 ratio with either wild-type *Bd-bcp-1* or the subdomain deletions mutants. **(D)** CDI mediated competition assay of AU0158 strains. *Bd*-Δ*bcp*-1Δ*bcp*-2 (recipient) co-cultured at 1:1 ratio with either wild-type *Bd-bcp-1* or the subdomain deletion mutants.

(*, P<0.01; **, P<0.001; ***, P<0.0001; ns, not significant).

**A)** Adapted from Ruhe, Z. C. et al., 2018 (190).

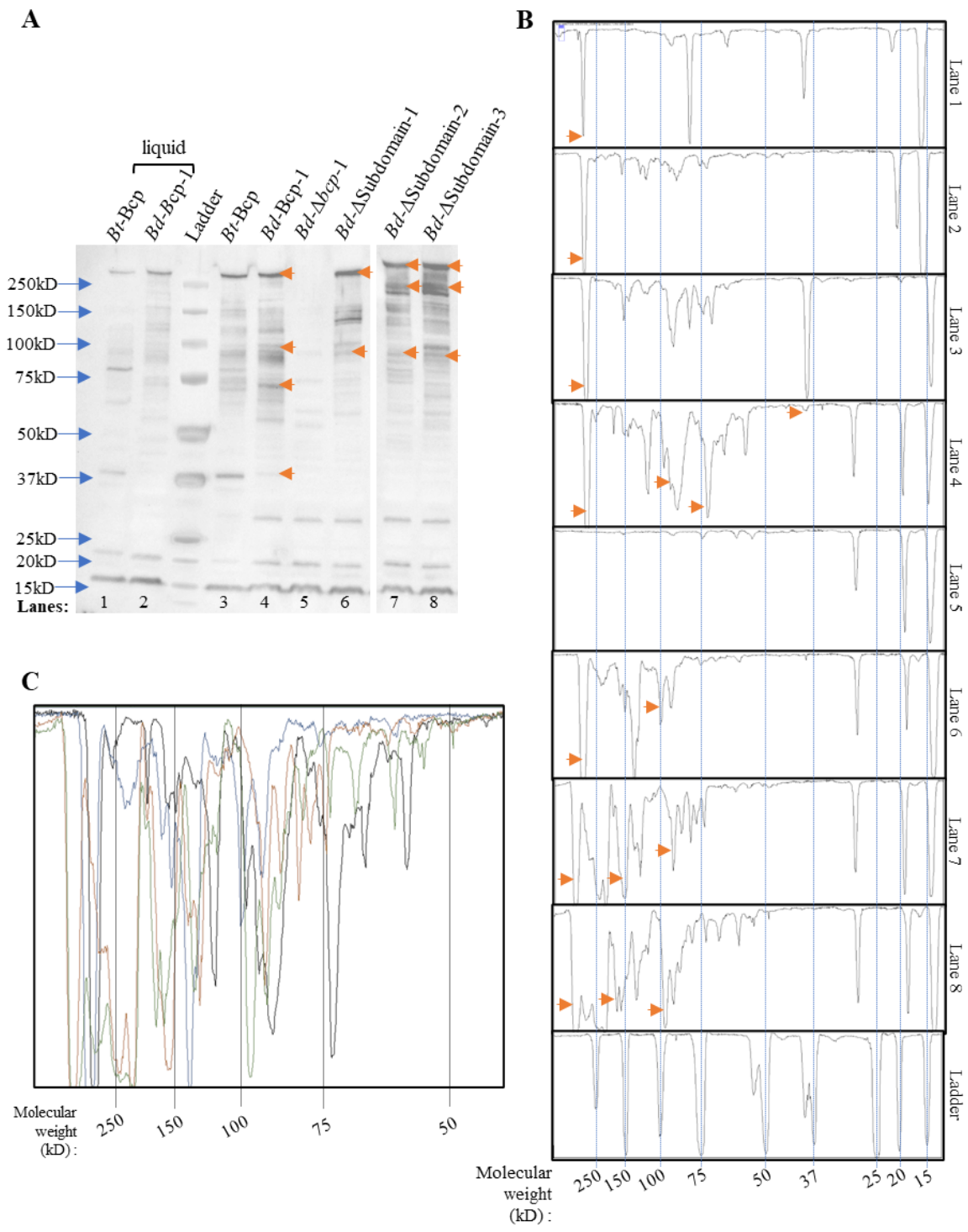


**Figure 4.4. Banding patterns between pre-toxin region deletions mutants vary from wild-type BcpA-1.**

**Figure 4.4: Banding patterns between pre-toxin region deletions mutants vary from wild-type BcpA-1.**

**(A)** Western blot of whole cell lysate of *B. thailandensis* (E264) and *B. dolosa* (AU0158) constitutively expressing E264 *Bt-bcpAIOB* or AU0158 *Bd-bcpAIOB*-1 locus. Whole cell lysis were collected from either liquid cultures, left, or harvested from plates, right. Constitutive expression of the AU0158 *Bd*-BcpA subdomain-1, subdomain-2, and subdomain-3 deletions were harvested from plates. The deletion of the locus *Bd-bcp*-1 was used as the negative antibody control. Prior to cell lysis, cultures were standardized to the same $OD_{600}$. Membrane probed with αBcpA C-terminal primary antibodies and fluorescent αRabbit secondary antibodies. **(B)** ImageJ software gel lane analysis of each lane and plotted the banding patterns with X-axis referring to the length of the gel and Y-axis referring to intensity of the bands. **(C)** Overlay of the ImageJ band plots of wild-type AU0158 BcpA-1 (black), BcpA subdomain-1 (blue), subdomain-2 (orange), subdomain-3 (green).

### 4.4. Discussion

Deletion of the pre-toxin region in *B. dolosa* that encompasses part of the FHA-2 domain, and smaller deletion mutants of the pre-toxin domain all result in AU0158 BcpA-1 inability to carrying out CDI-associated competition. The *E. coli* CdiA trafficking model suggests that both the FHA-2 and the pre-toxin region pass through the donor cell membranes into the recipient cell outer membrane and are hypothesized to specifically aid in transport of the C-terminal toxin into the cytoplasm.

Our data show that the deletion of the pre-toxin region in AU0158 does not inhibit production of BcpA-1 but remains incapable of CDI. These results are consistent with our understanding of CdiA/BcpA translocation. At this time, I cannot determine where in the trafficking process loss of the pre-toxin region obstructs carryout CDI.

The requirements for BcpA translocation, assuming the C-terminal toxin activity is dependent on localization to the cytoplasm of the recipient cell, are that the protein must 1.) be produced, 2) trafficked into the periplasm of the donor cell, 3) pass through the outer membrane of the donor cell, 4) cross through the inner membrane of the recipient cell, and 5) be exported into the cytoplasm from the recipient cell periplasm. Where in the trafficking process the pre-toxin region impedes functional CDI cannot be determined. The lethality of the pre-toxin region in E264 suggests there to be a function in the donor.

The differential banding patterns I observe in AU0158 BcpA-1 compared to the multiple pre-toxin region mutants can be the result of altered trafficking, both in the donor and to the recipient cell, or degradation and instability of the BcpA protein. I hypothesize that there is a mixture of both. The different banding results cannot be

distinguished as to where in the BcpA trafficking process the BcpA fragments correlate to.

Currently, the membrane receptors in the recipient cells required for BcpA translocation remain unknown in *Burkholderia* species. Thus, determining donor from recipient from whole cell lysate cannot be done. If the OMR of the recipient cells were identified and deletion mutants created, the BcpA banding patterns in ΔOMR mutants could only come from either BcpA degradation or donor cell BcpA processing. Banding patterns specific to the donor could indicate if loss of the pre-toxin region plays a role in BcpA stability or donor cell trafficking.

Support that the current Western blot may be capturing both BcpA in the donor in addition to the recipient is that there are AU0158 specific bands at about 37kD and 75kD only found in WT *Bd*-Bcp collected from solid media (Figure 4.4). These bands, based on size, are predicted to correspond to the catalytic toxin (37kD) and the pre-toxin variable region through the toxin domain (75kD). The band at 37kD of the catalytic toxin is hypothesized to be cleaved during BcpA translocation into the cytoplasm of the recipient cell. The band at 75kD encompassing the pre-toxin region and toxin domain is hypothesized to be the intermediate cleavage in the recipient cell periplasm prior to final translocation into cytoplasm. Future studies will be aimed at identifying the sequence of the 37kD and 75kD bands through mass spectrometry to confirm our hypothesis. If the sequence does confirm that 37kD is the catalytic C-terminal toxin and the 75kD band is the pre-toxin and toxin, then it further supports that the pre-toxin region plays a role in C-terminal toxin cleavage required for CDI.

Both the WT BcpA of E264 and AU0158 under constitutive promoters were compared to bacteria collected from solid or liquid cultures (Figure 4.3A& Figure 4.4A). As the promoters for all the over expression mutants are the same, the differences in BcpA production between the two environments are surprising. These results could indicate that the constitutive promoter is altered when bacteria are grown in different environments, although the nutrients remain consistent, or that the BcpA protein is being degraded or unstable in bacteria growing in liquid cultures compared to solid media. To determine if the constitutive promoter expression is altered in liquid compared to solid media, *lacZ* mutants of BcpA can be made for use in a β-galactosidase activity assay to measure *lacZ* expression. LacZ production can then be compared from the bacteria collected from liquid cultures to that collected from solid cultures, both of which *bcpA-lacZ* was under the same constitutive promoter. These results would support that the constitutive promoter is altered under the different types of bacterial growth environments. If the production of LacZ remains similar under the constitutive promoter in bacteria from solid and liquid, then the difference in BcpA production observed in the Western blots may be associated with BcpA protein being degraded or unstable in bacteria growing in liquid cultures compared to solid media.

Staying under the assumption that *E. coli* model of CdiA trafficking is similar to the trafficking of BcpA in *Burkholderia*, I hypothesize that in addition to export of the C-terminal toxin into the cytoplasm of the recipient cell, the pre-toxin region plays an additional role in trafficking within the donor cell.

# Chapter 5: Transposon mutagenesis used to identify genes associated with CDI susceptibility.

## 5.1. Summary

To identify genes associated with CDI susceptibility in *B. dolosa* recipient cells, transposon mutagenesis selection approaches were used to enrich for CDI-resistant mutants. Loss of the quorum sensing pathway receptor, CepR, resulted in protection against both BcpA-1 and BcpA-2 associated CDI. Transposon insertions in regulatory and metabolic genes conferred resistance to both BcpA-1 and BcpA-2 toxins. However, deletion of the same identified genes provided only partial protection from BcpA-1 alone. Using whole genome sequencing, additional mutations were identified in the transposon mutants. Mutations identified were in the same locus encoding for proteins used in lipopolysaccharide production and structure regulation. Disruptions in the LPS regulation genes are sufficient for full protection from both CDI systems produced in *B. dolosa* AU0158. These findings provide insight into the complexity of CDI sensitivity.

## 5.2. Introduction

Toxicity from BcpA is dependent on a variety of susceptibility factors required in the recipient cell. The current model for translocation of the CDI toxin, using *E. coli* CDI system proteins, involves the toxin interacting with specific outer membrane receptors on the recipient cell surface (197, 268). Further translocation of the C-terminal toxin into the cytoplasm requires periplasmic associated receptors (191, 197, 198, 201). Data from *E. coli* show that membrane receptors can vary from strain to strain leading to specificity in

which bacteria are susceptible to each individual toxin. CDI toxins use of these receptors does not always require function of said proteins (197).

Less is known about *Burkholderia* susceptibility factors and translocation of BcpA. Recent studies show the recipient cells for *B. multivorans*, CGD2M, requires *gltJK* in CDI sensitivity (203). *Burkholderia pseudomallei* 1026b chimeric BcpA is shown to require specific LPS structures for BcpA translocation as well as proteins encoded by *B. thailandensis* genes: BTH_10359, BTH_110599, and BTH_10986. The identified genes are specific to susceptibility to 1026b C-terminus and CDI via *B. thailandensis* E264 was not altered (202). Similarly, to *E. coli* factors, sensitivity to CDI protein intoxication differ significantly between closely related species. In addition to membrane specific proteins, some *E. coli* CDI systems can require specific cytoplasmic proteins for susceptibility in recipient cells. Examples of which include *O*-acetylserine sulfhydrylase A (CysK), Elongation Factor Thermo-Unstable (EF-Tu), and the Elongation Factor Thermo-Stable (EF-Ts), each associated with tRNase activity of the CDI toxin. The necessity for the intracellular factors varies amongst *E.coli* strains (205, 206, 273). There has yet, to our knowledge, been cytoplasmic factors identified for *Burkholderia* CDI systems.

Previous studies indicate that recipient cell CDI sensitivity factors differ between species and toxin variants. To identify genes associated with CDI susceptibility in *B. dolosa* recipient cells, transposon mutagenesis selection was used to enrich for CDI-resistant mutants to either BcpA-1 or BcpA-2. Transposon insertions in regulatory and metabolic genes conferred with resistance to both BcpA-1 and BcpA-2 toxins. Deletion of the candidate genes showed that deletion of *hisD*, *cspD*, or *cepR* provided partial, but significant protection from either BcpA-1 or BcpA-2 intoxication. Additional mutations

were identified by whole genome sequencing. Mutations identified were in gene predicted to encode for proteins associated with LPS biosynthesis. Disruptions to LPS resulted in resistance to both B. *dolosa* CDI systems. Overall, our findings provide insight into the complexity of CDI sensitivity and suggest that alterations to recipient cell metabolism and regulatory networks may nonspecifically impact CDI in *Burkholderia* spp..

## 5.3. Results

### 5.3.1. Selection of *Burkholderia dolosa* mutants resistant to CDI system-1 or CDI system-2.

*B. dolosa* strain AU0158 encodes three distinct CDI systems, two of which mediate CDI under conditions of native gene expression in the laboratory (188). To understand the mechanism of *Burkholderia* CDI system toxin import, we sought to identify recipient cell factors necessary for susceptibility to the two active *B. dolosa* CDI systems. *B. dolosa* mutants lacking both CDI system-1 and CDI system-2 (Δ*bcp-1* Δ*bcp-2*) were subjected to random mutagenesis using a miniTn5-based transposon. Isolated transposon mutants were pooled and competed against *B. dolosa* donor cells that contained either CDI system-1 (Δ*bcp-2*) or CDI system-2 (Δ*bcp-1*) (Figure 5.1A,B). Output recipient CFUs were pooled and re-competed against the appropriate donor bacteria. CDI-resistant transposon mutants were enriched through three rounds of competitions, at which point the competitive indices of each transposon mutant pool were either not significantly different (Figure 5.1A), or more resistant than recipients expressing cognate *bcpI* (Figure 5.1B). Individual CDI-resistant colonies ($n$=16) were randomly selected from the pool of resistant mutants and individually competed against the appropriate donor bacteria (Figure 5.1C,D). All

competed colonies had an average $\log_{10}$ competitive index of $\leq 0.4$, indicating that they were not outcompeted by the CDI+ donor strain.

Transposon insertion sites were identified from nine resistant clones using nested arbitrary PCR and sequencing across the transposon-chromosome junction. Only one unique transposon insertion site was identified, in gene BDAG_00967, from individual colonies collected from the mutant pool resistant to CDI system-2 (Table 5.1). Surprisingly, a mutant with an identical transposon insertion in BDAG_00967 (likely clones) was also isolated from the CDI system-1 resistant pool. Transposon disruptions in three additional genes, BDAG_02644 (*cspD*), BDAG_02714 (*hisD*), and BDAG_03544 (*cepR*), were also identified from the pool of CFUs resistant to CDI system-1 (Table 5.1). For all of the identified mutants, the Tn5 disruptions occur close to the 5' end. Disruptions early in the gene typically will cause domains to be impacted creating a nonfunctional gene (Figure 5.2). Two of the Tn5 disrupted genes, BDAG_02644 (*cspD*) and BDAG_03544 (*cepR*), are predicted to be isolated within their own locus and would not likely disrupt any other genes (Figure 5.2 A,B). BDAG_02714 (*hisD*) and BDAG_00967 are in loci that contain additional downstream genes (Figure 5.2 C,D). Potentially, the CDI resistance observed in competition may not be due to the gene disrupted for *hisD* or BDAG_00967, but instead due to a polar effect on the other genes in the locus.

Transposon mutants were selected for resistance against only one *B. dolosa* CDI system, but the recovery of BDAG_00967::miniTn5 from both selection pools indicated that this mutant was resistant to both CDI system-1 and CDI system-2. To determine whether the remaining mutants were specifically or generally resistant to *B. dolosa* CDI systems, individual mutants were competed against both Δ*bcp-1* and Δ*bcp-2* mutant donor

bacteria. Mutants Tn2-2 and Tn2-3 (*hisD*:miniTn5) and Tn2-7 (*cspD*:miniTn5) were not outcompeted by either donor type, suggesting that the resistance conferred by these disruptions generally protects from CDI and is not specific to a particular BcpA variant (Figure 5.3). By contrast, mutant Tn2-8 (*cepR*:miniTn5) was outcompeted by Δ*bcp-1* donor bacteria that deploy CDI system-2, although not to the same degree as the Δ*bcp-1* Δ*bcp-2* parent strain, suggesting that the mutation in Tn2-8 confers greater resistance against CDI system-1.

### 5.3.2. Deletion of candidate genes does not alter *B. dolosa* growth.

To determine the roles of the four candidate genes identified from the transposon selection, chromosomal deletions were made by allelic exchange in the parental Δ*bcp-1* Δ*bcp-2* mutant lacking both CDI system-1 and CDI system-2. Interbacterial competition assay used to measure CDI assumes that donor and recipient bacteria have similar growth rates. Confirmation that competition phenotypes for the Tn5 identified gene deletion mutants are due to CDI and not alterations to the growth rate, growth curves for each chromosomal deletion mutant were plotted by growing in low-salt LB duplicate cultures and measuring optical density at λ600 (OD600) at various time points, taken ~ every 90m, until 24 h. There was no significant difference between liquid growth for any of the Tn5 associated deletion mutants (Δ*cepR,* Δ*cspD,* Δ*hisD,* Δ*00967)* compared to the parental Δ*bcp-1* Δ*bcp-2* mutant (Figure 5.4).

### 5.3.3. Quorum sensing regulator CepR influences CDI efficiency.

Transposon mutagenesis screening identified Tn2-8 with disruption in *cepR* (Table 5.1). The gene, *cepR,* encodes for the cytoplasmic receptor, CepR. The quorum system CepI/CepR, synthesizes and responds to the autoinducer *N*-octanoyl L-homoserine lactone ($C_8$-AHL) via the CepI synthase and CepR receptor, respectively. Quorum sensing is a global gene regulator in Bcc members and has been demonstrated to control virulence in various eukaryotic models (39, 40, 229, 274). One of the CepR/CepI system homologs in *B. thailandensis* activates the expression of the *bcpAIOB* CDI operon, although it is unknow if the regulation is direct (195). There is still much unknown about the role of quorum sensing in regard to CDI systems.

Initial competition of Tn 2-8 (*cepR*::miniTn5) were resistant against Δ*bcp-1* and had comparably less resistance to Δ*bcp-2* donors (Figure 5.3). To determine the role CepR plays in differential CDI system susceptibility, competitions were performed using the *cepR* deletion mutant made in the parental Δ*bcp*-1 Δ*bcp*-2 background (Δ*cepR*). Initial competitions against both Δ*bcp*-1 or Δ*bcp*-2 donors had large variability in Δ*cepR* competitive index outcomes between experimental replicates (data not shown).

Variability in the previous *cepR* mutant competitions were due to initial input cultures at differential points within stationary growth phase. Co-culture competitions in which recipient input bacteria were started with cultures from mid-log phase (6 h), early stationary (11 h), and late stationary (24 h) against donors from overnight cultures (17 h). At 6 h, all donor cells were resistant against CDI from system-1 and system-2. The recipient mutant, Δ*cepR,* at 11 h was as resistant as the complemented immunity strain, Δ*bcp*-1 Δ*bcp*-2 +*bcpI*-1 or Δ*bcp*-1 Δ*bcp*-2+*bcpI*-2. In both cases the parental strain, Δ*bcp*-1 Δ*bcp*-2, was out-competed by both BcpA-1 and BcpA-2 producing donor cells. However, 24 h

the recipient Δ*cepR* mutant did not significant difference in sensitivity from the Δ*bcp*-1 Δ*bcp*-2 parent, with both mutants being out competed by BcpA-1 by ~ 2.5 logs and BcpA-2 by ~3 logs (Figure 5.5). Altering the growth phase for recipient cells compared to the donor cells influenced the outcome of competition significantly allowing the cells from earlier growth phases to have advantage over the 'older' competing cells.

Limiting the external variability of differential stationary phase growth of recipient to donor bacteria, all cultures were inoculated and grown for 24h. The outcomes of the bacterial competitions observed Δ*cepR* mutants had significantly more protections against both BcpA-1 and BcpA-2 CDI compared to the parental strain (Figure 5.6 A,B). Competitive indices of Δ*cepR*, on average, were 0.6 logs and 0.7 logs more resistant against CDI from system-1 and system-2 than Δ*bcp*-1 Δ*bcp*-2. Complementing with the *cepR* expressing plasmid, sensitivity was restored (Figure 5.6 AB).To compare the compounding competitive effect of CDI from both systems, Δ*cepR* mutants were then competed against wild-type bacteria. The Δ*cepR* mutant was more resistant against wild-type CDI than the parental Δ*bcp*-1 Δ*bcp*-2 with a difference of 1.25 logs in the competitive indices (Figure 5.6C).

In the growth curve assay (Figure 5.4), there was no defect for any of the chromosomal deletion mutants. However, growth in liquid culture is a different environment than that of competitions on solid media. In a mock competition in which Δ*bcp*-1 Δ*bcp*-2 was the 'donor', Δ*cepR* outcompeted the parental strain by 0.55 logs. As neither the donor nor recipient cells are capable of CDI, these results indicate that there is a minor growth advantage to in the Δ*cepR* mutant. The competitive index was restored to near 0 when Δ*cepR* was complemented, Δ*cepR*+*cepR* (Figure 5.6 D).

Taken together, loss of the quorum sensing receptor, CepR, in recipient cells protects moderately against BcpA-1 and BcpA-2 intoxication both individually and in combination. However, as the loss of CepR resulted in a growth advantage during the mock competitions, the extent to which CepR plays in CDI is more difficult to tease apart.

### 5.3.4. Genes *cspD* and *hisD* have a minor contribution to recipient cell CDI susceptibility.

The gene *cspD* encodes for a cold shock-like protein, CspD, which is predicted to bind to DNA. Homologs of *cspD* in *E. coli* inhibit DNA replication and are induced by nutritional-limitation stress (275, 276). To identify the extent to which CspD plays in CDI-sensitivity in recipient cells, the in-frame triple deletion mutant, Δ*bcp*-1 Δ*bcp*-2 Δ*cspD* (Δ*cspD*), was competed against both Δ*bcp-1* and Δ*bcp-2*. The outcomes of the bacterial competitions showed no significant differences in Δ*cspD* mutant sensitivity to the parental strain when competed against Δ*bcp*-1 (Figure 5.7 A). Differential results were observed when the triple deletion mutant Δ*cspD* was competed against Δ*bcp*-2 having partial protection compared to the parent. Comparing the competitive indices of Δ*cspD* and Δ*bcp*-1 Δ*bcp*-2 there was a mean difference of 0.7 logs (Figure 5.7 B). Although the Δ*cspD* mutant did have partial protection against Δ*bcp-2*, resistance against either CDI donor did not mimic that of the *cspD*::miniTn5 transposon mutant (Tn2-7) which had resistance comparable with the cognate immunity mutants (+*bcpI-1* or +*bcpI-2*) (Figure 5.3). Overexpression of CspD has been shown to be toxic in other bacteria and, similarly, we were unable to complement our mutants with cspD, either under the S12 constitutive

promotor or the native promoter (data not shown). These results taken together support that CspD does play a partial role in sensitivity to BcpA-1.

Transposon mutagenesis identified HisD as a potential candidate for CDI susceptibility. Gene *hisD* encodes a histidinol dehydrogenase that catalyzes the last two steps of L-histidine biosynthesis (277, 278). As other components of the biosynthesis pathway may be altered due to *hisD* gene's location in the locus (Figure 5.2), histidine auxotrophy was tested. Neither the *hisD*::miniTn5 transposon mutant (Tn2-3) nor a Δ*hisD* mutant could grow in minimal medium. Growth was restored by supplementation with exogenous histidine or complementation the Δ*hisD* mutant with constitutive *hisD* at an attTn7 site (Figure 5.8). These results indicate that supplementing cultures with L-histidine is sufficient to restore the growth of the auxotrophic mutants in minimal media.

HisD in CDI sensitivity was identified by competing the deletion mutant, Δ*hisD*, against Δ*bcp-1* and Δ*bcp-2* donors. Susceptibility of Δ*hisD* mutant followed similar trends as Δ*cspD* with the competitive index differing between BcpA-1 and BcpA-2 donors. Sensitivity to Δ*bcp-1* was not altered between the parental Δ*bcp-1* Δ*bcp-2* and the *hisD* deletion mutant (Δ*hisD*), having an average competitive index of 2.7 and 2.6logs (Figure 5.7 C). Deletion of *hisD* did result in partial protection against Δ*bcp-2*. The average competitive index of Δ*hisD* was 0.7logs more resistant that the parental Δ*bcp-1* Δ*bcp-2* (Figure 5.7 D). In competitions against either Δ*bcp-1* and Δ*bcp-2* donors, over expression of *hisD* resulted in significantly more sensitivity compared to the parent strain regardless of expression in the parent of the triple deletion mutant Δ*hisD* (Figure 5.7 C,D).

The loss of production of either CspD or HisD results in partial protection against CDI system-1 and remains fully susceptible to CDI system-2. In all co-culture

competitions, the deletion mutants Δ*cspD* and Δ*hisD* do not mimic the protection observed in their prospective transposon mutants (Tn2-7 and Tn2-3, respectively).

### 5.3.5. Intracellular membrane associated proteins encoded by BDAG_00967 and BDAG_00966 do not alter CDI susceptibility.

The regulatory gene, BDAG_00967, encodes a dGTP triphosphohydrolase protein predicted to be localized to the cytoplasmic membrane and contains GGDEF/EAL domains. Orthologs of BDAG_00967 and other GGDEF/EAL domain containing proteins are associated with regulating biofilm formation, motility, and other stress-associated phenotypes (279). BDAG_00967 is predicted to encode for a cytoplasmic membrane bound dGTP triphosphohydrolase. The predicted membrane bound protein could be a candidate for the inner membrane receptor (IMR) required in BcpA translocation. To investigate the function BDAG_00967 plays in *B. dolosa* CDI susceptibility, a deletion mutant for BDAG_00967 (Δ*00967*) was constructed in the Δ*bcp-1* Δ*bcp-2* parental background strain. As done with the other CDI susceptibility candidates, Δ*00967* was competed against both Δ*bcp-1* and Δ*bcp-2* donors. Experimental replicates were pooled, and no significant difference were observed between Δ*00967,* and the CDI-sensitive Δ*bcp*-1 Δ*bcp*-2 parent strain regardless of the donor (Figure 5.9 A,B). Overexpression of BDAG_00967 under the constitutive promoter (+00967) mutants have increased sensitivity to the Δ*bcp*-1 Δ*bcp*-2 parental strain in competitions against CDI system-2 (Δ*bcp*-1) (Figure 5.9A). Altering expression of BDAG_00967 had no significant effect of the competitive index in Δ*bcp-2* co- cultures (Figure 5.9B). The marginal influence of

BDAG_00967 expression on CDI susceptibility to either BcpA-1 or BcpA-2 indicates that it is unlikely to encode for the IMR protein used as a BcpA translocation factor.

BDAG_00967 is located 196bp 3' upstream of another gene encoding a cytoplasmic bound protein, BDAG_00966. Homologs of BDAG_00966, *chrA*, encode for a chromate efflux pump used to remove toxic chromium from the bacterium (280, 281). Due to the limitations of transposon mutagenesis resulting in polar effects in downstream genes, we complemented the Tn5 insertion mutant for BDAG_00967, Tn1-2, with BDAG_00967 (+00967), BDAG_00966 (+00966), or both genes, BDAG_00967-00966 (+00967-66), all of which are under the S12 constitutive promoter. Bacterial competitions were co-cultured at 1:1 ratio of donor to recipients as described above. However, calculating the competitive index was done by subtracting the single antibiotic-resistance marked donor CFUs from the recipient CFUs marked with both kanamycin (BDAG_00967:miniTn5) and tetracycline (complementary plasmids) resistance. Complementation of any combination of BDAG_00967 and BDAG_00966 did not alter resistance to (BDAG_00967:miniTn5 (Tn1-2) during competitions against CDI system-2 (Figure 5.9 C).

However, complementation of BDAG_00967 and BDAG_00967-66 in Tn1-2 did restore partial sensitivity to BcpA-1 intoxication with an average difference in the competitive index being 1.2 logs and 1.6 logs, respectively, compared to the parental Tn1-2 mutant (Figure 5.9 D). Tn5+00966 did not restore sensitivity to the tn5 mutant against either Δ*bcp-1* or Δ*bcp-2* (Figure 5.9 C,D). Due to the variability in the extent to which BDAG_00967 alters CDI susceptibility, we further confirmed a role of BDAG_00966 in CDI. Deletion of BDAG_00966 was constructed in the Δ*bcp*-1 Δ*bcp*-2 parental strain

(Δ*00966*). Deletion of BDAG_00966 did not provide any protection against intoxication by either BcpA-1 or BcpA-2 (Figure 5.9 E,F). These data support that BDAG_00967 has a small effect in CDI susceptibility, and similarly to *cspD* and *hisD*, do not correlate with the resistance observed in the corresponding transposon mutants.

Although the role that BDAG_00967 plays in CDI is minimal, other GGDEF/EAL domain containing proteins alter biofilm formation (279). To determine if BDAG_00967 similarly regulates biofilm formation in *B. dolosa*, static biofilms for the BDAG_00967 mutants were grown. Growth of bacteria in microtiter plates wells followed by staining of attached cells with crystal violet serves as a common method for quantifying biofilm formation. Measuring the absorbance of the crystal violet-stained attached cells, found all mutants were inhibited in biofilm formation compared to wild-type. Additionally, deletion of BDAG_00967 in the Δ*bcp*-1 Δ*bcp*-2 parent strain had increased absorbance compared to the parent. Complementing the triple deletion mutant, Δ*00967*, returned to absorbance levels comparable to the Δ*bcp*-1 Δ*bcp*-2 parent (Figure 5.10 A).

Crystal violet staining only gives a crude means of measuring biofilm formation, and does not show the influence of BDAG_00967 may have on the unique biofilm architecture characteristics of *B. dolosa* AU0158 (247). Using confocal microscopy and *gfp*-expressing mutants, biofilms were imaged, and Z-stacks compiled from wild-type bacteria, Δ*bcp*-1 Δ*bcp*-2, and Δ*00967*. Biofilms from wild-type and Δ*bcp*-1 Δ*bcp*-2 cultures were consistent with the structures specific to *B. dolosa* AU0158 (247). However, the architecture of the BDAG_00967 biofilm was drastically different (Figure 5.10 B). The biomass for each biofilm was calculated from the Z-stacks using COMSTAT biofilm analysis software. The biomass calculated for BDAG_00967 was over 3x that of wild-type

and almost 7x more than Δ*bcp-1* Δ*bcp-2* (Figure 5.10 C). One of the limitations in the confocal imaging experiment was not having the complemented BDAG_00967 strain to find if the *B. dolosa* architecture would be restored. Altogether, although BDAG_00967 does not seem to alter CDI significantly, it does regulate the formation and architecture of *B. dolosa* biofilms.

### 5.3.6. Whole Genome Sequencing identified additional unique mutations in the chromosomes of resistant transposon mutants.

Whole genome sequencing (WGS) was performed on isolates of singular clonal transposon mutants Tn1-2 (BDAG_00967:miniTn5), Tn2-2 (*hisD*:miniTn5), Tn2-7 (*cspD*:miniTn5), and Tn2-8 (*cepR*:miniTn5) and compared against parental Δ*bcp*-1 Δ*bcp*-2 to find unique genetic mutations. The parameter used to identify unique mutations required >25 reads with a frequency of 85% and mutation occur in genes with Genebank accession numbers found in the reported AU0158 sequenced genome. Each transposon mutant had at least one unique mutation in the genome (Table 5.2). Full list of genomic mutations parental mutations and inclusion of mutations in the transposon mutants are included in appendix E. A single unique mutation in Tn2-8 (*cepR*:miniTn5) identified an amino acid change in the Major Facilitator Superfamily (MFS) sugar transporter encoding gene, BDAG_0462. Unlike the other identified CDI resistant mutants, Tn2-8 and Δ*cepR* were consistent with CDI resistant phenotypes with one another, we do not predict that the mutation alters CDI sensitivity. Two sequenced transposons, Tn1-2 (BDAG_00967:miniTn5) and Tn2-7 (*cspD*:miniTn5) had different unique mutations, both of which were in BDAG_01006. A downstream gene BDAG_01005 had a unique repeat

contraction in Tn2-2 (*hisD*:miniTn5). These chromosomal mutations indicate that the locus containing BDAG_01005 and BDAG_01006 could potentially be the reason the resistance to CDI differ between transposon mutants and the corresponding gene deletions mutants. BDAG_01006 and BDAG_01005 both are associated in regulating lipopolysaccharide production and structure. Tn2-7 (*cspD*:miniTn5) had an additional amino acid mutation in BDAG_00967 (Table 5.2). Mutations in both BDAG_00967 and the BDAG_01006-01005 locus may have a compounding effect resulting in the CDI resistance of the Tn2-7 transposon mutant.

### 5.3.7. Alteration in LPS regulation locus correlates with resistance to CDI indiscriminately.

The three transposon mutants in which the deletion of the miniTn5 disrupted genes did not correlate with similar resistance to CDI to either BcpA-1 or BcpA-2 in the corresponding deletion mutants, supports that the unique mutations identified in the WGS are driving the CDI resistance phenotype in the transposon mutants. BDAG_01005 and BDAG_01006 are located in a locus that includes a *wabO* homolog (Figure 5.11 A). WabO in AU0158 is predicted as a glycosyl transferase. In *B. cenocepacia*, WabO was found to play a role in LPS biosynthesis (282). Similarly, BDAG_01006 is also predicted to encode for glycosyl transferase Although *wabO* and BDAG_01006 both encode for glycosyl transferase proteins, the amino acid sequencing is distinct from one another with 16% identity. BDAG_01005 is predicted as an O-antigen ligase. Together this locus is predicted to be critical in LPS structure and biosynthesis. For each strain, the LPS was isolated and denatured to specifically stain for LPS after running samples through 10%-20% Tricine

gel. The structure of LPS between Wildtype, parental Δ*bcp*-1 Δ*bcp*-2, and Tn2-8 (*cepR*:miniTn5) are consistent with two bands both in size and intensity within the core and lipid A region, with long and intense expression of banding patterns in the O-antigen region (Figure 5.11 B). Transposon mutants with additional unique mutations in either BDAG_01005 or BDAG_01006 had significantly different LPS banding patterns. Tn2-2 (*hisD*:miniTn5) was identified to have a mutation in BDAG_01005. The LPS banding patterns in the Tn2-2 mutant were unique with a single band in the core-lipid A region and a single band in the O-antigen region. Both Tn1-2 (00967:miniTn5) and Tn2-7 (*cspD*:miniTn5) share similar banding patterns in the core-lipid A region, and O-antigen. The similar LPS banding patterns for both Tn1-2 and Tn2-7 suggest that both BDAG_01006 and BDAG_00967 mutants alter LPS (Figure 5.11 C).

Disruption mutants of BDAG_01005 and BDAG_01006 were created to test the role the genes play in both LPS structure and CDI sensitivity. Due to the organization of the locus, disruption mutant of BDAG_01006 (::pD01006) might also disrupt the downstream gene BDAG_01005 (Figure 5.11 A). The LPS structure was consistent between wild-type, Δ*bcp*-1 Δ*bcp*-2, and the Δ00967 mutants. These results support that BDAG_00967 does not alter the LPS. Disruption in BDAG_01005 reproduces the LSP changes identified in Tn 2-2 (*hisD*::miniTn5) as anticipated. Disruption in BDAG_01006, regardless of the background, either Δ*bcp*-1 Δ*bcp*-2 or Δ00967, had similar LPS banding patterns (Figure 5.11 D). Disruptions in BDAG_01005 and BDAG_01006 both result in unique LPS banding patterns compared to both Δ*bcp*-1 Δ*bcp*-2 and wild-type bacteria.

To determine the role of these genes in recipient cell sensitivity, disruption mutants were competed against wild-type bacteria expressing both CDI system encoding loci. As

all of the transposon mutants were resistant to both BcpA-1 and BcpA-2, using wild-type donors will indicate if BDAG_01005 or BDAG_01006 mutations confer resistance generally against CDI systems. The CDI resistance of BDAG_01005 disruption mutant (::pD01005) was equivalent to mutants expressing both of the cognate immunities(*+bcpI-1 +bcpI-2*). Disruption in BDAG_01006 (::pD01006) was slightly more sensitive to wild-type intoxication that the immunity control, but still remained significantly more resistant compared to the parental Δ*bcp*-1 Δ*bcp*-2. However, the BDAG_01006 disruption mutant was slightly more sensitive to wild-type CDI system intoxication than the immune recipient. When the BDAG_01006 mutant was disrupted in the mutant also lacking BDAG_00967, the mutant was significantly more resistant than the BDAG_01006 disruption alone (Figure 5.11F). These results might indicate that mutations in both BDAG_00967 and BDAG_01006 have a compounding influence on recipient cell sensitivity. Taken all together, these results indicate that BDAG_01005 and BDAG_01006 plays a role in LPS biosynthesis and structure in addition to CDI sensitivity. However, it is unknown if the CDI sensitivity associated with BDAG_01005 and BDAG_01006 is specific as wild-type bacteria produces CDI system-1 and system-2.

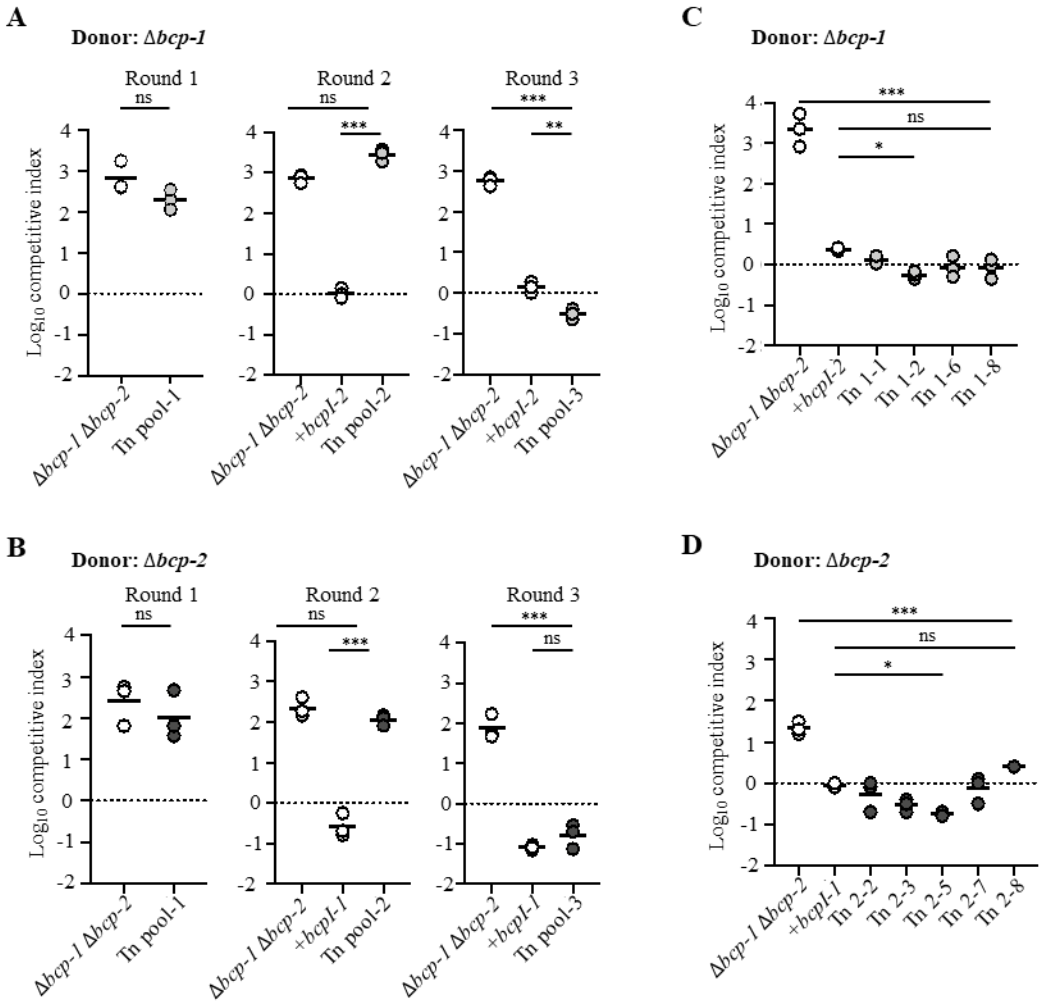


**Figure 5.1. Selection of CDI-resistant *B. dolosa* transposon mutants.**

**Figure 5.1. Selection of CDI-resistant *B. dolosa* transposon mutants.**

Interbacterial competition assays between **A)** Δ*bcp-1* or **B)** Δ*bcp-2* donor bacteria and the indicated recipient controls Δ*bcp-1* Δ*bcp-2* parent, Δ*bcp-1* Δ*bcp-2* complemented with cognate *bcpI* (indicated with open symbols) and the experimental CDI-resistant transposon mutants (Tn) isolated in sequential rounds of co-cultured competitions. **C)** Δ*bcp-1* or **D)** Δ*bcp-2* donor bacteria competed against 8 individually selected colonies from the Round 3 pool of resistant mutants and controls as described above. Only the competitive indices for colonies identifiable via nested arbitrary PCR are shown. Experimental recipient mutants are colored to indicate the donor competed against (Δ*bcp-1* are colored light grey and Δ*bcp-2* are dark grey). Symbols represent competitive index values from one biological replicate and bars show the mean (n=3). Dashed line shows competitive index = 0 (1:1 ratio of donor to recipient). The competitive indices were calculated as (output donor CFU/recipient CFU) divided by (input donor CFU/recipient CFU). A one-way ANOVA was used to report significance (ns; not significant, *; $p<0.05$, **; $p<0.005$, and ***; $p<0.0005$).

**Table 5.1. Chromosomal insertion sites of CDI-resistant *B. dolosa* miniTn5 mutants.**

| Tn mutant[b] | Locus tag | Gene | Annotation | Insertion after gene |
|---|---|---|---|---|
| Tn1-1, Tn1-2, Tn1-4, Tn1-6, Tn1-8, Tn2-5* | AK34_755 (BDAG_00967) | | EAL domain-containing protein | 224bp |
| Tn2-7* | AK34_2642 (BDAG_02644) | *cspD* | Cold-shock protein | 35bp |
| Tn2-2*, Tn2-3* | AK34_2721 (BDAG_02714) | *hisD* | Histidinol dehydrogenase | 373bp |
| Tn2-8* | AK34_3773 (BDAG_03544) | *cepR* | Autoinducer binding domain-containing protein | 117bp |

[a] Mutants isolated for resistance to *B. dolosa* BcpAIOB-2 are labeled "1-x". Mutants isolated for resistance to BcpAIOB-1 are labeled "2-x" and denoted with (*).

[b] Multiple transposon mutants are listed when sequencing results indicated they were clones with identical insertion sites.

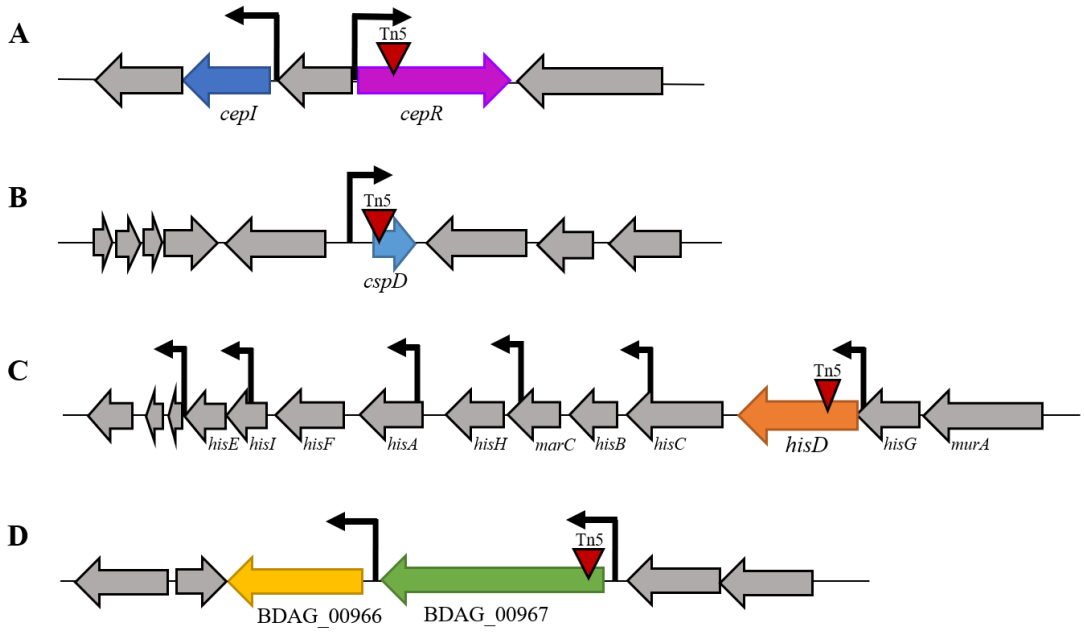


**Figure 5.2. Diagram of identified transposon disruptions.**

**A)** Locus organization of BDAG_03544 (*cepR*) in purple, including the upstream gene BDAG_03546 (*cepI)* in dark blue. **B)** Locus organization of BDAG_02644 (*cspD*) in light blue. **C)** Locus organization of BDAG_02714 (*hisD*) in orange. Name of the genes that encode for proteins within the same histidine biosynthesis pathway are included. **D)** Locus organization of BDAG_00967 in green and the downstream gene BDAG_00966 in yellow. Black arrows represent promoter locations predicted using the Softberry BPROM program. Red triangle indicated with in the gene the Tn5 transposon was inserted.

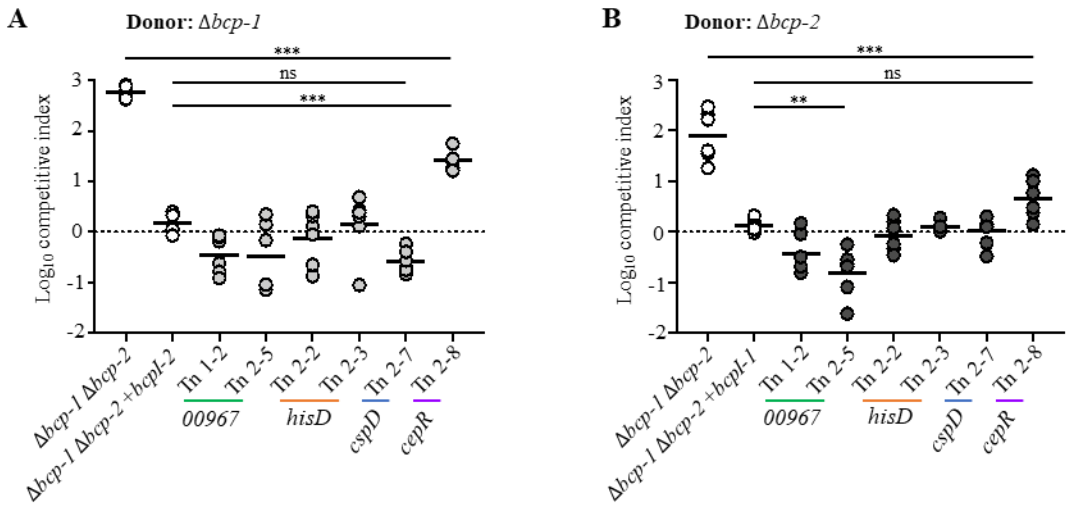


**Figure 5.3. Susceptibility of identified transposon mutants to BcpAIOB-1 and BcpAIOB-2.**

**Figure 5.3. Susceptibility of identified transposon mutants to BcpAIOB-1 and BcpAIOB-2.**

Interbacterial competition assays between **A)** Δ*bcp-1* or **B)** Δ*bcp-2* donor bacteria and the indicated control recipient cells: Δ*bcp-1* Δ*bcp-2* (parent), Δ*bcp-1* Δ*bcp-2* complemented with cognate *bcpI* (indicated with open symbols), and experimental recipient isolates CDI-resistant transposon mutants. Single colonies isolates from transposon resistant Round 3 pools to either Δ*bcp-1* or Δ*bcp-2* donor bacteria are competed in tandem with Δ*bcp-1* or Δ*bcp-2* regardless of the original CDI-system resistance colonies were selected from. Only the competitive indices for colonies identifiable via nested arbitrary PCR are shown. Colored lines indicate the disrupted gene in the transposon mutants. Experimental recipient mutants are colored to indicate the donor competed against (Δ*bcp-1* are colored light grey and Δ*bcp-2* are dark grey). Symbols represent competitive index values from two biological replicate and bars show the mean ($n$=6). Dashed line shows competitive index = 0 (1:1 ratio of donor to recipient). The competitive indices were calculated as (output donor CFU/recipient CFU) divided by (input donor CFU/recipient CFU). A one-way ANOVA was used to report significance (ns; not significant, *; $p$<0.05, **; $p$<0.005, and ***; $p$<0.0005).

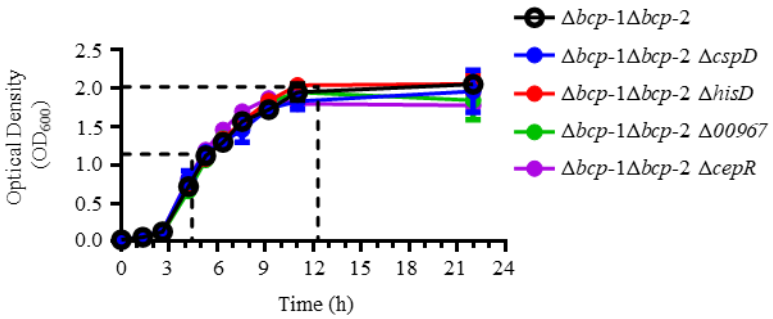


**Figure 5.4. Liquid culture bacterial growth of deletion of regulatory, stress response or quorum sensing genes.**

Growth curve experiments performed with deletion mutants of transposon identified candidates, Δ*cspD*, Δ*hisD*, Δ00967, Δ*cepR*, in the parental Δ*bcp-1* Δ*bcp-2* background. Growth curves of candidate deletion mutants were compares to the parental Δ*bcp-1* Δ*bcp-2* mutant. Optical density for all strains were measured in duplicate through 0-24h, symbols represent the mean with standard deviation. A one-way ANOVA was used to report significance from each time point and no significant differences were found between the $OD_{600}$ between any of the strains.

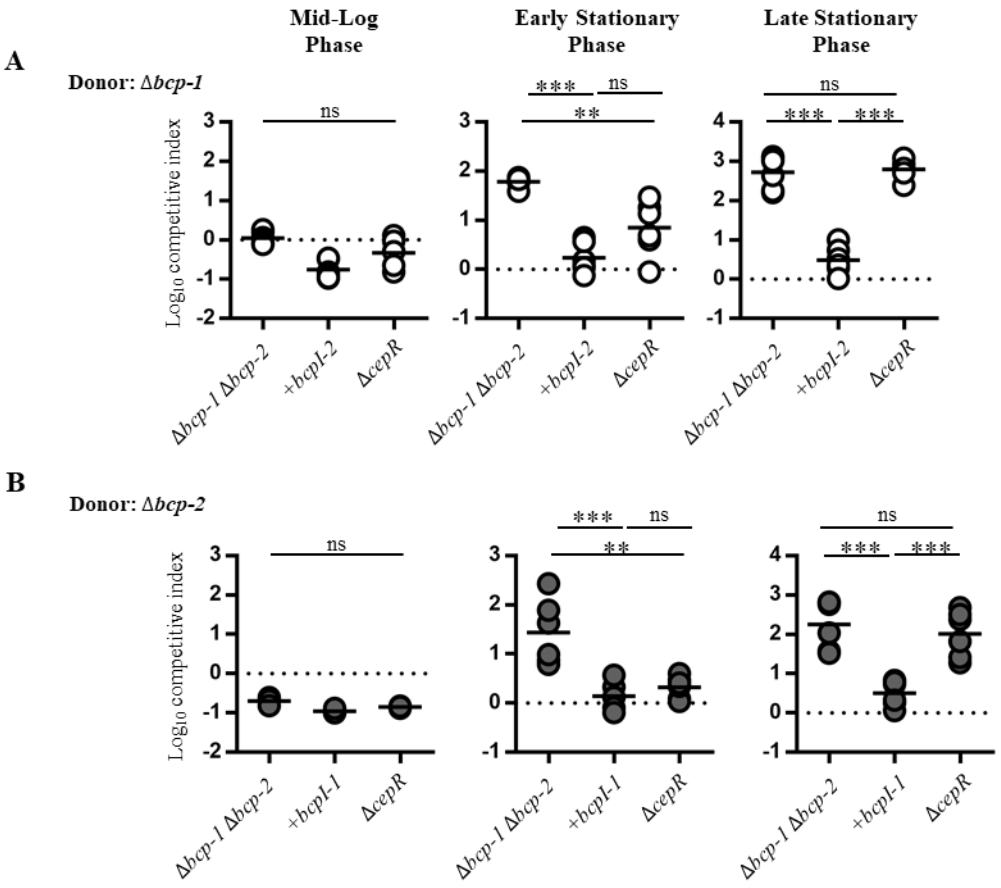


**Figure 5.5. Recipient cell susceptibility tested at different growth phases.**

**Figure 5.5. Recipient cell susceptibility tested at different growth phases.**

Interbacterial competition assays between **A)** Δ*bcp-1* or **B)** Δ*bcp-2* donor bacteria and the indicated control recipient cells: Δ*bcp-1* Δ*bcp-2* (parent), Δ*bcp-1* Δ*bcp-2* complemented with cognate *bcpI* (indicated with open symbols), and experimental Δ*cepR* mutants. $OD_{600}$=0.02 of recipient cell cultures were inoculates and competitions setup at three time points: mid-log phase (6 h), early-stationary phase (11 h), and late-stationary phase (24 h). Donor cells were grown from overnights and competitions setup from cultures at 17 h. Experimental recipient mutants are colored to indicate the donor competed against (Δ*bcp-1* are colored light grey and Δ*bcp-2* are dark grey). Symbols represent competitive index values from two biological replicate and bars show the mean ($n$=6). Dashed line shows competitive index = 0 (1:1 ratio of donor to recipient). The competitive indices were calculated as (output donor CFU/recipient CFU) divided by (input donor CFU/recipient CFU). A one-way ANOVA was used to report significance (ns; not significant, *; $p$<0.05, **; $p$<0.005, and ***; $p$<0.0005).

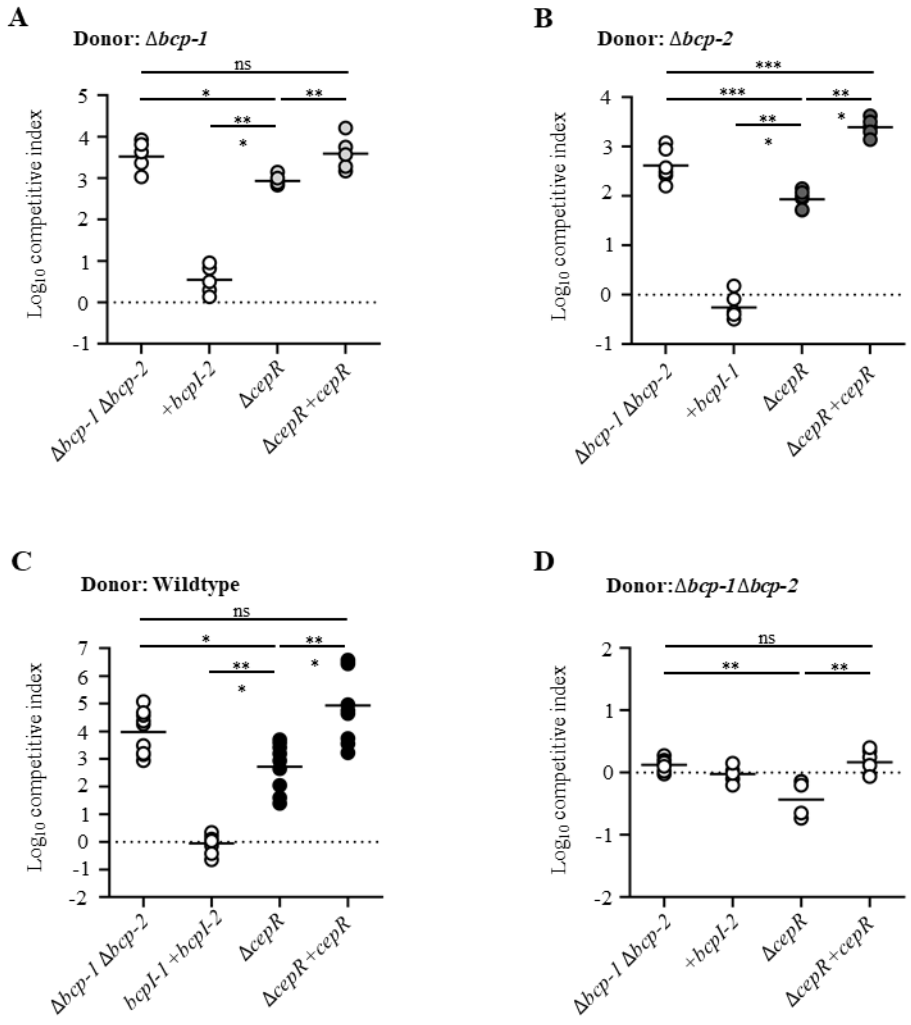


**Figure 5.6. Susceptibility to CDI tested for the transposon candidate quorum sensing regulation gene, *cepR*.**

**Figure 5.6. Susceptibility to CDI tested for the transposon candidate quorum sensing regulation gene, *cepR*.** Interbacterial competition assays between **A)** Δ*bcp-1*, **B)** Δ*bcp-2*, **C)** Wildtype, or **D)** Δ*bcp-2*Δ*bcp-2* donor bacteria between the indicated recipient controls Δ*bcp-1* Δ*bcp-2* (parent), Δ*bcp-1* Δ*bcp-2* complemented with cognate *bcpI* (indicated with open symbols) and deletion of *cepR* in parental background, Δ*cepR*. **A, B, D)** Symbols represent competitive index values from multiple (2) biological replicate and bars show the mean ($n$=6). **C)** Symbols represent competitive index values from multiple (3) biological replicate and bars show the mean ($n$=9). Complementation plasmids contain *cepR* driven by the S12 constitutive promoter at the *att*Tn7 site, +*cepR*. Experimental recipient mutants are colored to indicate the donor competed against (Δ*bcp-1* are colored light grey and Δ*bcp-2* are dark grey). Dashed line shows competitive index = 0 (1:1 ratio of donor to recipient). The competitive indices were calculated as described in Figure 1. A one-way ANOVA was used to report significance (ns; not significant, *; $p$<0.05, **; $p$<0.005, and ***; $p$<0.0005).

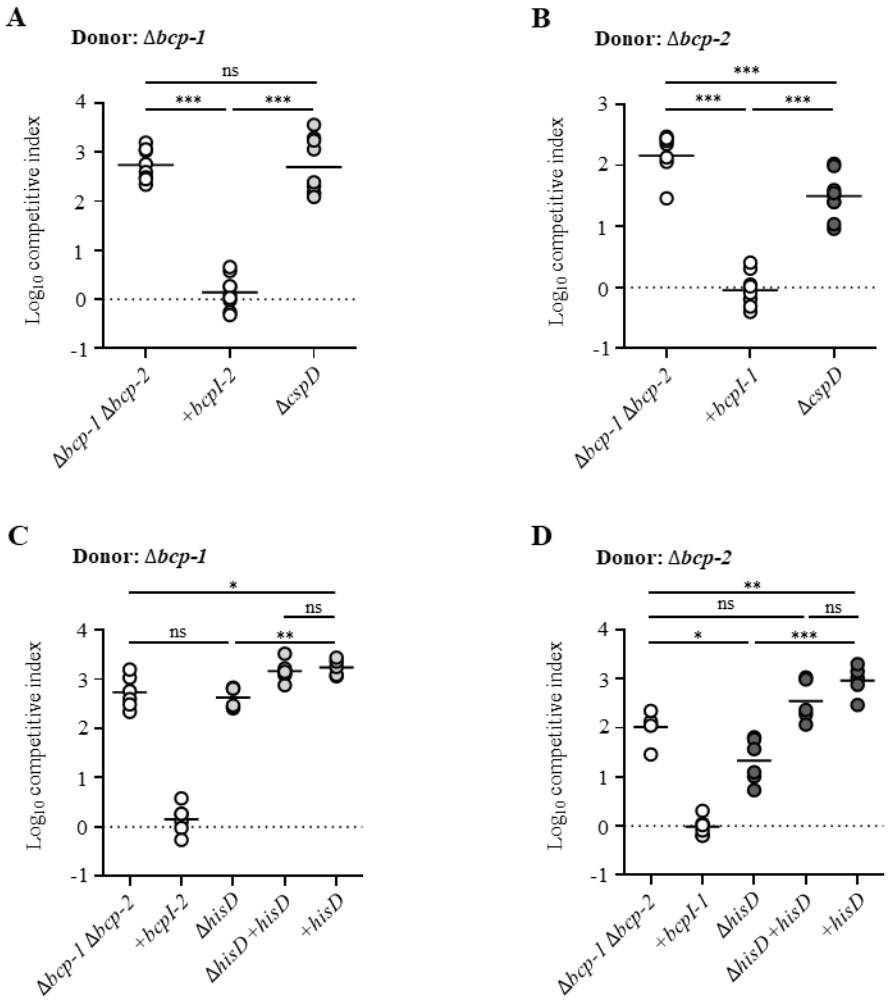


**Figure 5.7. Susceptibility to CDI tested for the transposon candidate genes, *cspD* and *hisD*.**

**Figure 5.7. Susceptibility to CDI tested for the transposon candidate genes, *cspD* and *hisD*.**

Interbacterial competition assays between **A)** Δ*bcp-1* or **B)** Δ*bcp-2* donor bacteria and the indicated recipient controls Δ*bcp-1* Δ*bcp-2* (parent), Δ*bcp-1* Δ*bcp-2* complemented with cognate *bcpI* (indicated with open symbols) and deletion of *cspD* in parental background. Symbols represent competitive index values from multiple (3) biological replicate and bars show the mean ($n$=9). **C)** Δ*bcp-1* or **D)** Δ*bcp-2* donor bacteria competed against the same control strains as above and triple deletion of *hisD* in the parental background. Complementation plasmids contain *hisD* driven by the S12 constitutive promoter at the *att*Tn7 site. Experimental recipient mutants are colored to indicate the donor competed against (Δ*bcp-1* are colored light grey and Δ*bcp-2* are dark grey). Symbols represent competitive index values from multiple (2) biological replicate and bars show the mean ($n$=5-6). Dashed line shows competitive index = 0 (1:1 ratio of donor to recipient). The competitive indices were calculated as described in Figure 1. A one-way ANOVA was used to report significance (ns; not significant, *; $p$<0.05, **; $p$<0.005, and ***; $p$<0.0005).

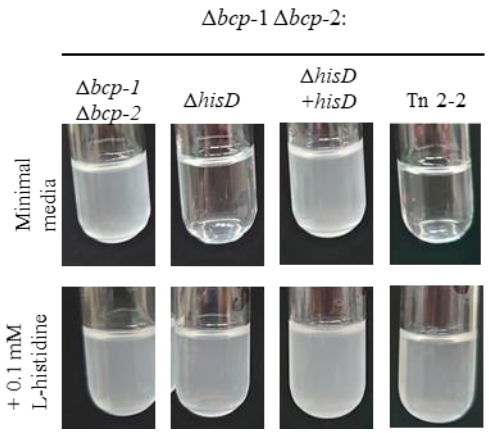


**Figure 5.8. Growth of *B. dolosa* Δ*hisD* mutant in minimal medium.**

Parental Δ*bcp-1* Δ*bcp-2* mutant, Δ*bcp-1* Δ*bcp-2* Δ*hisD* mutant, and Δ*bcp-1* Δ*bcp-2* Δ*hisD* complemented with *hisD* at an *att*Tn7 site, and *hisD*::MiniTn5 disruption clone (from left to right) were cultured in M63 minimal medium (top) or medium supplemented with 0.1mM L-histidine (bottom). Cultures were imaged after ~24 h aerated growth at 37°C.

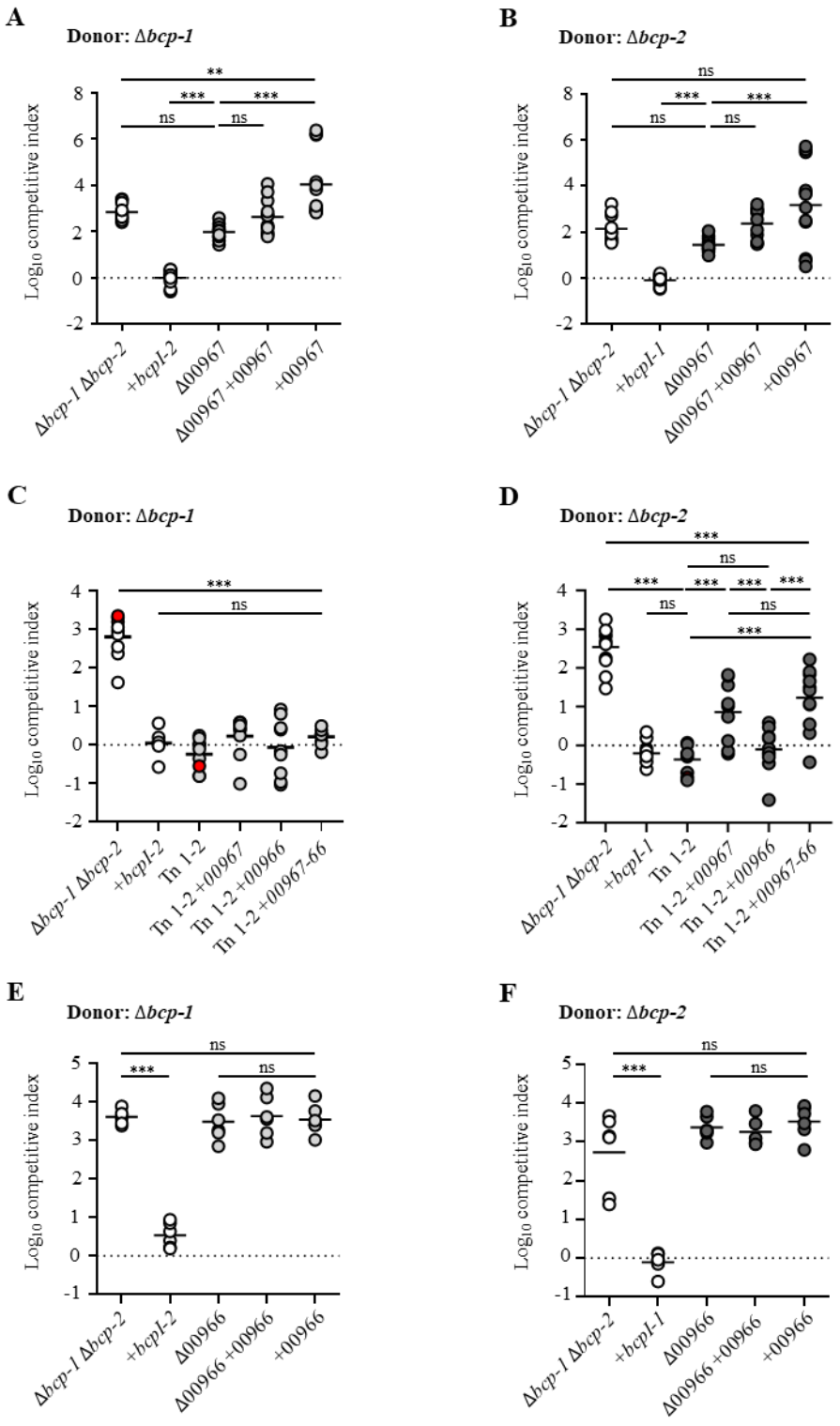


**Figure 5.9. Deletion and complementation of transposon identified inner membrane susceptibility factors encoded in BDAG_00967 and BDAG_00966 locus.**

**Figure 5.9. Deletion and complementation of transposon identified inner membrane susceptibility factors encoded in BDAG_00967 and BDAG_00966 locus.**

Interbacterial competition assays between **A)** Δ*bcp-1* or **B)** Δ*bcp-2* donor bacteria and the indicated recipient controls Δ*bcp-1* Δ*bcp-2* (parent), Δ*bcp-1* Δ*bcp-2* complemented with cognate *bcpI* (indicated with open symbols) and deletion of BDAG_00967 in parental background, Δ00967. Complementation plasmids contain BDAG_00967, +00967, driven by the S12 constitutive promoter at the *att*Tn7 site. Symbols represent competitive index values from multiple (4) biological replicate and bars show the mean (*n*=11-12). **E)** Δ*bcp-1* or **F)** Δ*bcp-2* donor bacteria between the indicated recipient controls Δ*bcp-1* Δ*bcp-2* (parent), Δ*bcp-1* Δ*bcp-2* complemented with cognate *bcpI* (indicated with open symbols) and deletion of BDAG_00966 in parental background, Δ00966. Symbols represent competitive index values from multiple (2) biological replicate and bars show the mean (*n*=6). Complementation plasmids contain BDAG_00966 driven by the S12 constitutive promoter at the *att*Tn7 site, +00966. The competitive indices were calculated as described in Figure 1.

**C)** Δ*bcp-1* or **D)** Δ*bcp-2* donor bacteria marked with only tetracycline resistance, $Tet^R$, are competed against recipient bacteria marked with kanamycin, $Km^R$, and tetracycline resistance, $Tet^R$ . Complementation of BDAG_00967, +00967, BDAG_00966, +00966, and BDAG_00967 through BDAG_00966, +00967-66 are under the S12 constitutive promoter via a tetracycline resistance parked plasmid at the *att*Tn7 site. The competitive indices were calculated as ((output $Tet^R$ CFU – recipient $Km^R$ CFU)/(recipient $Km^R$ CFU) divided by ((input $Tet^R$ CFU – recipient $Km^R$ CFU)/(recipient $Km^R$ CFU). Red symbol indicates recipient $Km^R$ CFU outnumber the recipient $Tet^R$ CFU and then were artificially

set with input ratio of 2:1 of $Tet^R$ CFUs to $Km^R$ CFUs. Experimental recipient mutants are colored to indicate the donor competed against (Δ*bcp-1* are colored light grey and Δ*bcp-2* are dark grey). Symbols represent competitive index values from multiple (3) biological replicate and bars show the mean ($n$=6-9). Dashed line shows competitive index = 0 (1:1 ratio of donor to recipient). A one-way ANOVA was used to report significance (ns; not significant, *; $p$<0.05, **; $p$<0.005, and ***; $p$<0.0005).

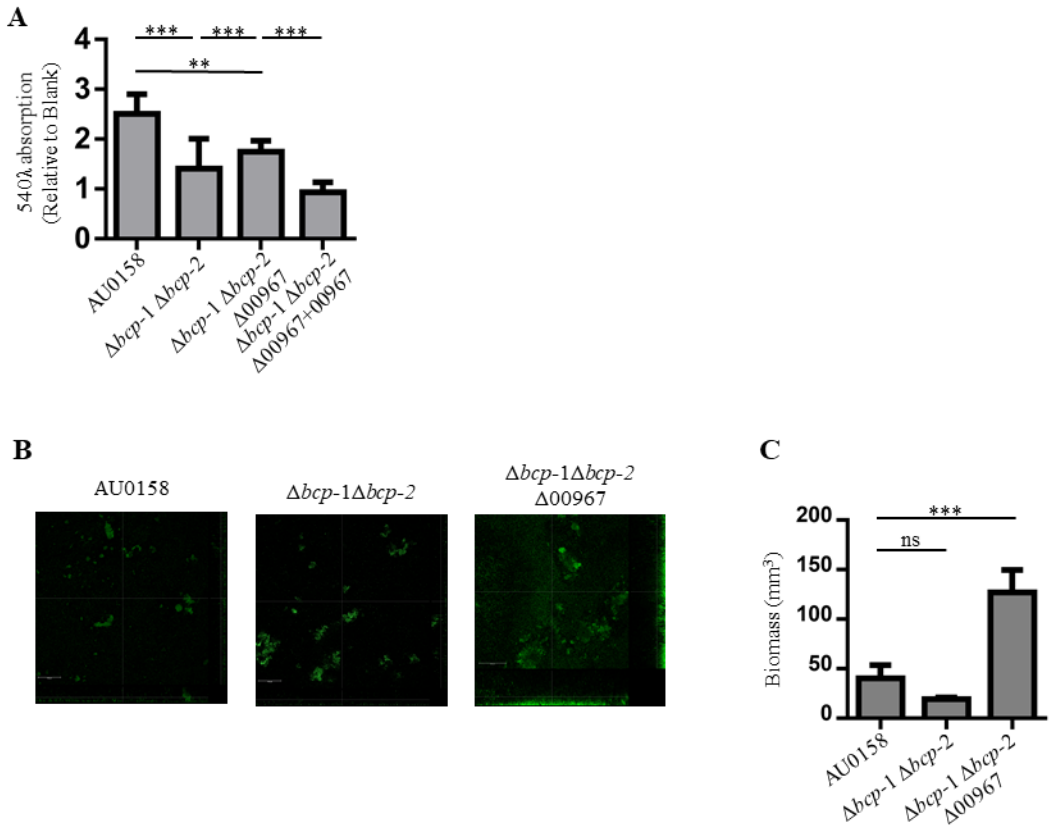


**Figure 5.10. Influence of BDAG_00967 on *B. dolosa* biofilm formation tested.**

**Figure 5.10. Influence of BDAG_00967 on *B. dolosa* biofilm formation tested.**

**A)** Crystal violet staining assay of *B. dolosa* for 48 h in TSB+1% glucose supplemented microtiter plates. Graph shows $OD_{540\lambda}$ values of Crystal violet bound cells normalized to the average measurement for the blanks (media alone wells). Data is of two biological replicate and bars show the mean ($n$=8). **B)** Confocal laser scanning microscopy of Biofilm formation in chambered well by *gfp* constitutive expressed *B. dolosa* strains. Bacteria were grown for 48h in TSB+1% glucose cultures grown in three biological replicate and bars show the mean ($n$=3). In Z stack renderings (48 h), cross-sections through the plane parallel to the coverslip (shown by large center image). Scale bars represent 100 μm. Images are representative. **C)** For each of the strains in (**B**), total biofilm mass was calculates using COMSTAT analysis of Z stacks collected after 48 h of biofilm growth development. A one-way ANOVA was used to report significance (ns; not significant, *; $p$<0.05, **; $p$<0.005, and ***; $p$<0.0005).

**Table 5.2. Unique variations[a] in *B. dolosa* transposon mutants identified by whole genome re-sequencing.**

| Tn mutant [b] | Chr | Position | Variation[c] | Locus tag | Annotation | Cov.[d] | Freq (%)[e] |
|---|---|---|---|---|---|---|---|
| Tn1-2 (BDAG_00967) | 1 | 860,238 | Δ17 bp* | AK34_796 (BDAG_01006) | glycosyl transferase | 88 | 100 |
| Tn1-2 (BDAG_00967) | 2 | 850,831 | C>G [A→G] | AK34_3910 (BDAG_03419) | nitrate/sulfite reductase | 109 | 100 |
| Tn2-2 (*hisD*) | 1 | 859,798 | (AGC) 4→3 [Δ L] | AK34_795 (BDAG_01005) | O-antigen ligase | 255 | 99.8 |
| Tn2-7 (*cspD*) | 1 | 810,641 | Δ1 bp* | AK34_755 (BDAG_00967) | EAL domain-containing protein | 115 | 100 |
| Tn2-7 (*cspD*) | 1 | 860,374 | A>G [L→P] | AK34_796 (BDAG_01006) | glycosyl transferase | 127 | 100 |
| Tn2-8 (*cepR*) | 3 | 562,405 | A>T [L→M] | AK34_5528 (BDAG_04624) | MFS transporter | 218 | 100 |

Chr, chromosome; Cov, coverage; Freq, frequency

[a] Variations relative to AU0158 reference genome occurring at >85% frequency in regions having >25 mapped reads, identified in the indicated transposon mutant and absent from Δ*bcpAIOB-1* Δ*bcpAIOB-2* parent mutant

[b] Parenthesis denote transposon-disrupted gene

[c] Brackets show amino acid change, where applicable. Mutations causing ORF frameshift are denoted with (*).

[d] Number of mapped reads

[e] % reads containing indicated mutation

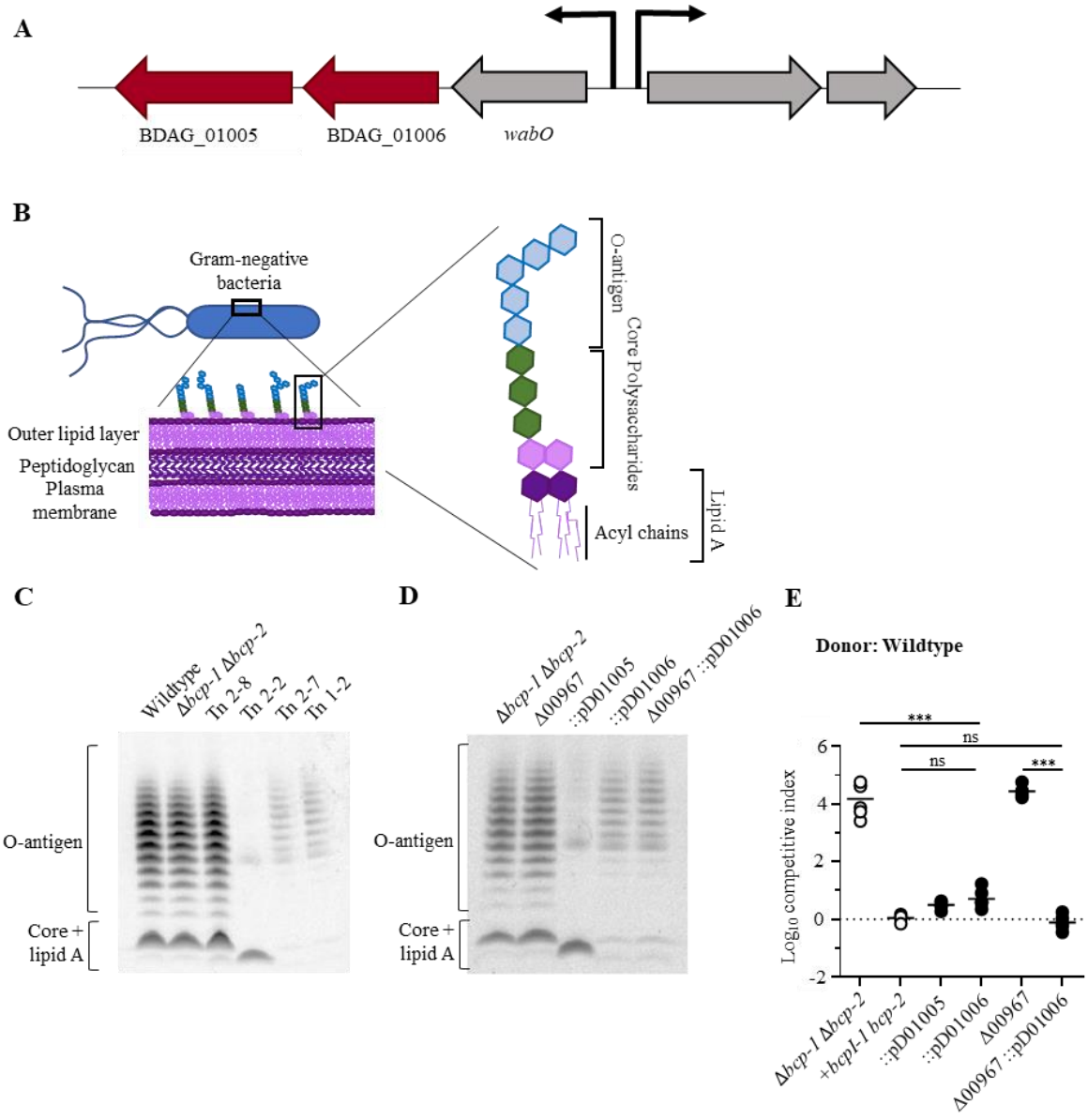


**Figure 5.11. LPS structure and CDI susceptibility for BDAG_01005 and BDAG_01005 mutants.**

**Figure 5.11. LPS structure and CDI susceptibility for BDAG_01005 and BDAG_01005 mutants.**

**A)** Locus organization of BDAG_01007 (*wabO*), BDAG_01006, and BDAG_01005. Red arrows represent the genes that whole genome sequencing identified unique mutations. **B)** Graphical representation of the location and structure of LPS in Gram-negative bacteria. **C)** LPS extracted from Wildtype, parental Δ*bcp-1* Δ*bcp-2,* and the four unique transposon insertion clones; Tn 2-8 (*cepR*::miniTn5), Tn2-2 (*hisD*:miniTn5), Tn 2-7 (*cspD*::miniTn5), and Tn 1-2 (00967::pminiTn5) **D)** LPS extracted from parental Δ*bcp-1* Δ*bcp-2,* triple deletion mutant Δ*bcp-1* Δ*bcp-2* Δ00967, and the disruption mutants in BDAG_01005 (::pD01005) and NDAG_01006 (::pD01006). Electrophoretic analysis of LPS of mutant strains. LPS extracted from *Burkholderia* cells was resolved in the Tricine 10-20% (Invitrogen) and visualized Pro-Q Emerald 300 LPS Gel Stain Kit (Molecular Probes). **E)** Interbacterial competitions between Wildtype donor bacteria and the indicated recipient controls; Δ*bcp-1* Δ*bcp-2* (parent), Δ*bcp-1* Δ*bcp-2* complemented with both cognate *bcpI* genes (indicated with open symbols). Experimental recipient bacteria mutants (indicated with black symbols) include genetic disruptions in BDAG_01005, ::pD01005, and BDAG_01006, ::pD01006. Disruptions for both genes were made in parental background and an additional BDAG_01006 was made in the triple deletion Δ*bcp-1* Δ*bcp-2*Δ00967 background, Δ00967:::pD01006. Symbols represent competitive index values from multiple (2) biological replicate and bars show the mean ($n$=5-6). The competitive indices were calculated as described in Figure 1. Dashed line shows competitive index = 0 (1:1 ratio of donor to recipient). A one-way ANOVA was used to report significance (ns; not significant, *; $p$<0.05, **; $p$<0.005, and ***; $p$<0.0005).

## 5.4. Discussion

Previous studies have shown that recipient cell sensitivity factors differ between species and may also differ between toxins expressed by a singular bacterium. With a small number of the studies identifying CDI susceptibility factors in *Burkholderia* spp., our understanding has been limited primarily to findings in *E. coli.* Each *B. dolosa* CDI system is distinct and may require both similar and different proteins for susceptibility in recipient bacterium. Intoxication via the CDI system protein BcpA requires both extracellular and intracellular receptors to facilitate translocation into the recipient cell, according to the current model (190). The majority of susceptibility factors have been identified in *E. coli* spp., with few studies identifying factors in *Burkholderia.*

Inner membrane proteins GltJK in *B. multivorans* and Bth_II0599 used by a *B. pseudomallei* CDI system have been associated with translocation of BcpA (201, 203). In this study, we used transposon mutagenesis to identify susceptibility factors to each BcpA expressed toxin in *B. dolosa.* Four genes with unique transposon insertions were identified and further found to have partial protection against *B. dolosa* BcpA intoxication.

The output of identified unique transposon insertions was limited which suggests a bottleneck during selection and isolation of resistant mutants. Only a single mutant was identified for resistance against BcpA-2, disrupting BDAG_00967. However, when unique transposon insertion mutants were competed, three of the four identified were resistant to both BcpA-1 and BcpA-2. Due to these data and limitations of the procedure, we believe that the identified genes are not exhaustive.

The gene *cepR* encodes the protein CepR, a LuxR-type receptor in the CepI/CepR quorum sensing complex mediated by an *N*-acyl L-homoserine lactone (AHL) signal (195,

225, 261, 274). In *B. thailandensis*, the CepR/CepI quorum sensing homologs alter expression of the *bcpAIOB* locus and the ability of donor cells to outcompete susceptible recipient bacteria by CDI (195). While it is not known whether CepI/CepR system similarly influences the expression of the *B. dolosa* CDI encoding loci, this study did show that quorum sensing impacts CDI susceptibility in recipient cells through an unknown mechanism. As the quorum sensing system is associated with global gene expression changes, we do not know if the relationship between CepR/CepI quorum sensing system is acing directly or indirectly with the *B. dolosa* CDI susceptibility factors. Alteration in encoding for the CDI susceptibility factors could be under direct quorum sensing regulation or alter additional components such as LPS or exopolysaccharides that may alter CDI sensitivity indirectly. As this study showed loss of CepR altered susceptibility to both BcpA-1 and BcpA-2, may indicate a general effect on CDI systems instead of direct. Our data is limited in ability to separate the role of CepR from the CepI synthase as donors are still capable of wild-type quorum sensing. The dissection of the relative contributions of genetic and environmental influence of quorum sensing in CDI sensitivity will provide insight into the role socio-microbiology plays in CDI (283, 284).

The additional deletion mutants in CDI-susceptibility factors had limited effects in recipient cells. The intermediate effects of the *hisD, cspD* and BDAG_00967 gene deletions provide insight into the complexity of CDI's influence on signaling and gene expression, even if indirectly (Figure 5.7 and Figure 5.9).

Deletions of *hisD* resulted in partial protection only to BcpA-1. Additionally, the *hisD* deletion resulted in histidine auxotrophy; mutants were able to supplement this deficiency with histidine from the Low Salt LB media during growth (Figure 5.8) These

results indicate that the upstream genes may not be additionally disrupted as supplementing with L-histidine alone restored growth. As histidine in Low Salt LB is sufficient for Δ*hisD* growth comparable to the parental Δ*bcp*-1Δ*bcp*-2 strain, we speculate that deletion of *hisD* could result in build-up of intermediate products such as L-histidinol, which may indirectly effect CDI efficiency of BcpA-1 while not altering BcpA-2 CDI.

Like *hisD*, deletion of *cspD* had partial protection against BcpA-1 intoxication while remaining as susceptible as the parental strain to BcpA-2. The gene *cspD* encodes for a cold shock-like protein, CspD, predicted to bind to DNA and respond to stress from DNA damage. Homologs of *cspD* in *E. coli* inhibit DNA replication and is induced during stationary phase to limit growth. Overproduction of this CspD is thus toxic to the cells (276, 276, 285). As the Δ*cspD* was unable to be complemented with a *cspD* expressing cassette, supports that overexpression of *cspD* in *Burkholderia* is similarly toxic.

The regulatory gene BDAG_00967 encodes a dGTP triphosphohydrolase protein, also known as dGTPase enzyme. The function of dGTP triphosphohydrolase is to regulate the ubiquitous intracellular secondary messenger cyclic-di-GMP. BDAG_00967 homologs regulate C-di-GMP production using the functional GGDEF and EAL protein domains to synthesize and degrade, respectively. Cyclic-di-GMP regulates biological processes by binding to diverse receptors resulting in complex control of cellular processes. Cyclic-di-GMP in other *Burkholderia* spp. regulates the transition between planktonic and motility, biofilm formation, and network-components (279, 286). BDAG_00967 influences *B. dolosa* biofilm formation, both in biomass and architecture (Figure 5.10). However, these data show an ‘all or nothing’ effect comparing wild-type expression of BDAG_00967 and

the deletion mutant. The loss of both GGDEF and EAL domains does not inform about the extent to which each domain regulates *B. dolosa* biofilms.

The *hisD, cspD* and BDAG_00967 gene deletions only resulted in intermediate protection against donor CDI systems and did not reproduce comparable levels of protection as the respective transposon mutants, additional chromosomal mutations were suspected. Whole genome sequencing identified three resistant transposon mutants possessed the additional mutations in the same locus. The resistance of the transposon mutants was most likely the result of the mutations in BDAG_01005 or BDAG_01006 genes and not the transposon disruptions. The transposon mutants *cspD*, Tn5 2-7, and BDAG_00967, Tn5 1-2, had mutations in both BDAG_01006 and the cyclic-di-GMP regulator gene BDAG_00967. Deletion of BDAG_00967 was insufficient for CDI protection, the disruption of BDAG_01006 and loss of BDAG_00967 mutant was significantly more resistant to CDI than either mutation alone, indicating that the loss of both gene has a compounding effect on susceptibility (Figure 5.11 E).

As disruptions in both BDAG_01005 and BDAG_01006 alter the LPS, although differently, this suggests that LPS biosynthesis and structure alters recipient cell susceptibility to CDI (Figure 5.11). LPS has already been shown to protect against *B. pseudomallei* CDI, although the identified LPS associated genes are different (202). These data support the hypothesis that LPS alteration inhibits CDI of donor bacteria generally and is not specific to any one CDI system. Thus far LPS is the only recipient cell surface molecule identified to participate in *Burkholderia* CDI.

Although the majority of the susceptibility candidates identified had limited influence on CDI susceptibility to either BcpA-1 and BcpA-2, these finding show how interwoven the alteration in genetic expression and CDI susceptibility are.

The amount of protection against CDI required in donor bacteria to survive within a given environmental niche is yet to be understood, however marginal resistance maybe sufficient for bacterial survival in the long run. Future directions aimed at identifying the extent to which partial compared to complete CDI resistance to a specific system influences bacterial survival in a specific niche will add critical insight into the complexity CDI and benefit of high rates of mutations withing non-kin recipient bacteria for survival.

## Chapter 6: Discussion and Future Directions

Elucidating how bacteria interact with one another, either through competition or cooperation, enhances our understanding of polymicrobial environments and, in turn, the impact these environments have on infectious disease transmission, progression, and treatment. Microbes utilize a wide range of mechanisms to carry out cell-to-cell interaction, and the work herein investigates the use and mechanism of contact-dependent growth inhibition systems (CDI) by *Burkholderia* species. CDI systems are found across many pathogenic Gram-negative bacteria including *Yersinia pestis* and *Pseudomonas aeruginosa* (183). Using *Burkholderia* species as the model organism places our findings in a clinically significant context.

CDI systems fall into two major functional classes, "*E. coli*-type", and "*Burkholderia*-type." (185, 187, 197). Although *Burkholderia* BcpA does share functional similarities with *E. coli* CdiA, their differences include, though are not limited to, organization of genes in the CDI-associated locus, *Burkholderia*-type CDI systems encoding of BcpO, and *E. coli*'s ability to perform CDI in liquid environments where as *Burkholderia* are limited to competition on solid media (185). Additionally, *Burkholderia* CDI systems can be further divided into two subclasses, class I and class II (192).

Much of this work compares the subclasses of *Burkholderia* CDI systems. Since the patient isolated *B. dolosa* strain AU0158 encodes for CDI systems from each subclass, I was able to directly compare each system in their native context and under native gene expression. Aside from the functional C-terminal toxin domain of BcpA, most of the sequence variability is found upstream of the conserved LYN sequence termed the pre-

toxin region (Figure 3.1A). The variable sequence is primarily a 100aa region but variability can extend up to 500aa upstream of the LYN sequence (Figure 4.1A).

Currently BcpA chimeras have been limited to swapping the C-terminus of BcpA toxins from the same class (192, 193). I hypothesized that chimeras could be made if the C-terminus contained the C-terminal toxin and the pre-toxin region. The pre-toxin regions are conserved within their own classes, therefore, exchanging the whole variable region should be enough to create functional chimeras. BcpA of E264 and BcpA-1 in AU0158 class I toxins have shown that BcpO is required for CDI efficiency (185, 188). Currently we do not know the role BcpO plays, nor if it directly interacts with BcpA. BcpO is predicted to be a membrane bound protein. Therefore, BcpO and the pre-toxin and toxin regions could be in proximity and interact within the periplasmic space.

Following the hypothesis that the BcpA toxin is similarly structured as E. coli CdiA; the functional toxin domain, the pre-toxin region, and part of the *Filamentous* hemagglutinin (FHA) domain; remains in the periplasm until binding to recipient cell outer membrane receptor, triggering toxin translocation diagramed in Figure 4.1B (190). This predicted region held in the periplasm includes the variable regions separating class I BcpA from class II. As this variable domain could be interacting with BcpO, we will learn more about the function of BcpO in regards to BcpA translocation and differentiation between the uses of BcpO in class I from class II.

Future experiments can use cross-class chimeric strains to identify BcpA-BcpO interaction regions. If BcpO interacted with the variable pre-toxin and toxin domain then chimeric strains containing the N-terminal conserved regions fused with class II pre-toxin and toxin domain would not see a change in CDI efficiency in the absence of BcpO.

However, if BcpO interacts with the N-terminus of the toxin then presence or absence of BcpO will result in different competition efficiency.

The E264 BcpA is 83.0% identical to the *B. dolosa* BcpA-1 and 89% identical in the catalytic C-terminal toxin domain. Although the function of E264 BcpA is yet to be fully determined, the C-terminus shares secondary structures similar to Holliday junction reductase and archaeal species endonucleases. These similarities to DNA cleaving proteins indicates that E264 BcpA toxicity is likely due to inducing DNA damage to carryout CDI (192, 209).

Since E264 BcpA and AU0158 BcpA-1 toxins are hypothesized to be nucleases, then CDI requires toxins be translocated into the cytoplasm of the recipient cell. Additionally, BcpA translocation requires passing through the recipient cell and is hypothesized to include the pre-toxin region following the *E. coli* model. I identified 2 unique bands specific AU0158 wild-type BcpA-1 at 37kD and 75kD (Figure 4.4). These bands, based on size, are predicted to correspond to the catalytic toxin (37kD) and the pre-toxin variable region through the toxin domain (75kD). The band at 37kD of the catalytic toxin is hypothesized to be cleaved during BcpA translocation into the cytoplasm of the recipient cell. The band at 75kD encompassing the pre-toxin region and toxin domain is hypothesized to be the intermediate cleavage in the recipient cell periplasm prior to final translocation into cytoplasm. Future studies will be aimed at identifying the sequence of the 37kD and 75kD bands through mass spectrometry to confirm our hypothesis.

Currently, we do not have antibodies against AU058 BcpA-2, hindering the ability to perform similar experiments to compare and identify BcpA-2 cleavage regions during translocation into recipient cells. Furthermore, AU0158 BcpA-2 is only toxic under the

constitutive S12 promoter. However, as a class II toxin, identifying banding patterns for BcpA-2 will help us determine if translocation cleavage sites differ from class I to class II and which are unique to each toxin. The pre-toxin regions in *Burkholderia*-type BcpA proteins correlate with the location of *E. coli* CdiA inner membrane receptor binding regions. I would suspect that the cleavage site for both class-I and class-II would be similarly located, as the sequences prior to the pre-toxin domains are conserved. However, AU0158 BcpA-2 C-terminal toxin activity is not known and may not require translocation into the recipient cell cytoplasm.

The evidence presented in this body of work supports the hypothesis that AU0158 BcpA-2 is functionally different than BcpA-1. In Chapter 5, I identified multiple factors that influence BcpA-1 and BcpA-2 CDI efficiency. Further the differences in recipient deletion mutant susceptibility from BcpA-1 and BcpA-2 indicates that the variability between the proteins result in functionally distinct indirect effects.

Two of these factors are HisD and CspD. Deletion of *cspD* or *hisD* inhibits the full extent of BcpA-1 and does not influence BcpA-2 CDI efficiency (Figure 5.6). How these factors influence BcpA-1 CDI is unknown. Both proteins are associated with regulating the cell either through metabolism or stress. Loss of either gene could result in a large cascade altering cellular physiology, global gene expression, and other cellular components. Due to the cascade of changes that could occur with deletion of the *cspD* or *hisD*, speculation on the reason loss of these genes influence BcpA-1 toxicity specifically, is practically endless. Changes that would alter the ability for BcpA translocation could include altering the ability for the toxin to bind to the membrane receptors, inhibiting efficient BcpA translocation, or altering the expression of a cytoplasmic factor that interacts with BcpA.

If these genes, specifically *cspD*, influence CDI toxicity in the cytoplasm then this would indicate that the difference in protection from BcpA-1 compared to BcpA-2 is because of the C-terminal toxin. The *cspD* gene encodes for a cold shock protein associated with responding to cellular stress from DNA damage (285). These results lead to an interesting question: why is loss of a DNA damage response factor beneficial to recipient cells experiencing nuclease stress? The regulation of cellular behavior requires the specific coordination of different biological processes and factors at the molecular level. This regulation is essential for cellular homeostasis, cellular development, and responding to the environment. Loss of CspD most likely causes global changes and alters the signaling web in recipient cells. These changes can alter the recipient cells susceptibility through inhibiting BcpA-1 specific translocation, or the BcpA-1 nuclease activity the cellular stress response to differ.

As BcpA-2 toxicity activity is unknown, it is possible that loss of CspD does not alter the ability of BcpA-2 to carry out CDI because DNA is not being damaged. CDI toxic activities typically are nucleases, although not always DNases. Multiple *E. coli* toxins are associated with RNase activity, specifically targeting tRNA.

Using the same secondary structure prediction software (254) found BcpA-2 has matches, although with 20% confidence, to ribosome inactivating proteins (RIPs). In *E. coli* and related strains, the toxic effects of RIPs are due to binding to the large 60S ribosomal subunit and act as an N-glycosidase. By binding to the ribosomal subunit, *E. coli* RIPs specifically cleave the adenine base A4324 in the 28S ribosomal rRNA subunit, resulting in the inability of the ribosome to bind elongation factor 2, blocking protein translation (287, 288). *E.coli* CdiA EC869 has been shown to function similarly, requiring

interaction with elongation factor-Tu (EF-Tu) disruption with delivery aminoacyl-tRNA to the ribosome (206). Due to the low confidence of the prediction software, this is primarily speculation as to BcpA-2 toxicity. However, the predicted secondary structures similarities of RIPs to the BcpA-2 C-terminal toxin does support my hypothesis that its toxicity is carried out in a different manner than BcpA-1.

Another factor identified to have influence on CDI susceptibility to BcpA-1 and BcpA-2 is CepR. The gene *cepR* encodes for the quorum sensing receptor, CepR. The CepR/CepI quorum sensing system synthesizes and responds to *N*-octanoyl L-homoserine lactone ($C_8$-AHL) (274, 289, 290). All *Burkholderia* spp. sequences within the Bcc umbrella encode for at least one CepR/CepI quorum sensing complex (290). The CepR/CepI system is associated with regulating *Burkholderia* spp. physiology and virulence (291–293). Motility is one of the major physiological phenotypes regulated by CepR/CepI in Burkholderia species including: *B. cepacia, B. cenocepacia,* and *B. multivorans* (261, 290, 294). In *B. thailandensis* the CepR/CepI quorum sensing systems regulate expression of the *bcpAIOB* CDI encoding locus. *B. thailandensis* has three CeprR/CepI systems. Of the three systems, only one, *btaR/I-1,* activates expression of the CDI locus. Deletion of *btaI-1 I* alone had partial inhibition on the ability of donor cells to carryout CDI, but not to the extent that the triple deletion mutants inhibited donor cell CDI (195).

The role of CepR in *B. dolosa* AU0158 recipient cells were ascertained (Figure 18). Recipient cells with *cepR* deleted had a competitive index 1 log below the susceptible parent strain when competed against Bcp-1 system. In comparison, competition against Bcp-2 system, the *cepR* deletion mutant had 0.5 log more resistance than the parental strain.

The role CepR/CepI plays in the donor cells is still unknown for *B. dolosa*. Often the expression of the *cepR* and *cepI* gene are coupled, thus deletion of *cepR* would inhibit the expression of *cepI* as well (295, 296). Future studies will aim to tease apart the role of quorum sensing in AU0158 CDI competitions for both the recipient cells and donor cells.

In the CepR/CepI *B. thailandensis* quorum sensing system, the quorum sensing system alters expression of genes that encode polysaccharides associated with the capsule or exopolysaccharides (195). Although, in Chapter 5, we identify that lipopolysaccharide structures effect recipient cell susceptibility, the Tn5-*cepR* mutant did not have altered LPS (Figure 5.10). However, we did not look at exopolysaccharide or capsular polysaccharides. The list of potential reasons that deletion of *cepR* has partial protection against BcpA-1 and, to a lesser extent, BcpA-2 is extensive as CepR/CepI quorum sensing systems cause global gene regulation changes. However, our findings in Chapter 5 support the idea that alterations to the cellular membrane surface influences the CDI susceptibility and provides a solid starting point for future studies.

The role of LPS in Gram negative bacteria is critical in changes to the cell's physiology and is often associated with virulence (297, 298). One of the major ways bacteria evade host immune systems are by altering the LPS structure (299, 300). Similarly, many colicins, such as ColN, use LPS as the initial binding factor, creating a tighter interaction between the colicin and the outer membrane receptor. Mutations to the LPS structure hinder the ability for colicins to first bind to the LPS and thus cannot carry out their toxic activity intracellularly (301, 302).

Disruption of BDAG_01006 and BDAG_01005 both resulted in resistance to WT CDI. Indicating that recipient cells are resistant to both AU0158 BcpA-1 and BcpA-2

intoxication [Chap 5 last figure]. Due to the orientation of the genes in the locus, disruptions in BDAG_01006 are predicted to have polar effects on BDAG_01005. However, in the images of the LPS gels, both disruption mutants had altered LPS, but changed in different ways. Disruptions in both BDAG_01005 and BDAG_01006 had changes to the O-antigen, however, BDAG_01005 also had changes to the core and lipid A portion of LPS. These results suggest that there is not a polar effect in the BDAG_01006 mutant. If there was a polar effect, I would suspect that both LPS changes would affect the core and lipid A regions similarly to what is seen in the BDAG_01005 mutant alone (Figure 5.10).

Disrupting BDAG_01006 was not as effective as disrupting BDAG_01005. The BDAG_01005 mutant was as resistant against WT CDI as recipient cell expressing both immunity proteins. As BDAG_01006 still has partial susceptibility, I would suspect that if BDAG_01006 was competed against the CDI systems under expression of the S12 constitutive promoter, BDAG_01006 recipient cells would have increased. If sensitivity of the recipient BDAG_01006 mutant is altered, then these results would support would that the alterations to the O-antigen of LPS is not completely inhibiting CDI but instead hindering CDI. The same experiment can be used to determine the extent to which alterations in the core and lipid A protects against CDI using the BDAG_01005 disruption mutant.

Another gene in the BDAG_01005 and BDAG_01006 locus is BDAG_01007, or *wabO*. Like BDAG_01005 and BDAG_01006, *wabO* encodes for LPS production factors. In *B. cenocepacia,* the *wabO* gene, when mutated resulted in mutations to the LPS core (282). Keeping with my hypothesis, if *wabO* mutation in *B. dolosa* we would expect to

LPS alterations and correlate with CDI resistance in recipient cells. Future experiments will be focused on the effects of in-frame deletion mutants for LPS regulatory genes, including *B. dolosa wabO.*

LPS genes have also been associated with CDI susceptibility of recipient cell to *B. pseudomallei*, Bp10266, BcpA-2 toxin. In the Majerczyk et al., 2014 manuscript, the Bp10266 CDI system-2 is produced in *B. thailandensis* E264, and transposon mutagenesis used to identify recipient cell susceptibility factors. The BTH_10986 LPS associated gene in E264 provided specific protection against Bp10266 BcpA-2, but the native E264 BcpA was still capable of carrying out WT levels of CDI. Because of these results, the researcher proposes that LPS is either the receptor or co-receptor for Bp10266 BcpA-2. Using flow cytometry found CDI competent cells had less binding affinity to the BTH_I0986 deletion mutants. Similarly, WT cells had low binding to cells lacking CDI systems (195). As the cells without CDI systems still had native production of BTH_I0986, if BTH_I0986 was an outer membrane receptor, Bp10266 BcpA-2 should still be able to bind efficiently. However, these findings still support that LPS is playing a role in CDI susceptibility.

Despite almost 20 years of research in CDI mechanism many large questions still remain for the field to answer. Although recipient susceptibility factors are being identified and characterized recently, the amount of toxin required to carry out CDI is still unknown. Another large question is what happens after the toxins are cleaved? How does the donor cell degrade the remaining N-terminus of the protein? While the biological and pathogenic relevance of CDI has not been fully elucidated and utilized, studies suggest there is some contribution, still requires basic research and fundamental understanding before these larger clinical questions can be answered. Future studies will be aimed at comparing Bcc

pathogen CDI systems to identify conserved features. investigating the environmental influences such as quorum sensing factors will add to the field's understanding the socio-microbiology of donor: recipient CDI interactions. Before complex questions surrounding CDI and its impact on disease can be answered, basic research on CDI mechanism must be performed in order to build the foundation of our understanding.

## References


1. De Vos P, De Ley J. 1983. Intra- and Intergeneric Similarities of Pseudomonas and Xanthomonas Ribosomal Ribonucleic Acid Cistrons. International Journal of Systematic Bacteriology 33:487–509.

2. Coenye T, Vandamme P, Govan JRW, LiPuma JJ. 2001. Taxonomy and Identification of the Burkholderia cepacia Complex. J Clin Microbiol 39:3427–3436.

3. Coenye T, Vandamme P. 2003. Diversity and significance of Burkholderia species occupying diverse ecological niches. Environmental Microbiology 5:719–729.

4. Yabuuchi E, Kosako Y, Oyaizu H, Yano I, Hotta H, Hashimoto Y, Ezaki T, Arakawa M. 1992. Proposal of Burkholderia gen. nov. and Transfer of Seven Species of the Genus Pseudomonas Homology Group II to the New Genus, with the Type Species Burkholderia cepacia (Palleroni and Holmes 1981) comb. nov. Microbiology and Immunology 36:1251–1275.

5. Yabuuchi E, Kosako Y, Yano I, Hotta H, Nishiuchi Y. 1995. Transfer of Two Burkholderia and An Alcaligenes Species to Ralstonia Gen. Nov. Microbiology and Immunology 39:897–904.

6. Depoorter E, Bull MJ, Peeters C, Coenye T, Vandamme P, Mahenthiralingam E. 2016. Burkholderia: an update on taxonomy and biotechnological potential as antibiotic producers. Appl Microbiol Biotechnol 100:5215–5229.

7. Stopnisek N, Bodenhausen N, Frey B, Fierer N, Eberl L, Weisskopf L. 2014. Genus-wide acid tolerance accounts for the biogeographical distribution of soil Burkholderia populations. Environmental Microbiology 16:1503–1512.

8. Fierer N, Jackson RB. 2006. The diversity and biogeography of soil bacterial communities. Proceedings of the National Academy of Sciences 103:626–631.

9. Vandamme P, Dawyndt P. 2011. Classification and identification of the Burkholderia cepacia complex: Past, present and future. Systematic and Applied Microbiology 34:87–95.

10. Parke JL, Gurian-Sherman D. 2001. Diversity of the Burkholderia Cepacia Complex and Implications for Risk Assessment of Biological Control Strains. Annual Review of Phytopathology 39:225.

11. Mars AE, Houwing J, Dolfing J, Janssen DB. 1996. Degradation of Toluene and Trichloroethylene by Burkholderia cepacia G4 in Growth-Limited Fed-Batch Culture. Appl Environ Microbiol 62:886–891.

12. Snyder RA, Millward JD, Steffensen WS. 2000. Aquifer Protist Response and the Potential for TCE Bioremediation with Burkholderia cepacia G4 PR1. Microb Ecol 40:189–199.

13. Kang JW, Doty SL. 2014. Cometabolic degradation of trichloroethylene by Burkholderia cepacia G4 with poplar leaf homogenate. Canadian Journal of Microbiology 60:487–490.

14. Isles A, Maclusky I, Corey M, Gold R, Prober C, Fleming P, Levison H. 1984. Pseudomonas cepacia infection in cystic fibrosis: An emerging problem. The Journal of Pediatrics 104:206–210.

15. Burns JL, Lien DM, Hedin LA. 1989. Isolation and characterization of dihydrofolate reductase from trimethoprim-susceptible and trimethoprim-resistant Pseudomonas cepacia. Antimicrobial Agents and Chemotherapy 33:1247–1251.

16. Dave J, Springbett R, Padmore H, Turner P, Smith G. 1993. Pseudomonas cepacia pseudobacteraemia. Journal of Hospital Infection 23:72–73.

17. Greenberg DE, Goldberg JB, Stock F, Murray PR, Holland SM, LiPuma JJ. 2009. Recurrent Burkholderia Infection in Patients with Chronic Granulomatous Disease: 11-Year Experience at a Large Referral Center. Clin Infect Dis 48:1577–1579.

18. Rey MM, Bonk MP, Hadjiliadis D. 2019. Cystic Fibrosis: Emerging Understanding and Therapies. Annu Rev Med 70:197–210.

19. Lyczak JB, Cannon CL, Pier GB. 2002. Lung Infections Associated with Cystic Fibrosis. Clinical Microbiology Reviews 15:194–222.

20. Uehlinger S, Schwager S, Bernier SP, Riedel K, Nguyen DT, Sokol PA, Eberl L. 2009. Identification of Specific and Universal Virulence Factors in Burkholderia cenocepacia Strains by Using Multiple Infection Hosts. Infect Immun 77:4102–4110.

21. O'Grady EP, Sokol PA. 2011. Burkholderia cenocepacia Differential Gene Expression during Host–Pathogen Interactions and Adaptation to the Host Environment. Front Cell Infect Microbiol 1.

22. Garcia BA, Carden JL, Goodwin DL, Smith TA, Gaggar A, Leon K, Antony VB, Rowe SM, Solomon GM. 2018. Implementation of a successful eradication protocol for Burkholderia Cepacia complex in cystic fibrosis patients. BMC Pulm Med 18:35.

23. LiPUMA JJ, Spilker T, Gill LH, Campbell PW, Liu L, Mahenthiralingam E. 2001. Disproportionate Distribution of Burkholderia cepacia Complex Species and Transmissibility Markers in Cystic Fibrosis. Am J Respir Crit Care Med 164:92–96.

24. LiPuma JJ. 2010. The Changing Microbial Epidemiology in Cystic Fibrosis. Clin Microbiol Rev 23:299–323.

25. Tablan OC, Martone WJ, Doershuk CF, Stern RC, Thomassen MJ, Klinger JD, White JW, Carson LA, Jarvis WR. 1987. Colonization of the Respiratory Tract with Pseudomonas cepacia in Cystic Fibrosis. Chest 91:527–532.

26. Sajjan US, Sun L, Goldstein R, Forstner JF. 1995. Cable (cbl) type II pili of cystic fibrosis-associated Burkholderia (Pseudomonas) cepacia: nucleotide sequence of the cblA major subunit pilin gene and novel morphology of the assembled appendage fibers. J Bacteriol 177:1030–1038.

27. Ganesan S, Sajjan US. 2012. Host Evasion by Burkholderia cenocepacia. Front Cell Infect Microbiol 1.

28. Conway B-AD, Venu V, Speert DP. 2002. Biofilm Formation and Acyl Homoserine Lactone Production in the Burkholderia cepacia Complex. J Bacteriol 184:5678–5685.

29. Desai M. 1998. Increasing resistance of planktonic and biofilm cultures of Burkholderia cepacia to ciprofloxacin and ceftazidime during exponential growth. Journal of Antimicrobial Chemotherapy 42:153–160.

30. Golini G, Favari F, Marchetti F, Fontana R. 2004. Bacteriostatic and bactericidal activity of levofloxacin against clinical isolates from cystic fibrosis patients. Eur J Clin Microbiol Infect Dis 23:798–800.

31. Peeters E, Nelis HJ, Coenye T. 2009. In vitro activity of ceftazidime, ciprofloxacin, meropenem, minocycline, tobramycin and trimethoprim/sulfamethoxazole against planktonic and sessile Burkholderia cepacia complex bacteria. Journal of Antimicrobial Chemotherapy 64:801–809.

32. Guglierame P, Pasca MR, De Rossi E, Buroni S, Arrigo P, Manina G, Riccardi G. 2006. Efflux pump genes of the resistance-nodulation-division family in Burkholderia cenocepacia genome. BMC Microbiol 6:66.

33. Vinion-Dubiel AD, Spilker T, Dean CR, Monteil H, LiPuma JJ, Goldberg JB. 2004. Correlation of wbiI Genotype, Serotype, and Isolate Source within Species of the Burkholderia cepacia Complex. J Clin Microbiol 42:4121–4126.

34. Loutet SA, Valvano MA. 2011. Extreme Antimicrobial Peptide and Polymyxin B Resistance in the Genus Burkholderia. Front Microbiol 2:159.

35. Rhodes KA, Schweizer HP. 2016. Antibiotic resistance in Burkholderia species. Drug Resistance Updates 28:82–90.

36. Lefebre MD, Valvano MA. 2001. In vitro resistance of Burkholderia cepacia complex isolates to reactive oxygen species in relation to catalase and superoxide dismutase production. Microbiology, 147:97–109.

37. Riedel K, Arevalo-Ferro C, Reil G, Görg A, Lottspeich F, Eberl L. 2003. Analysis of the quorum-sensing regulon of the opportunistic pathogen Burkholderia cepacia H111 by proteomics. ELECTROPHORESIS 24:740–750.

38. Venturi V, Friscina A, Bertani I, Devescovi G, Aguilar C. 2004. Quorum sensing in the Burkholderia cepacia complex. Research in Microbiology 155:238–244.

39. Lewenza S, Sokol PA. 2001. Regulation of Ornibactin Biosynthesis andN-Acyl-l-Homoserine Lactone Production by CepR in Burkholderia cepacia. Journal of Bacteriology 183:2212–2218.

40. Sokol PA, Darling P, Lewenza S, Corbett CR, Kooi CD. 2000. Identification of a Siderophore Receptor Required for Ferric Ornibactin Uptake in Burkholderia cepacia. Infection and Immunity 68:6554–6560.

41. Glendinning KJ, Parsons YN, Duangsonk K, Hales BA, Humphreys D, Hart CA, Winstanley C. 2004. Sequence divergence in type III secretion gene clusters of the Burkholderia cepacia complex. FEMS Microbiology Letters 235:229–235.

42. Coenye T, LiPuma JJ, Henry D, Hoste B, Vandemeulebroecke K, Gillis M, Speert DP, Vandamme P. 2001. Burkholderia cepacia genomovar VI, a new member of the Burkholderia cepacia complex isolated from cystic fibrosis patients. International Journal of Systematic and Evolutionary Microbiology 51:271–279.

43. Vermis K, Coenye T, LiPuma JJ, Mahenthiralingam E, Nelis HJ, Vandamme P. 2004. Proposal to accommodate Burkholderia cepacia genomovar VI as Burkholderia dolosa sp. nov. International Journal of Systematic and Evolutionary Microbiology, 54:689–691.

44. Biddick R, Spilker T, Martin A, LiPuma JJ. 2003. Evidence of transmission of *Burkholderia cepacia* , *Burkholderia multivorans* and *Burkholderia dolosa* among persons with cystic fibrosis. FEMS Microbiology Letters 228:57–62.

45. Kalish LA, Waltz DA, Dovey M, Potter-Bynoe G, McAdam AJ, LiPuma JJ, Gerard C, Goldmann D. 2006. Impact of Burkholderia dolosa on Lung Function and Survival in Cystic Fibrosis. Am J Respir Crit Care Med 173:421–425.

46. Caraher E, Duff C, Mullen T, Mc Keon S, Murphy P, Callaghan M, McClean S. 2007. Invasion and biofilm formation of Burkholderia dolosa is comparable with Burkholderia cenocepacia and Burkholderia multivorans. Journal of Cystic Fibrosis 6:49–56.

47. Sahl JW, Vazquez AJ, Hall CM, Busch JD, Tuanyok A, Mayo M, Schupp JM, Lummis M, Pearson T, Shippy K, Colman RE, Allender CJ, Theobald V, Sarovich DS, Price EP, Hutcheson A, Korlach J, LiPuma JJ, Ladner J, Lovett S, Koroleva G, Palacios G, Limmathurotsakul D, Wuthiekanun V, Wongsuwan G, Currie BJ, Keim P, Wagner DM. 2016. The Effects of Signal Erosion and Core Genome Reduction on the Identification of Diagnostic Markers. mBio 7.

48. Butler D. 2012. Viral research faces clampdown. Nature News 490:456.

49. Whitmore A. 1913. An Account of a Glanders-like Disease occurring in Rangoon. J Hyg (Lond) 13:1-34.1.

50. Singh M, Mahmood M. 2017. Melioidosis: the great mimicker. Journal of Community Hospital Internal Medicine Perspectives 7:245–247.

51. Currie BJ, Ward L, Cheng AC. 2010. The Epidemiology and Clinical Spectrum of Melioidosis: 540 Cases from the 20 Year Darwin Prospective Study. PLoS Negl Trop Dis 4.

52. Chaowagul W, White NJ, Dance DAB, Wattanagoon Y, Naigowit P, Davis TME, Looareesuwan S, Pitakwatchara N. 1989. Melioidosis: A Major Cause of Community-Acquired Septicemia in Northeastern Thailand. The Journal of Infectious Diseases 159:890–899.

53. Smith MD, Angus BJ, Wuthiekanun V, White NJ. 1997. Arabinose assimilation defines a nonvirulent biotype of Burkholderia pseudomallei. Infect Immun 65:4319–4321.

54. Brett PJ, DeShazer D, Woods DE. 1998. Burkholderia thailandensis sp. nov., a Burkholderia pseudomallei-like species. International Journal of Systematic Bacteriology 48:317–320.

55. Yu Y, Kim HS, Chua HH, Lin CH, Sim SH, Lin D, Derr A, Engels R, DeShazer D, Birren B, Nierman WC, Tan P. 2006. Genomic patterns of pathogen evolution revealed by comparison of Burkholderia pseudomallei, the causative agent of melioidosis, to avirulent Burkholderia thailandensis. BMC Microbiol 6:46.

56. Haraga A, West TE, Brittnacher MJ, Skerrett SJ, Miller SI. 2008. Burkholderia thailandensis as a Model System for the Study of the Virulence-Associated Type III Secretion System of Burkholderia pseudomallei. Infection and Immunity 76:5402–5411.

57. Nierman WC, DeShazer D, Kim HS, Tettelin H, Nelson KE, Feldblyum T, Ulrich RL, Ronning CM, Brinkac LM, Daugherty SC, Davidsen TD, Deboy RT, Dimitrov G, Dodson RJ, Durkin AS, Gwinn ML, Haft DH, Khouri H, Kolonay JF, Madupu R, Mohammoud Y, Nelson WC, Radune D, Romero CM, Sarria S, Selengut J, Shamblin C, Sullivan SA, White O, Yu Y, Zafar N, Zhou L, Fraser CM. 2004. Structural flexibility in the Burkholderia mallei genome. Proc Natl Acad Sci U S A 101:14246–14251.

58. Song H, Hwang J, Yi H, Ulrich RL, Yu Y, Nierman WC, Kim HS. 2010. The Early Stage of Bacterial Genome-Reductive Evolution in the Host. PLoS Pathog 6.

59. Losada L, Ronning CM, DeShazer D, Woods D, Fedorova N, Stanley Kim H, Shabalina SA, Pearson TR, Brinkac L, Tan P, Nandi T, Crabtree J, Badger J, Beckstrom-Sternberg S, Saqib M, Schutzer SE, Keim P, Nierman WC. 2010. Continuing Evolution of Burkholderia mallei Through Genome Reduction and Large-Scale Rearrangements. Genome Biol Evol 2:102–116.

60. Van Melderen L. 2010. Toxin–antitoxin systems: why so many, what for? Current Opinion in Microbiology 13:781–785.

61. Unterholzner SJ, Poppenberger B, Rozhon W. 2013. Toxin–antitoxin systems. Mobile Genetic Elements 3:e26219.

62. Gerdes K, Christensen SK, Løbner-Olesen A. 2005. Prokaryotic toxin–antitoxin stress response loci. Nat Rev Microbiol 3:371–382.

63. Jensen RB, Gerdes K. 1995. Programmed cell death in bacteria: proteic plasmid stabilization systems. Molecular Microbiology 17:205–210.

64. Gerdes K, Rasmussen PB, Molin S. 1986. Unique type of plasmid maintenance function: postsegregational killing of plasmid-free cells. Proceedings of the National Academy of Sciences 83:3116–3120.

65. Dy RL, Richter C, Salmond GPC, Fineran PC. 2014. Remarkable Mechanisms in Microbes to Resist Phage Infections. Annu Rev Virol 1:307–331.

66. Harms A, Maisonneuve E, Gerdes K. 2016. Mechanisms of bacterial persistence during stress and antibiotic exposure. Science 354.

67. Travisano M, Velicer GJ. 2004. Strategies of microbial cheater control. Trends in Microbiology 12:72–78.

68. Strassmann JE, Gilbert OM, Queller DC. 2011. Kin Discrimination and Cooperation in Microbes. Annu Rev Microbiol 65:349–367.

69. Kirkup BC, Riley MA. 2004. Antibiotic-mediated antagonism leads to a bacterial game of rock–paper–scissors in vivo. 6981. Nature 428:412–414.

70. Stefanic P, Kraigher B, Lyons NA, Kolter R, Mandic-Mulec I. 2015. Kin discrimination between sympatric *Bacillus subtilis* isolates. Proc Natl Acad Sci USA 112:14042–14047.

71. Harms A, Brodersen DE, Mitarai N, Gerdes K. 2018. Toxins, Targets, and Triggers: An Overview of Toxin-Antitoxin Biology. Molecular Cell https://doi.org/10.1016/j.molcel.2018.01.003.

72. Pandey DP, Gerdes K. 2005. Toxin–antitoxin loci are highly abundant in free-living but lost from host-associated prokaryotes. Nucleic Acids Res 33:966–976.

73. Leplae R, Geeraerts D, Hallez R, Guglielmini J, Drèze P, Van Melderen L. 2011. Diversity of bacterial type II toxin–antitoxin systems: a comprehensive search and functional analysis of novel families. Nucleic Acids Res 39:5513–5525.

74. Rainey PB, Travisano M. 1998. Adaptive radiation in a heterogeneous environment. 6688. Nature 394:69–72.

75. Spiers AJ, Bohannon J, Gehrig SM, Rainey PB. 2003. Biofilm formation at the air-liquid interface by the Pseudomonas fluorescens SBW25 wrinkly spreader requires an acetylated form of cellulose. Mol Microbiol 50:15–27.

76. Boles BR, Thoendel M, Singh PK. 2004. Self-generated diversity produces "insurance effects" in biofilm communities. Proc Natl Acad Sci U S A 101:16630–16635.

77. Nadell CD, Bassler BL, Levin SA. 2008. Observing bacteria through the lens of social evolution. J Biol 7:27.

78. Nakatsuji T, Chen TH, Narala S, Chun KA, Two AM, Yun T, Shafiq F, Kotol PF, Bouslimani A, Melnik AV, Latif H, Kim J-N, Lockhart A, Artis K, David G, Taylor P, Streib J, Dorrestein PC, Grier A, Gill SR, Zengler K, Hata TR, Leung DYM, Gallo RL. 2017. Antimicrobials from human skin commensal bacteria protect against Staphylococcus aureus and are deficient in atopic dermatitis. Sci Transl Med 9.

79. Monod J. 1949. The growth of bacterial cultures. Annu Rev Microbiol 3:371–394.

80. Case TJ, Gilpin ME. 1974. Interference Competition and Niche Theory. Proceedings of the National Academy of Sciences of the United States of America 71:3073–3077.

81. Mao J, Blanchard AE, Lu T. 2015. Slow and Steady Wins the Race: A Bacterial Exploitative Competition Strategy in Fluctuating Environments. ACS Synth Biol 4:240–248.

82. Schoener TW. 1983. Field Experiments on Interspecific Competition. The American Naturalist 122:240–285.

83. Gardner A, West SA. 2006. Demography, altruism, and the benefits of budding. Journal of Evolutionary Biology 19:1707–1716.

84. Hamilton WD. 1964. The genetical evolution of social behaviour. I. Journal of Theoretical Biology 7:1–16.

85. Bijma P, Wade MJ. 2008. The joint effects of kin, multilevel selection and indirect genetic effects on response to genetic selection. Journal of Evolutionary Biology 21:1175–1188.

86. Kümmerli R, Berg PVD, Griffin AS, West SA, Gardner A. 2010. Repression of competition favours cooperation: experimental evidence from bacteria. Journal of Evolutionary Biology 23:699–706.

87. Van Dyken JD. 2010. THE COMPONENTS OF KIN COMPETITION. Evolution 64:2840–2854.

88. Van Dyken JD, Wade MJ. 2012. Origins of altruism diversity I: The diverse ecological roles of altruistic strategies and their evolutionary responses to local competition. Evolution 66:2484–2497.

89. Wade MJ. 1985. Soft Selection, Hard Selection, Kin Selection, and Group Selection. The American Naturalist 125:61–73.

90. Lyons NA, Kraigher B, Stefanic P, Mandic-Mulec I, Kolter R. 2016. A Combinatorial Kin Discrimination System in Bacillus subtilis. Current Biology 26:733–742.

91. Gardner A, West SA. 2010. Greenbeards. Evolution 64:25–38.

92. Dawkins R. 1982. The extended phenotype: the gene as the unit of selection. Freeman, Oxford [Oxfordshire] ;

93. Bernard Williams. 2014. The Selfish Gene, by Richard Dawkins, New Scientist (1976). Princeton University Press.

94. West SA, Murray MG, Machado CA, Griffin AS, Herre EA. 2001. Testing Hamilton's rule with competition between relatives. Nature 409:510–513.

95. Gardner A, West SA. 2004. Spite and the scale of competition. Journal of Evolutionary Biology 17:1195–1203.

96. Gardner A, West SA, Barton NH. 2007. The Relation between Multilocus Population Genetics and Social Evolution Theory. The American Naturalist 169:207–226.

97. Stacy A, McNally L, Darch SE, Brown SP, Whiteley M. 2016. The biogeography of polymicrobial infection. Nat Rev Microbiol 14:93–105.

98. Nomura M. 1963. Mode of Action of Colicines. Cold Spring Harb Symp Quant Biol 28:315–324.

99. James R, Kleanthous C, Moore GR. 1996. The biology of E colicins: paradigms and paradoxes. Microbiology, 142:1569–1580.

100. Luirink J, Clark DM, Ras J, Verschoor EJ, Stegehuis F, de Graaf FK, Oudega B. 1989. pCloDF13-encoded bacteriocin release proteins with shortened carboxyl-terminal segments are lipid modified and processed and function in release of cloacin DF13 and apparent host cell lysis. J Bacteriol 171:2673–2679.

101. Herranz C, Driessen AJM. 2005. Sec-Mediated Secretion of Bacteriocin Enterocin P by Lactococcus lactis. Appl Environ Microbiol 71:1959–1963.

102. McCormick JK, Worobo RW, Stiles ME. 1996. Expression of the antimicrobial peptide carnobacteriocin B2 by a signal peptide-dependent general secretory pathway. Appl Environ Microbiol 62:4095–4099.

103. Atanaskovic I, Kleanthous C. 2019. Tools and Approaches for Dissecting Protein Bacteriocin Import in Gram-Negative Bacteria. Front Microbiol 10:646.

104. Riley MA, Wertz JE. 2002. Bacteriocins: Evolution, Ecology, and Application. Annu Rev Microbiol 56:117–137.

105. Panina I, Krylov N, Nolde D, Efremov R, Chugunov A. 2020. Environmental and dynamic effects explain how nisin captures membrane-bound lipid II. Sci Rep 10:8821.

106. Chen H, Tian F, Li S, Xie Y, Zhang H, Chen W. 2012. Cloning and heterologous expression of a bacteriocin sakacin P from Lactobacillus sakei in Escherichia coli. Appl Microbiol Biotechnol 94:1061–1068.

107. Denkovskienė E, Paškevičius Š, Misiūnas A, Stočkūnaitė B, Starkevič U, Vitkauskienė A, Hahn-Löbmann S, Schulz S, Giritch A, Gleba Y, Ražanskienė A. 2019. Broad and Efficient Control of Klebsiella Pathogens by Peptidoglycan-Degrading and Pore-Forming Bacteriocins Klebicins. Sci Rep 9:15422.

108. Sabo SS, Converti A, Ichiwaki S, Oliveira RPS. 2019. Bacteriocin production by Lactobacillus plantarum ST16Pa in supplemented whey powder formulations. Journal of Dairy Science 102:87–99.

109. Pandey N, Malik RK, Kaushik JK, Singroha G. 2013. Gassericin A: a circular bacteriocin produced by Lactic acid bacteria Lactobacillus gasseri. World J Microbiol Biotechnol 29:1977–1987.

110. Kim YC, Tarr AW, Penfold CN. 2014. Colicin import into E. coli cells: A model system for insights into the import mechanisms of bacteriocins. Biochimica et Biophysica Acta (BBA) - Molecular Cell Research 1843:1717–1731.

111. McCaughey LC, Grinter R, Josts I, Roszak AW, Waløen KI, Cogdell RJ, Milner J, Evans T, Kelly S, Tucker NP, Byron O, Smith B, Walker D. 2014. Lectin-Like Bacteriocins from Pseudomonas spp. Utilise D-Rhamnose Containing Lipopolysaccharide as a Cellular Receptor. PLoS Pathog 10:e1003898.

112. McCaughey LC, Josts I, Grinter R, White P, Byron O, Tucker NP, Matthews JM, Kleanthous C, Whitchurch CB, Walker D. 2016. Discovery, characterization and in vivo activity of pyocin SD2, a protein antibiotic from Pseudomonas aeruginosa. Biochem J 473:2345–2358.

113. Govan JR, Harris G. 1985. Typing of Pseudomonas cepacia by bacteriocin susceptibility and production. J Clin Microbiol 22:490–494.

114. Knappe TA, Linne U, Zirah S, Rebuffat S, Xie X, Marahiel MA. 2008. Isolation and Structural Characterization of Capistruin, a Lasso Peptide Predicted from the Genome Sequence of Burkholderia thailandensis E264. J Am Chem Soc 130:11446–11454.

115. Bakkal S, Robinson SM, Ordonez CL, Waltz DA, Riley MA. 2010. Role of bacteriocins in mediating interactions of bacterial isolates taken from cystic fibrosis patients. Microbiology 156:2058–2067.

116. Ghequire MGK, Canck E, Wattiau P, Winge I, Loris R, Coenye T, Mot R. 2013. Antibacterial activity of a lectin-like Burkholderia cenocepacia protein. Microbiologyopen 2:566–575.

117. Ghequire MGK, De Mot R. 2015. Distinct colicin M-like bacteriocin-immunity pairs in Burkholderia. Sci Rep 5.

118. Soltani S, Hammami R, Cotter PD, Rebuffat S, Said LB, Gaudreau H, Bédard F, Biron E, Drider D, Fliss I. 2021. Bacteriocins as a new generation of antimicrobials: toxicity aspects and regulations. FEMS Microbiology Reviews 45.

119. Meade E, Slattery MA, Garvey M. 2020. Bacteriocins, Potent Antimicrobial Peptides and the Fight against Multi Drug Resistant Species: Resistance Is Futile? Antibiotics (Basel) 9:32.

120. 2007. The spatial distribution of microbes in the environment. Springer, Dordrecht.

121. Kadam SV, Velicer GJ. 2006. Variable patterns of density-dependent survival in social bacteria. Behavioral Ecology 17:833–838.

122. Mølbak L, Molin S, Kroer N. 2007. Root growth and exudate production define the frequency of horizontal plasmid transfer in the Rhizosphere. FEMS Microbiology Ecology 59:167–176.

123. Krašovec R, Richards H, Gifford DR, Belavkin RV, Channon A, Aston E, McBain AJ, Knight CG. 2018. Opposing effects of final population density and stress on Escherichia coli mutation rate. ISME J 12:2981–2987.

124. Tecon R, Ebrahimi A, Kleyer H, Levi SE, Or D. 2018. Cell-to-cell bacterial interactions promoted by drier conditions on soil surfaces. PNAS 115:9791–9796.

125. Stubbendieck RM, Straight PD. 2016. Multifaceted Interfaces of Bacterial Competition. J Bacteriol 198:2145–2155.

126. Nudleman E, Wall D, Kaiser D. 2005. Cell-to-Cell Transfer of Bacterial Outer Membrane Lipoproteins. Science 309:125–127.

127. Dey A, Wall D. 2014. A Genetic Screen in Myxococcus xanthus Identifies Mutants That Uncouple Outer Membrane Exchange from a Downstream Cellular Response. Journal of Bacteriology 196:4324–4332.

128. Pathak DT, Wei X, Dey A, Wall D. 2013. Molecular recognition by a polymorphic cell surface receptor governs cooperative behaviors in bacteria. PLoS Genet 9:e1003891.

129. Vassallo CN, Cao P, Conklin A, Finkelstein H, Hayes CS, Wall D. 2017. Infectious polymorphic toxins delivered by outer membrane exchange discriminate kin in myxobacteria. eLife 6:e29397.

130. Schwechheimer C, Kuehn MJ. 2015. Outer-membrane vesicles from Gram-negative bacteria: biogenesis and functions. Nat Rev Microbiol 13:605–619.

131. Nieves W, Petersen H, Judy BM, Blumentritt CA, Russell-Lodrigue K, Roy CJ, Torres AG, Morici LA. 2014. A Burkholderia pseudomallei Outer Membrane Vesicle Vaccine Provides Protection against Lethal Sepsis. Clin Vaccine Immunol 21:747–754.

132. Baker SM, Davitt CJH, Motyka N, Kikendall NL, Russell-Lodrigue K, Roy CJ, Morici LA. 2017. A Burkholderia pseudomallei Outer Membrane Vesicle Vaccine Provides Cross Protection against Inhalational Glanders in Mice and Non-Human Primates. Vaccines (Basel) 5.

133. Williams SG, Varcoe LT, Attridge SR, Manning PA. 1996. Vibrio cholerae Hcp, a secreted protein coregulated with HlyA. Infection and Immunity 64:283–289.

134. Bladergroen MR, Badelt K, Spaink HP. 2003. Infection-Blocking Genes of a Symbiotic Rhizobium leguminosarum Strain That Are Involved in Temperature-Dependent Protein Secretion. MPMI 16:53–64.

135. Pukatzki S, Ma AT, Sturtevant D, Krastins B, Sarracino D, Nelson WC, Heidelberg JF, Mekalanos JJ. 2006. Identification of a conserved bacterial protein secretion system in Vibrio cholerae using the Dictyostelium host model system. PNAS 103:1528–1533.

136. Boyer F, Fichant G, Berthod J, Vandenbrouck Y, Attree I. 2009. Dissecting the bacterial type VI secretion system by a genome wide in silico analysis: what can be learned from available microbial genomic resources? BMC Genomics 10:104.

137. Chang Y, Rettberg LA, Ortega DR, Jensen GJ. 2017. In vivo structures of an intact type VI secretion system revealed by electron cryotomography. EMBO Rep 18:1090–1099.

138. Silverman JM, Brunet YR, Cascales E, Mougous JD. 2012. Structure and Regulation of the Type VI Secretion System. Annu Rev Microbiol 66:453–472.

139. Cascales E, Cambillau C. 2012. Structural biology of type VI secretion systems. Philos Trans R Soc Lond B Biol Sci 367:1102–1111.

140. Records AR. 2011. The Type VI Secretion System: A Multipurpose Delivery System with a Phage-Like Machinery. MPMI 24:751–757.

141. Quentin D, Ahmad S, Shanthamoorthy P, Mougous JD, Whitney JC, Raunser S. 2018. Mechanism of loading and translocation of type VI secretion system effector Tse6. Nat Microbiol 3:1142–1152.

142. Li M, Le Trong I, Carl MA, Larson ET, Chou S, De Leon JA, Dove SL, Stenkamp RE, Mougous JD. 2012. Structural Basis for Type VI Secretion Effector Recognition by a Cognate Immunity Protein. PLoS Pathog 8:e1002613.

143. Monjarás Feria J, Valvano MA. 2020. An Overview of Anti-Eukaryotic T6SS Effectors. Front Cell Infect Microbiol 10:584751.

144. Burtnick MN, DeShazer D, Nair V, Gherardini FC, Brett PJ. 2010. Burkholderia mallei Cluster 1 Type VI Secretion Mutants Exhibit Growth and Actin Polymerization Defects in RAW 264.7 Murine Macrophages. Infect Immun 78:88–99.

145. Schwab U, Abdullah LH, Perlmutt OS, Albert D, Davis CW, Arnold RR, Yankaskas JR, Gilligan P, Neubauer H, Randell SH, Boucher RC. 2014. Localization of Burkholderia cepacia Complex Bacteria in Cystic Fibrosis Lungs and Interactions with Pseudomonas aeruginosa in Hypoxic Mucus. Infect Immun 82:4729–4745.

146. Hood RD, Singh P, Hsu F, Güvener T, Carl MA, Trinidad RRS, Silverman JM, Ohlson BB, Hicks KG, Plemel RL, Li M, Schwarz S, Wang WY, Merz AJ, Goodlett DR, Mougous JD. 2010. A Type VI Secretion System of Pseudomonas aeruginosa Targets a Toxin to Bacteria. Cell Host Microbe 7:25–37.

147. Trunk K, Peltier J, Liu Y-C, Dill BD, Walker L, Gow NAR, Stark MJR, Quinn J, Strahl H, Trost M, Coulthurst SJ. 2018. The Type VI secretion system deploys anti-fungal effectors against microbial competitors. Nat Microbiol 3:920–931.

148. Alteri CJ, Mobley HLT. 2016. The Versatile Type VI Secretion System. Microbiol Spectr 4:10.1128/microbiolspec.VMBF-0026–2015.

149. Russell AB, Peterson SB, Mougous JD. 2014. Type VI secretion effectors: poisons with a purpose. Nat Rev Microbiol 12:137–148.

150. Russell AB, Singh P, Brittnacher M, Bui NK, Hood RD, Carl MA, Agnello DM, Schwarz S, Goodlett DR, Vollmer W, Mougous JD. 2012. A widespread bacterial type VI secretion effector superfamily identified using a heuristic approach. Cell Host Microbe 11:538–549.

151. Whitney JC, Chou S, Russell AB, Biboy J, Gardiner TE, Ferrin MA, Brittnacher M, Vollmer W, Mougous JD. 2013. Identification, Structure, and Function of a Novel Type VI Secretion Peptidoglycan Glycoside Hydrolase Effector-Immunity Pair. J Biol Chem 288:26616–26624.

152. Chou S, Bui NK, Russell AB, Lexa K, Gardiner TE, LeRoux M, Vollmer W, Mougous JD. 2012. Structure of a peptidoglycan amidase effector targeted to Gram-negative bacteria by the type VI secretion system. Cell Rep 1:656–664.

153. Russell AB, LeRoux M, Hathazi K, Agnello DM, Ishikawa T, Wiggins PA, Wai SN, Mougous JD. 2013. Diverse type VI secretion phospholipases are functionally plastic antibacterial effectors. Nature 496:508–512.

154. Whitney JC, Quentin D, Sawai S, LeRoux M, Harding BN, Ledvina HE, Tran BQ, Robinson H, Goo YA, Goodlett DR, Raunser S, Mougous JD. 2015. An Interbacterial NAD(P)+ Glycohydrolase Toxin Requires Elongation Factor Tu for Delivery to Target Cells. Cell 163:607–619.

155. Tang JY, Bullen NP, Ahmad S, Whitney JC. 2018. Diverse NADase effector families mediate interbacterial antagonism via the type VI secretion system. Journal of Biological Chemistry 293:1504–1514.

156. Coulthurst S 2019. The Type VI secretion system: a versatile bacterial weapon. Microbiology 165:503–515.

157. Ting S-Y, Bosch DE, Mangiameli SM, Radey MC, Huang S, Park Y-J, Kelly KA, Filip SK, Goo YA, Eng JK, Allaire M, Veesler D, Wiggins PA, Peterson SB, Mougous JD. 2018. Bifunctional Immunity Proteins Protect Bacteria against FtsZ-Targeting ADP-Ribosylating Toxins. Cell 175:1380-1392.e14.

158. Fridman CM, Keppel K, Gerlic M, Bosis E, Salomon D. 2020. A comparative genomics methodology reveals a widespread family of membrane-disrupting T6SS effectors. Nat Commun 11:1085.

159. Allsopp LP, Bernal P, Nolan LM, Filloux A. 2020. Causalities of war: The connection between type VI secretion system and microbiota. Cell Microbiol 22:e13153.

160. Navarro-Garcia F, Ruiz-Perez F, Cataldi Á, Larzábal M. 2019. Type VI Secretion System in Pathogenic Escherichia coli: Structure, Role in Virulence, and Acquisition. Front Microbiol 10.

161. Koskiniemi S, Lamoureux JG, Nikolakakis KC, t'Kint de Roodenbeke C, Kaplan MD, Low DA, Hayes CS. 2013. Rhs proteins from diverse bacteria mediate intercellular competition. Proc Natl Acad Sci U S A 110:7032–7037.

162. Unterweger D, Kitaoka M, Miyata ST, Bachmann V, Brooks TM, Moloney J, Sosa O, Silva D, Duran-Gonzalez J, Provenzano D, Pukatzki S. 2012. Constitutive Type VI Secretion System Expression Gives Vibrio cholerae Intra- and Interspecific Competitive Advantages. PLoS One 7:e48320.

163. Kirchberger PC, Unterweger D, Provenzano D, Pukatzki S, Boucher Y. 2017. Sequential displacement of Type VI Secretion System effector genes leads to evolution of diverse immunity gene arrays in Vibrio cholerae. Sci Rep 7:45133.

164. Alteri CJ, Himpsl SD, Zhu K, Hershey HL, Musili N, Miller JE, Mobley HLT. 2017. Subtle variation within conserved effector operon gene products contributes to T6SS-mediated killing and immunity. PLoS Pathog 13:e1006729.

165. Pilatz S, Breitbach K, Hein N, Fehlhaber B, Schulze J, Brenneke B, Eberl L, Steinmetz I. 2006. Identification of Burkholderia pseudomallei Genes Required for the Intracellular Life Cycle and In Vivo Virulence. Infect Immun 74:3576–3586.

166. Shalom G, Shaw JG, Thomas MS. 2007. In vivo expression technology identifies a type VI secretion system locus in Burkholderia pseudomallei that is induced upon invasion of macrophages. Microbiology, 153:2689–2699.

167. Schell MA, Ulrich RL, Ribot WJ, Brueggemann EE, Hines HB, Chen D, Lipscomb L, Kim HS, Mrázek J, Nierman WC, DeShazer D. 2007. Type VI secretion is a major virulence determinant in Burkholderia mallei. Molecular Microbiology 64:1466–1485.

168. Burtnick MN, Brett PJ, Harding SV, Ngugi SA, Ribot WJ, Chantratita N, Scorpio A, Milne TS, Dean RE, Fritz DL, Peacock SJ, Prior JL, Atkins TP, DeShazer D. 2011. The Cluster 1 Type VI Secretion System Is a Major Virulence Determinant in Burkholderia pseudomallei. Infect Immun 79:1512–1525.

169. Hunt TA, Kooi C, Sokol PA, Valvano MA. 2004. Identification of Burkholderia cenocepacia Genes Required for Bacterial Survival In Vivo. Infect Immun 72:4010–4022.

170. Spiewak HL, Shastri S, Zhang L, Schwager S, Eberl L, Vergunst AC, Thomas MS. 2019. Burkholderia cenocepacia utilizes a type VI secretion system for bacterial competition. Microbiologyopen 8.

171. Green ER, Mecsas J. 2016. Bacterial Secretion Systems – An overview. Microbiol Spectr 4:10.1128/microbiolspec.VMBF-0012–2015.

172. Souza DP, Oka GU, Alvarez-Martinez CE, Bisson-Filho AW, Dunger G, Hobeika L, Cavalcante NS, Alegria MC, Barbosa LRS, Salinas RK, Guzzo CR, Farah CS. 2015. Bacterial killing via a type IV secretion system. Nat Commun 6:6453.

173. Sgro GG, Oka GU, Souza DP, Cenens W, Bayer-Santos E, Matsuyama BY, Bueno NF, dos Santos TR, Alvarez-Martinez CE, Salinas RK, Farah CS. 2019. Bacteria-Killing Type IV Secretion Systems. Front Microbiol 10.

174. Wallden K, Rivera-Calzada A, Waksman G. 2010. Type IV secretion systems: versatility and diversity in function. Cell Microbiol 12:1203–1212.

175. Fronzes R, Christie PJ, Waksman G. 2009. The structural biology of type IV secretion systems. Nat Rev Microbiol 7:10.1038/nrmicro2218.

176. Cao Z, Casabona MG, Kneuper H, Chalmers JD, Palmer T. 2016. The type VII secretion system of Staphylococcus aureus secretes a nuclease toxin that targets competitor bacteria. Nat Microbiol 2:1–11.

177. Ulhuq FR, Gomes MC, Duggan GM, Guo M, Mendonca C, Buchanan G, Chalmers JD, Cao Z, Kneuper H, Murdoch S, Thomson S, Strahl H, Trost M, Mostowy S, Palmer T. 2020. A membrane-depolarizing toxin substrate of the Staphylococcus aureus type VII secretion system mediates intraspecies competition. PNAS 117:20836–20847.

178. Chatterjee A, Willett JLE, Dunny GM, Duerkop BA. 2021. Phage infection and sub-lethal antibiotic exposure mediate Enterococcus faecalis type VII secretion system dependent inhibition of bystander bacteria. PLOS Genetics 17:e1009204.

179. Kneuper H, Cao ZP, Twomey KB, Zoltner M, Jäger F, Cargill JS, Chalmers J, van der Kooi-Pol MM, van Dijl JM, Ryan RP, Hunter WN, Palmer T. 2014. Heterogeneity in ess transcriptional organization and variable contribution of the Ess/Type VII protein secretion system to virulence across closely related Staphylocccus aureus strains. Mol Microbiol 93:928–943.

180. Garcia EC. 2018. Contact-dependent interbacterial toxins deliver a message. Curr Opin Microbiol 42:40–46.

181. Aoki SK, Pamma R, Hernday AD, Bickham JE, Braaten BA, Low DA. 2005. Contact-Dependent Inhibition of Growth in Escherichia coli. Science 309:1245–1248.

182. Mazar J, Cotter PA. 2007. New insight into the molecular mechanisms of two-partner secretion. Trends in Microbiology 15:508–515.

183. Aoki SK, Diner EJ, de Roodenbeke C t'Kint, Burgess BR, Poole SJ, Braaten BA, Jones AM, Webb JS, Hayes CS, Cotter PA, Low DA. 2010. A widespread family of polymorphic contact-dependent toxin delivery systems in bacteria. Nature 468:439–442.

184. Poole SJ, Diner EJ, Aoki SK, Braaten BA, Roodenbeke C t'Kint de, Low DA, Hayes CS. 2011. Identification of Functional Toxin/Immunity Genes Linked to Contact-Dependent Growth Inhibition (CDI) and Rearrangement Hotspot (Rhs) Systems. PLOS Genetics 7:e1002217.

185. Anderson MS, Garcia EC, Cotter PA. 2012. The Burkholderia bcpAIOB Genes Define Unique Classes of Two-Partner Secretion and Contact Dependent Growth Inhibition Systems. PLOS Genetics 8:e1002877.

186. Lemonnier M, Levin BR, Romeo T, Garner K, Baquero M-R, Mercante J, Lemichez E, Baquero F, Blázquez J. 2008. The evolution of contact-dependent inhibition in non-growing populations of Escherichia coli. Proc Biol Sci 275:3–10.

187. Nikolakakis K, Amber S, Wilbur JS, Diner EJ, Aoki SK, Poole SJ, Tuanyok A, Keim PS, Peacock S, Hayes CS, Low DA. 2012. The toxin/immunity network of Burkholderia pseudomallei contact-dependent growth inhibition (CDI) systems. Mol Microbiol 84:516–529.

188. Perault AI, Cotter PA. 2018. Three Distinct Contact-Dependent Growth Inhibition Systems Mediate Interbacterial Competition by the Cystic Fibrosis Pathogen Burkholderia dolosa. Journal of Bacteriology 200:e00428-18.

189. Willett JLE, Ruhe ZC, Goulding CW, Low DA, Hayes CS. 2015. Contact-Dependent Growth Inhibition (CDI) and CdiB/CdiA Two-Partner Secretion Proteins. Journal of Molecular Biology 427:3754–3765.

190. Ruhe ZC, Subramanian P, Song K, Nguyen JY, Stevens TA, Low DA, Jensen GJ, Hayes CS. 2018. Programmed Secretion Arrest and Receptor-Triggered Toxin Export during Antibacterial Contact-Dependent Growth Inhibition. Cell 175:921-933.e14.

191. Aoki SK, Webb JS, Braaten BA, Low DA. 2009. Contact-Dependent Growth Inhibition Causes Reversible Metabolic Downregulation in Escherichia coli. J Bacteriol 191:1777–1786.

192. Anderson MS, Garcia EC, Cotter PA. 2014. Kind Discrimination and Competitive Exclusion Mediated by Contact-Dependent Growth Inhibition Systems Shape Biofilm Community Structure. PLOS Pathogens 10:e1004076.

193. Myers-Morales T, Oates AE, Byrd MS, Garcia EC. 2019. Burkholderia cepacia Complex Contact-Dependent Growth Inhibition Systems Mediate Interbacterial Competition. J Bacteriol 201.

194. Roussin M, Rabarioelina S, Cluzeau L, Cayron J, Lesterlin C, Salcedo SP, Bigot S. 2019. Identification of a Contact-Dependent Growth Inhibition (CDI) System That Reduces Biofilm Formation and Host Cell Adhesion of Acinetobacter baumannii DSM30011 Strain. Front Microbiol 10.

195. Majerczyk C, Brittnacher M, Jacobs M, Armour CD, Radey M, Schneider E, Phattarasokul S, Bunt R, Greenberg EP. 2014. Global Analysis of the Burkholderia thailandensis Quorum Sensing-Controlled Regulon. Journal of Bacteriology 196:1412–1424.

196. Ocasio AB, Cotter PA. 2019. CDI/CDS system-encoding genes of Burkholderia thailandensis are located in a mobile genetic element that defines a new class of transposon. PLOS Genetics 15:e1007883.

197. Aoki SK, Malinverni JC, Jacoby K, Thomas B, Pamma R, Trinh BN, Remers S, Webb J, Braaten BA, Silhavy TJ, Low DA. 2008. Contact-dependent growth inhibition requires the essential outer membrane protein BamA (YaeT) as the receptor and the inner membrane transport protein AcrB. Mol Microbiol 70:323–340.

198. Beck CM, Willett JLE, Cunningham DA, Kim JJ, Low DA, Hayes CS. 2016. CdiA Effectors from Uropathogenic Escherichia coli Use Heterotrimeric Osmoporins as Receptors to Recognize Target Bacteria. PLOS Pathogens 12:e1005925.

199. Ruhe ZC, Nguyen JY, Xiong J, Koskiniemi S, Beck CM, Perkins BR, Low DA, Hayes CS. 2017. CdiA Effectors Use Modular Receptor-Binding Domains To Recognize Target Bacteria. mBio 8:e00290-17.

200. Ruhe ZC, Wallace AB, Low DA, Hayes CS. 2013. Receptor Polymorphism Restricts Contact-Dependent Growth Inhibition to Members of the Same Species. mBio 4:e00480-13.

201. Willett JLE, Gucinski GC, Fatherree JP, Low DA, Hayes CS. 2015. Contact-dependent growth inhibition toxins exploit multiple independent cell-entry pathways. PNAS 112:11341–11346.

202. Koskiniemi S, Garza-Sánchez F, Edman N, Chaudhuri S, Poole SJ, Manoil C, Hayes CS, Low DA. 2015. Genetic Analysis of the CDI Pathway from Burkholderia pseudomallei 1026b. PLOS ONE 10:e0120265.

203. Myers-Morales T, Sim MMS, DuCote TJ, Garcia EC. 2021. Burkholderia multivorans requires species-specific GltJK for entry of a contact-dependent growth inhibition system protein. Mol Microbiol https://doi.org/10.1111/mmi.14783.

204. Diner EJ, Beck CM, Webb JS, Low DA, Hayes CS. 2012. Identification of a target cell permissive factor required for contact-dependent growth inhibition (CDI). Genes Dev 26:515–525.

205. Jones AM, Garza-Sánchez F, So J, Hayes CS, Low DA. 2017. Activation of contact-dependent antibacterial tRNase toxins by translation elongation factors. PNAS 114:E1951–E1957.

206. Michalska K, Quan Nhan D, Willett JLE, Stols LM, Eschenfeldt WH, Jones AM, Nguyen JY, Koskiniemi S, Low DA, Goulding CW, Joachimiak A, Hayes CS. 2018. Functional plasticity of antibacterial EndoU toxins. Mol Microbiol 109:509–527.

207. Blanchard AE, Celik V, Lu T. 2014. Extinction, coexistence, and localized patterns of a bacterial population with contact-dependent inhibition. BMC Syst Biol 8:23.

208. Bottery MJ, Passaris I, Dytham C, Wood AJ, van der Woude MW. 2019. Spatial Organization of Expanding Bacterial Colonies Is Affected by Contact-Dependent Growth Inhibition. Curr Biol 29:3622-3634.e5.

209. Garcia EC, Anderson MS, Hagar JA, Cotter PA. 2013. Burkholderia BcpA mediates biofilm formation independently of interbacterial contact dependent growth inhibition. Mol Microbiol 89:1213–1225.

210. Garcia EC, Perault AI, Marlatt SA, Cotter PA. 2016. Interbacterial signaling via Burkholderia contact-dependent growth inhibition system proteins. Proc Natl Acad Sci U S A 113:8296–8301.

211. Allen JP, Hauser AR. 2019. Diversity of Contact-Dependent Growth Inhibition Systems of Pseudomonas aeruginosa. J Bacteriol 201:e00776-18.

212. Mercy C, Ize B, Salcedo SP, de Bentzmann S, Bigot S. 2016. Functional Characterization of Pseudomonas Contact Dependent Growth Inhibition (CDI) Systems. PLoS One 11:e0147435.

213. Allen JP, Ozer EA, Minasov G, Shuvalova L, Kiryukhina O, Satchell KJF, Hauser AR. 2020. A comparative genomics approach identifies contact-dependent growth inhibition as a virulence determinant. Proc Natl Acad Sci U S A 117:6811–6821.

214. Melvin JA, Gaston JR, Phillips SN, Springer MJ, Marshall CW, Shanks RMQ, Bomberger JM. 2017. Pseudomonas aeruginosa Contact-Dependent Growth Inhibition Plays Dual Role in Host-Pathogen Interactions. mSphere 2:e00336-17.

215. Ogier J-C, Duvic B, Lanois A, Givaudan A, Gaudriault S. 2016. A New Member of the Growing Family of Contact-Dependent Growth Inhibition Systems in Xenorhabdus doucetiae. PLoS One 11:e0167443.

216. Trent MS, Worsham LMS, Ernst-Fonberg ML. 1998. The Biochemistry of Hemolysin Toxin Activation: Characterization of HlyC, an Internal Protein Acyltransferase. Biochemistry 37:4644–4652.

217. Rojas CM, Ham JH, Deng W-L, Doyle JJ, Collmer A. 2002. HecA, a member of a class of adhesins produced by diverse pathogenic bacteria, contributes to the attachment, aggregation, epidermal cell killing, and virulence phenotypes of Erwinia chrysanthemi EC16 on Nicotiana clevelandii seedlings. Proc Natl Acad Sci U S A 99:13142–13147.

218. Killiny N, Almeida RPP. 2014. Factors Affecting the Initial Adhesion and Retention of the Plant Pathogen Xylella fastidiosa in the Foregut of an Insect Vector. Appl Environ Microbiol 80:420–426.

219. Gottig N, Garavaglia BS, Garofalo CG, Orellano EG, Ottado J. 2009. A Filamentous Hemagglutinin-Like Protein of Xanthomonas axonopodis pv. citri, the Phytopathogen Responsible for Citrus Canker, Is Involved in Bacterial Virulence. PLoS One 4:e4358.

220. Talà A, Progida C, Stefano MD, Cogli L, Spinosa MR, Bucci C, Alifano P. 2008. The HrpB–HrpA two-partner secretion system is essential for intracellular survival of Neisseria meningitidis. Cellular Microbiology 10:2461–2482.

221. De Gregorio E, Esposito EP, Zarrilli R, Di Nocera PP. 2018. Contact-Dependent Growth Inhibition Proteins in Acinetobacter baylyi ADP1. Curr Microbiol 75:1434–1440.

222. De Gregorio E, Zarrilli R, Di Nocera PP. 2019. Contact-dependent growth inhibition systems in Acinetobacter. Sci Rep 9:154.

223. Harding CM, Pulido MR, Di Venanzio G, Kinsella RL, Webb AI, Scott NE, Pachón J, Feldman MF. 2017. Pathogenic Acinetobacter species have a functional type I secretion system and contact-dependent inhibition systems. Journal of Biological Chemistry 292:9075–9087.

224. Fuqua C, Parsek MR, Greenberg EP. 2001. Regulation of Gene Expression by Cell-to-Cell Communication: Acyl-Homoserine Lactone Quorum Sensing. Annu Rev Genet 35:439–468.

225. Rutherford ST, Bassler BL. 2012. Bacterial Quorum Sensing: Its Role in Virulence and Possibilities for Its Control. Cold Spring Harb Perspect Med 2:a012427.

226. Schluter J, Schoech AP, Foster KR, Mitri S. 2016. The Evolution of Quorum Sensing as a Mechanism to Infer Kinship. PLOS Computational Biology 12:e1004848.

227. Thiel V, Kunze B, Verma P, Wagner-Döbler I, Schulz S. 2009. New Structural Variants of Homoserine Lactones in Bacteria. ChemBioChem 10:1861–1868.

228. Nealson KH, Platt T, Hastings JW. 1970. Cellular Control of the Synthesis and Activity of the Bacterial Luminescent System1. Journal of Bacteriology 104:313–322.

229. Malott RJ, Sokol PA. 2007. Expression of the bviIR and cepIR Quorum-Sensing Systems of Burkholderia vietnamiensis. Journal of Bacteriology 189:3006–3016.

230. Le Guillouzer S, Groleau M-C, Déziel E. The Complex Quorum Sensing Circuitry of Burkholderia thailandensis Is Both Hierarchically and Homeostatically Organized. mBio 8:e01861-17.

231. Pihl M, Chávez de Paz LE, Schmidtchen A, Svensäter G, Davies JR. 2010. Effects of clinical isolates of Pseudomonas aeruginosa on Staphylococcus epidermidis biofilm formation. FEMS Immunology & Medical Microbiology 59:504–512.

232. Escalas A, Hale L, Voordeckers JW, Yang Y, Firestone MK, Alvarez-Cohen L, Zhou J. 2019. Microbial functional diversity: From concepts to applications. Ecology and Evolution 9:12000–12016.

233. Zak J, Willig M, Moorhead D, Wildman H. 1994. Functional diversity of microbial communities: A quantitative approach. Soil Biology and Biochemistry 26:1101–1108.

234. Foster KR, Bell T. 2012. Competition, Not Cooperation, Dominates Interactions among Culturable Microbial Species. Current Biology 22:1845–1850.

235. Rumbaugh KP, Sauer K. 2020. Biofilm dispersion. Nat Rev Microbiol 18:571–586.

236. Bisht K, Wakeman CA. 2019. Discovery and Therapeutic Targeting of Differentiated Biofilm Subpopulations. Front Microbiol 0.

237. Lacqua A, Wanner O, Colangelo T, Martinotti MG, Landini P. 2006. Emergence of Biofilm-Forming Subpopulations upon Exposure of Escherichia coli to Environmental Bacteriophages. Applied and Environmental Microbiology 72:956–959.

238. Williamson KS, Richards LA, Perez-Osorio AC, Pitts B, McInnerney K, Stewart PS, Franklin MJ. 2012. Heterogeneity in Pseudomonas aeruginosa Biofilms Includes Expression of Ribosome Hibernation Factors in the Antibiotic-Tolerant Subpopulation and Hypoxia-Induced Stress Response in the Metabolically Active Population. J Bacteriol 194:2062–2073.

239. Pellizzoni E, Ravalico F, Scaini D, Delneri A, Rizzo R, Cescutti P. 2016. Biofilms produced by Burkholderia cenocepacia: influence of media and solid supports on composition of matrix exopolysaccharides. Microbiology (Reading) 162:283–294.

240. Murphy MP, Caraher E. 2015. Residence in biofilms allows Burkholderia cepacia complex (Bcc) bacteria to evade the antimicrobial activities of neutrophil-like dHL60 cells. Pathog Dis 73.

241. Butt A, Thomas M. 2017. Iron Acquisition Mechanisms and Their Role in the Virulence of Burkholderia Species. Frontiers in Cellular and Infection Microbiology 7.

242. Suárez-Moreno ZR, Caballero-Mellado J, Coutinho BG, Mendonça-Previato L, James EK, Venturi V. 2012. Common Features of Environmental and Potentially Beneficial Plant-Associated Burkholderia. Microb Ecol 63:249–266.

243. López CM, Rholl DA, Trunck LA, Schweizer HP. 2009. Versatile Dual-Technology System for Markerless Allele Replacement in Burkholderia pseudomallei. Appl Environ Microbiol 75:6496–6503.

244. Choi K-H, Mima T, Casart Y, Rholl D, Kumar A, Beacham IR, Schweizer HP. 2008. Genetic Tools for Select-Agent-Compliant Manipulation of Burkholderia pseudomallei. Appl Environ Microbiol 74:1064–1075.

245. Choi K-H, Gaynor JB, White KG, Lopez C, Bosio CM, Karkhoff-Schweizer RR, Schweizer HP. 2005. A Tn7-based broad-range bacterial cloning and expression system. Nat Methods 2:443–448.

246. Garcia EC. 2017. Burkholderia thailandensis: genetic manipulation. Curr Protoc Microbiol 45:4C.2.1-4C.2.15.

247. Schaefers MM, Liao TL, Boisvert NM, Roux D, Yoder-Himes D, Priebe GP. 2017. An Oxygen-Sensing Two-Component System in the Burkholderia cepacia Complex Regulates Biofilm, Intracellular Invasion, and Pathogenicity. PLoS Pathog 13.

248. Heydorn A, Nielsen AT, Hentzer M, Sternberg C, Givskov M, Ersbøll BK, Molin SY 2000. Quantification of biofilm structures by the novel computer program comstat. Microbiology 146:2395–2407.

249. de Lorenzo V, Herrero M, Jakubzik U, Timmis KN. 1990. Mini-Tn5 transposon derivatives for insertion mutagenesis, promoter probing, and chromosomal insertion of cloned DNA in gram-negative eubacteria. J Bacteriol 172:6568–6572.

250. Intile PJ, Balzer GJ, Wolfgang MC, Yahr TL. 2015. The RNA Helicase DeaD Stimulates ExsA Translation To Promote Expression of the Pseudomonas aeruginosa Type III Secretion System. Journal of Bacteriology 197:2664–2674.

251. Price MN, Zane GM, Kuehl JV, Melnyk RA, Wall JD, Deutschbauer AM, Arkin AP. 2018. Filling gaps in bacterial amino acid biosynthesis pathways with high-throughput genetics. PLOS Genetics 14:e1007147.

252. Ulrich RL, DeShazer D, Kenny TA, Ulrich MP, Moravusova A, Opperman T, Bavari S, Bowlin TL, Moir DT, Panchal RG. 2013. Characterization of the Burkholderia thailandensis SOS Response by Using Whole-Transcriptome Shotgun Sequencing. Appl Environ Microbiol 79:5830–5843.

253. Kearse M, Moir R, Wilson A, Stones-Havas S, Cheung M, Sturrock S, Buxton S, Cooper A, Markowitz S, Duran C, Thierer T, Ashton B, Meintjes P, Drummond A. 2012. Geneious Basic: An integrated and extendable desktop software platform for the organization and analysis of sequence data. Bioinformatics 28:1647–1649.

254. Kelley LA, Mezulis S, Yates CM, Wass MN, Sternberg MJE. 2015. The Phyre2 web portal for protein modeling, prediction and analysis. Nat Protoc 10:845–858.

255. Umarov RKh, Solovyev VV. 2017. Recognition of prokaryotic and eukaryotic promoters using convolutional deep learning neural networks. PLoS One 12:e0171410.

256. Winsor GL, Khaira B, Van Rossum T, Lo R, Whiteside MD, Brinkman FSL. 2008. The Burkholderia Genome Database: facilitating flexible queries and comparative analyses. Bioinformatics 24:2803–2804.

257. GraphPad Statistics Guide 579.

258. Allison DG, Sattenstall MA. 2007. The influence of green fluorescent protein incorporation on bacterial physiology: a note of caution. Journal of Applied Microbiology 103:318–324.

259. Nickzad A, Lépine F, Déziel E. 2015. Quorum Sensing Controls Swarming Motility of Burkholderia glumae through Regulation of Rhamnolipids. PLoS One 10:e0128509.

260. Kim J, Kang Y, Choi O, Jeong Y, Jeong J-E, Lim JY, Kim M, Moon JS, Suga H, Hwang I. 2007. Regulation of polar flagellum genes is mediated by quorum sensing and FlhDC in Burkholderia glumae. Mol Microbiol 64:165–179.

261. Huber B, Riedel K, Hentzer M, Heydorn A, Gotschlich A, Givskov M, Molin S, Eberl L. 2001. The cep quorum-sensing system of Burkholderia cepacia H111 controls biofilm formation and swarming motility. Microbiology 147:2517–2528.

262. Mountcastle SE, Vyas N, Villapun VM, Cox SC, Jabbari S, Sammons RL, Shelton RM, Walmsley AD, Kuehne SA. 2021. Biofilm viability checker: An open-source tool for automated biofilm viability analysis from confocal microscopy images. npj Biofilms Microbiomes 7:1–12.

263. van Duuren JBJH, Müsken M, Karge B, Tomasch J, Wittmann C, Häussler S, Brönstrup M. 2017. Use of Single-Frequency Impedance Spectroscopy to Characterize the Growth Dynamics of Biofilm Formation in Pseudomonas aeruginosa. Sci Rep 7:5223.

264. Melnikov SV, Stevens DL, Fu X, Kwok HS, Zhang J-T, Shen Y, Sabina J, Lee K, Lee H, Söll D. 2020. Exploiting evolutionary trade-offs for posttreatment management of drug-resistant populations. PNAS 117:17924–17931.

265. Xu Y, Buss EA, Boucias DG. 2016. Culturing and Characterization of Gut Symbiont Burkholderia spp. from the Southern Chinch Bug, Blissus insularis (Hemiptera: Blissidae). Appl Environ Microbiol 82:3319–3330.

266. Coutinho CP, de Carvalho CCCR, Madeira A, Pinto-de-Oliveira A, Sá-Correia I. 2011. Burkholderia cenocepacia Phenotypic Clonal Variation during a 3.5-Year Colonization in the Lungs of a Cystic Fibrosis Patient ▿. Infect Immun 79:2950–2960.

267. Steinmetz I, Rohde M, Brenneke B. 1995. Purification and characterization of an exopolysaccharide of Burkholderia (Pseudomonas) pseudomallei. Infect Immun 63:3959–3965.

268. Ruhe ZC, Wallace AB, Low DA, Hayes CS. Receptor Polymorphism Restricts Contact-Dependent Growth Inhibition to Members of the Same Species. mBio 4:e00480-13.

269. Relman DA, Domenighini M, Tuomanen E, Rappuoli R, Falkow S. 1989. Filamentous hemagglutinin of Bordetella pertussis: nucleotide sequence and crucial role in adherence. Proceedings of the National Academy of Sciences 86:2637–2641.

270. Kajava AV, Cheng N, Cleaver R, Kessel M, Simon MN, Willery E, Jacob-Dubuisson F, Locht C, Steven AC. 2001. Beta-helix model for the filamentous haemagglutinin adhesin of Bordetella pertussis and related bacterial secretory proteins. Molecular Microbiology 42:279–292.

271. Alsteens D, Martinez N, Jamin M, Jacob-Dubuisson F. 2013. Sequential Unfolding of Beta Helical Protein by Single-Molecule Atomic Force Microscopy. PLOS ONE 8:e73572.

272. Aoki SK, Poole SJ, Hayes CS, Low DA. 2011. Toxin on a stick. Virulence 2:356–359.

273. Kaundal S, Uttam M, Thakur KG. 2016. Dual Role of a Biosynthetic Enzyme, CysK, in Contact Dependent Growth Inhibition in Bacteria. PLOS ONE 11:e0159844.

274. Lewenza S, Conway B, Greenberg EP, Sokol PA. 1999. Quorum Sensing in Burkholderia cepacia: Identification of the LuxRI Homologs CepRI. J Bacteriol 181:748–756.

275. Yamanaka K, Inouye M. 1997. Growth-phase-dependent expression of cspD, encoding a member of the CspA family in Escherichia coli. J Bacteriol 179:5126–5130.

276. Yamanaka K, Zheng W, Crooke E, Wang Y-H, Inouye M. 2001. CspD, a novel DNA replication inhibitor induced during the stationary phase in Escherichia coli. Molecular Microbiology 39:1572–1584.

277. Ramos-Montañez S, Winkler ME. 2009. Biosynthesis of Histidine. EcoSal Plus 3.

278. Papaleo MC, Russo E, Fondi M, Emiliani G, Frandi A, Brilli M, Pastorelli R, Fani R. 2009. Structural, evolutionary and genetic analysis of the histidine biosynthetic "core" in the genus Burkholderia. Gene 448:16–28.

279. Richter AM, Fazli M, Schmid N, Shilling R, Suppiger A, Givskov M, Eberl L, Tolker-Nielsen T. 2019. Key Players and Individualists of Cyclic-di-GMP Signaling in Burkholderia cenocepacia. Front Microbiol 9.

280. Ri R-G, Mi R-D, C C. 2016. chr genes from adaptive replicons are responsible for chromate resistance by Burkholderia xenovorans LB400. World journal of microbiology & biotechnology 32.

281. Acosta-Navarrete YM, León-Márquez YL, Salinas-Herrera K, Jácome-Galarza IE, Meza-Carmen V, Ramírez-Díaz MI, Cervantes C. 2014. Expression of the six chromate ion transporter homologues of Burkholderia xenovorans LB400. Microbiology 160:287–295.

282. Ortega X, Silipo A, Saldías MS, Bates CC, Molinaro A, Valvano MA. 2009. Biosynthesis and Structure of the Burkholderia cenocepacia K56-2 Lipopolysaccharide Core Oligosaccharide. J Biol Chem 284:21738–21751.

283. Greenberg EP. 2011. THE NEW SCIENCE OF SOCIOMICROBIOLOGY AND THE REALM OF SYNTHETIC AND SYSTEMS ECOLOGYThe Science and Applications of Synthetic and Systems Biology: Workshop Summary. National Academies Press (US).

284. Parsek MR, Greenberg EP. 2005. Sociomicrobiology: the connections between quorum sensing and biofilms. Trends in Microbiology 13:27–33.

285. Keto-Timonen R, Hietala N, Palonen E, Hakakorpi A, Lindström M, Korkeala H. 2016. Cold Shock Proteins: A Minireview with Special Emphasis on Csp-family of Enteropathogenic Yersinia. Front Microbiol 7.

286. Kumar B, Sorensen JL, Cardona ST. 2018. A c-di-GMP-Modulating Protein Regulates Swimming Motility of Burkholderia cenocepacia in Response to Arginine and Glutamate. Frontiers in Cellular and Infection Microbiology 8:56.

287. Walsh MJ, Dodd JE, Hautbergue GM. 2013. Ribosome-inactivating proteins. Virulence 4:774–784.

288. Girbés T, Barbieri L, Ferreras M, Arias FJ, Rojo MA, Iglesias R, Alegre C, Escarmis C, Stirpe F. 1993. Effects of ribosome-inactivating proteins on Escherichia coli and Agrobacterium tumefaciens translation systems. J Bacteriol 175:6721–6724.

289. Gotschlich A, Huber B, Geisenberger O, Tögl A, Steidle A, Riedel K, Hill P, Tümmler B, Vandamme P, Middleton B, Camara M, Williams P, Hardman A, Eberl L. 2001. Synthesis of Multiple N-Acylhomoserine Lactones is Wide-spread Among the Members of the Burkholderia cepacia Complex. Systematic and Applied Microbiology 24:1–14.

290. Slinger BL, Deay JJ, Chandler JR, Blackwell HE. 2019. Potent modulation of the CepR quorum sensing receptor and virulence in a Burkholderia cepacia complex member using non-native lactone ligands. 1. Scientific Reports 9:13449.

291. Suppiger A, Schmid N, Aguilar C, Pessi G, Eberl L. 2013. Two quorum sensing systems control biofilm formation and virulence in members of the Burkholderia cepacia complex. Virulence 4:400–409.

292. Subramoni S, Sokol PA. 2012. Quorum sensing systems influence Burkholderia cenocepacia virulence. Future Microbiology 7:1373–1387.

293. McKeon SA, Nguyen DT, Viteri DF, Zlosnik JEA, Sokol PA. 2011. Functional Quorum Sensing Systems are Maintained during Chronic Burkholderia cepacia Complex Infections in Patients with Cystic Fibrosis. The Journal of Infectious Diseases 203:383–392.

294. Tomlin KL, Malott RJ, Ramage G, Storey DG, Sokol PA, Ceri H. 2005. Quorum-Sensing Mutations Affect Attachment and Stability of Burkholderia cenocepacia Biofilms. Appl Environ Microbiol 71:5208–5218.

295. O'Grady EP, Viteri DF, Sokol PA. 2012. A Unique Regulator Contributes to Quorum Sensing and Virulence in Burkholderia cenocepacia. PLoS One 7:e37611.

296. O'Grady EP, Viteri DF, Malott RJ, Sokol PA. 2009. Reciprocal regulation by the CepIR and CciIR quorum sensing systems in Burkholderia cenocepacia. BMC Genomics 10:441.

297. Maldonado RF, Sá-Correia I, Valvano MA. 2016. Lipopolysaccharide modification in Gram-negative bacteria during chronic infection. FEMS Microbiol Rev 40:480–493.

298. Matsuura M. 2013. Structural Modifications of Bacterial Lipopolysaccharide that Facilitate Gram-Negative Bacteria Evasion of Host Innate Immunity. Frontiers in Immunology 4:109.

299. Warren AE, Boulianne-Larsen CM, Chandler CB, Chiotti K, Kroll E, Miller SR, Taddei F, Sermet-Gaudelus I, Ferroni A, McInnerney K, Franklin MJ, Rosenzweig F. 2011. Genotypic and Phenotypic Variation in Pseudomonas aeruginosa Reveals Signatures of Secondary Infection and Mutator Activity in Certain Cystic Fibrosis Patients with Chronic Lung Infections ▿. Infect Immun 79:4802–4818.

300. Murray GL, Attridge SR, Morona R. 2006. Altering the Length of the Lipopolysaccharide O Antigen Has an Impact on the Interaction of Salmonella enterica Serovar Typhimurium with Macrophages and Complement. Journal of Bacteriology 188:2735–2739.

301. Johnson CL, Ridley H, Marchetti R, Silipo A, Griffin DC, Crawford L, Bonev B, Molinaro A, Lakey JH. 2014. The antibacterial toxin colicin N binds to the inner core of lipopolysaccharide and close to its translocator protein. Mol Microbiol 92:440–452.

302. Jansen KB, Inns PG, Housden NG, Hopper JTS, Kaminska R, Lee S, Robinson CV, Bayley H, Kleanthous C. 2020. Bifurcated binding of the OmpF receptor underpins import of the bacteriocin colicin N into Escherichia coli. Journal of Biological Chemistry 295:9147–9156.

303. Norris MH, Kang Y, Wilcox B, Hoang TT. 2010. Stable, Site-Specific Fluorescent Tagging Constructs Optimized for Burkholderia Species. Appl Environ Microbiol 76:7635–7640.

304. Martínez de Tejada G, Miller JF, Cotter PA. 1996. Comparative analysis of the virulence control systems of Bordetella pertussis and Bordetella bronchiseptica. Molecular Microbiology 22:895–908.

## Appendix A: Acronyms

| | |
|---|---|
| AA | Amino Acids |
| AHL | Acyl Homoserine Lactone |
| Amp | Ampicillin Antibiotics |
| AU1058 | *Burkholderia dolosa* Strain AU0158 |
| Bcc | *Burkholderia cepacia* Complex |
| Bcp | *Burkholderia* Contact Dependent Growth Inhibition Protein |
| *Bd* | *Burkholderia dolosa* |
| BP | DNA Base pair |
| BPC | *Burkholderia pseudomallei* complex |
| BSL | Bio-safety level |
| *Bt* | *Burkholderia thailandensis* |
| E264 | *Burkholderia thailandensis* strain E264 |
| CI | Competitive Index |
| C8-HSL | IV-Octanoyl Homoserine Lactone |
| CDC | Center for Disease Control |
| CDI | Contact-Dependent Growth Inhibition |
| CDS | Contact-Dependent Signaling |
| CF | Cystic Fibrosis |
| CFTR | Cystic Fibrosis Transmembrane Conductance Regulator |
| CFU | Colony Forming Units |

| | |
|---|---|
| CGD | Chronic Granulomatous Disease |
| CGD2M | *Burkholderia multivoran* strain CGD2M |
| Cm | Chloramphenicol |
| CspD | Cold Shock protein-D |
| C-Term | C-Terminus |
| CV | Crystal Violet |
| CysK | *O*-Acetylserine Sulfhydrylase A |
| DMSO | Dimethyl Sulfoxide |
| DNA | Deoxyribonucleic acid |
| DNase | Deoxyribonuclease |
| EF | Elongation Factor |
| EF-2 | Elongation Factor 2 |
| EF-T | Elongation Factor Thermo-Stable |
| EF-Tu | Elongation Factor Thermo-Unstable |
| EPS | Exopolysaccharides |
| FHA | Filamentous Hemagglutinin |
| GFP | Green Fluorescent Protein |
| GTPase | Guanosine Triphosphatase |
| H | Hours |
| IM | Inner Membrane |
| IMR | Inner Membrane Receptor |
| Kan | Kanamycin |
| kb | Kilo bases of DNA |

| | |
|---|---|
| kD | Kilodalton |
| LB | Lysogeny Broth |
| LPS | Lipopolysaccharide |
| LSLB | Low Salt Lysogeny Broth |
| LYN | Nx(E/Q)LYN conserved sequence in BcpA proteins |
| MMC | Mitomycin C |
| mRNA | Messenger Ribonucleic Acid |
| NCBI | National Center for Biotechnology Information |
| NS | Not Significant |
| N-Term | N Terminus |
| $OD_{420}$ | Optical Density, 420 nm |
| $OD_{540}$ | Optical Density, 540nm |
| $OD_{600}$ | Optical Density, 600 nm |
| OM | Outer Membrane |
| OME | Outer Membrane Exchange |
| OMR | Outer Membrane Receptor |
| OMR-BR | Outer Membrane Receptor-Binding Region |
| OMV | Outer Membrane Vesical |
| ONPG | Ortho-Nitrophenyl-β-Galactoside |
| ORF | Open Reading Frame |
| PBS | Phosphate-Buffered Saline |
| PBS-T | Phosphate-Buffered Saline-Tween |
| PCR | Polymerase Chain Reaction |

| | |
|---|---|
| PH | Potential Hydrogen |
| PVC | Polyvinyl Chloride |
| RHS | Rearrangement Hotspot |
| RIP | Ribosome Inactivating Protein |
| RNA | Ribonucleic Acid |
| RNase | Ribonuclease |
| rRNA | Ribosomal Ribonucleic Acid |
| SDS-PAGE | Sodium Dodecyl Sulfate-Polyacrylamide Gel Electrophoresis |
| SecSS | Sec Signal Sequence |
| SOS | ‘Save our ship’ – genes associated with responding to DNA damage |
| sRNA | Small Regulatory RNA |
| ssDNA | Single Stranded Deoxyribonucleic |
| T | Time |
| T3SS | Type III Secretion System |
| T4SS | Type IV Secretion System |
| T5SS | Type V Secretion System |
| T5SSb | Type Vb Secretion System |
| T6SS | Type VI Secretion System |
| T7SS | Type VII Secretion System |
| TA | Toxin-Antitoxin |
| Tet | Tetracycline |

| | |
|---|---|
| TPS | Two-Partner Secretion |
| tRNA | Transfer Ribonucleic Acid |
| TSB | Tryptic Soy Broth |
| WGS | Whole Genome Sequencing |
| WT | Wild-type |
| X-gal | 5-Bromo-4-Chloro-3-Indolyl-β-D-Galactopyranoside |
| YP | Tyrosine (Y) and Proline (P) Rich Region of CdiA |
| α | Antibody |
| β-ME | β-Mercaptoethanol |
| Δ | Deletion |

**Appendix B: Strains used in this body of work.**

| **Strain - laboratory stock annotation** | **Strain- dissertation annotation** | **Genotype** | **Source reference** |
|---|---|---|---|
| *E. coli* DH5α | | | |
| *E. coli* DH5α λpir | | | |
| *E. coli* RHO3 | | | |
| *B. dolosa* AU0158 | | | Taxonomy ID:3144971 |
| AU0158Δ*bcp*-1 | Δ*bcp-1* | *Bd*AU0158 Δ*bcpAIOB-1* | Garcia EC, 2016 (210) |
| AU0158 Δ*bcp*-2 | Δ*bcp-2* | *Bd*AU0158 Δ*bcpAIOB*-2 | Garcia EC, 2016 (210) |
| AU0158 Δ*bcp*-1 Δ*bcp*-2 | Δ*bcp-1* Δ*bcp-2* | *Bd*AU0158 Δ*bcpAIOB*-1 Δ*bcpAIOB*-2 | Garcia EC, 2016 (210) |
| AU0158 Kan | Wild-type | *Bd*AU0158-WT *att*Tn7::pUC18Tmini | |
| AU0158 Δ*bcp*-1 Kan | Δ*bcp*-1 | *Bd*AU0158 Δ*bcpAIOB*-1 *att*Tn7::pUCmini*gfp* | Oates AE, 2021 (*submitted*) |
| AU0158 Δ*bcp*-2 Kan | Δ*bcp*-2 | Δ*bcpAIOB*-2 *Bd*AU0158 *att*Tn7::pUC18Tmini-Tn7-km | Perault AI, 2018 (188) |
| AU0158 Δ*bcp*-1 Δ*bcp*-2 Kan | Δ*bcp*-1 Δ*bcp*-2 | *Bd*AU0158 Δ*bcpAIOB*-1 Δ*bcpAIOB*-2 *att*Tn7::pUC18Tmini-Tn7-km | Perault AI, 2018 (188) |
| AU0158 Tet | Wild-type | *Bd*AU0158-WT *att*Tn7::pUC18Tmini-Tn7-tet | Perault AI, 2018 (188) |
| AU0158 Δ*bcp*-1 Tet | Δ*bcp*-1 | *Bd*AU0158 Δ*bcpAIOB*-1 *att*Tn7::pUC18Tmini-Tn7-tet | Perault AI, 2018 (188) |
| AU0158 Δ*bcp*-2 Tet | Δ*bcp*-2 | *Bd*AU0158 Δ*bcpAIOB*-2 *att*Tn7::pUC18Tmini-Tn7-tet | Perault AI, 2018 (188) |

| | | | |
|---|---|---|---|
| AU0158 Δ*bcp*-1 Δ*bcp*-2 Tet | Δ*bcp*-1 Δ*bcp*-2 | *Bd*AU0158 Δ*bcpAIOB*-1 Δ*bcpAIOB*-2 *att*Tn7::pUC18Tmini-Tn7-tet | Perault AI, 2018 (188) |
| AU0158 Δ*bcp*-1 Δ*bcp*-2 +*bcpI*-1 | Δ*bcp*-1 Δ*bcp*-2 +*bcpI*-1 | *Bd*AU0158 Δ*bcpAIOB-1* Δ*bcpAIOB-2 att*Tn7::pAP3 | Perault AI, 2018 (188) |
| AU0158 Δ*bcp*-1 Δ*bcp*-2 +*bcpI*-2 | Δ*bcp*-1 Δ*bcp*-2 +*bcpI*-2 | *Bd*AU0158 Δ*bcpAIOB*-1 Δ*bcpAIOB*-2 *att*Tn7::pAP5 | Perault AI, 2018 (188) |
| AU0158 Δ*bcp*-1 Δ*bcp*-2 +bcpI-1 +*bcpI*-2 | Δ*bcp*-1 Δ*bcp*-2 +*bcpI*-2 | *Bd*AU0158 Δ*bcpAIOB*-1 Δ*bcpAIOB*-2 *att*Tn7::pAP3, *att*Tn7::pAP5 | This body of work |
| AU0158 *bcp-1* ::pAP6S12 | *bcp*-1$^{ON}$ | *Bd*AU0158 *bcpAIOB-1*ΩpAP6S12 | This body of work |
| AU0158 *bcp-2*::pAP7S12 | *bcp-2*$^{ON}$ | *Bd*AU0158 *bcpAIOB-2*ΩpAP7S12 | This body of work |
| AU0158 Δ*bcpO* | Δ*bcpO* | *Bd*AU0158 | Perault AI, 2018 (188) |
| AU0158 Δ*bcpO* +pAP6S12 | Δ*bcpO*$^{ON}$ | *Bd*AU0158 | This body of work |
| AU0158 +*gfp* | Wild-type +*gfp* | *Bd*AU0158 WT *att*Tn7::pUC*gfp* | This body of work |
| AU0158 Δ*bcp*-1 +*gfp* | Δ*bcp*-1 +*gfp* | *Bd*AU0158 Δ*bcpAIOB*-1 *att*Tn7::pUC*gfp* | This body of work |
| AU0158 Δ*bcp*-2 +*gfp* | Δ*bcp*-2 +*gfp* | *Bd*AU0158 Δ*bcpAIOB*-2 *att*Tn7::pUC*gfp* | This body of work |
| AU0158 Δ*bcp*-1 Δ*bcp*-2 +*gfp* | Δ*bcp*-1 Δ*bcp*-2 +*gfp* | *Bd*AU0158 Δ*bcpAIOB*-1 Δ*bcpAIOB*-2 *att*Tn7::pUC*gfp* | This body of work |
| AU0158 *bcpA*-1 △500aa | Δsubdom-1 | *Bd*AU0158-WT BcpA-1Δ2491-3003aa | This body of work |
| AU0158 *bcpA1*△subdom-1 | Δsubdom-2 | *Bd*AU0158-WT BcpA-1Δ2805-2855aa | This body of work |

| | | | |
|---|---|---|---|
| AU0158 *bcpA*1△subdom-2 | Δsubdom-3 | *Bd*AU0158-WT BcpA-1Δ2805-2905aa | This body of work |
| AU0158 *bcpA1*△500aa:: pAP6S12 | Δsubdom-$1^{ON}$ | *Bd*AU0158-WT *bcpAIOB-1*Ωp AP6S12 BcpA-1Δ2491-3003aa | This body of work |
| AU0158 *bcpA*1△subdom-1::pAP6S12 | Δsubdom-$2^{ON}$ | WT *bcpAIOB-1*ΩpAP6S12 BcpA-1Δ2805-2855aa | This body of work |
| AU0158 *bcpA*1△subdom-2::pAP6S12 | Δsubdom-$3^{ON}$ | *Bd*AU0158-WT *bcpAIOB-1*ΩpAP6S12 BcpA-1Δ2805-2905aa | This body of work |
| AU0158 *bcpA*1△500aa Kan | Δsubdom-1 | *Bd*AU0158-WT BcpA-1Δ2491-3003aa *att*Tn7::pUC18Tmini-Tn7-km | This body of work |
| AU0158 △*bcpA1*△subdom-1 Kan | Δsubdom-2 | *Bd*AU0158-WT BcpA-1Δ2805-2855aa *att*Tn7::pUC18Tmini-Tn7-km | This body of work |
| AU0158 *bcpA1*△subdom-2 Kan | Δsubdom-3 | *Bd*AU0158-WT BcpA-1 Δ2805-2905aa *att*Tn7::pUC18Tmini-Tn7-km | This body of work |
| AU0158 Δ*bcp*-1 Δ*bcp*-2 Δ*cepR* | Δ*cepR* | *Bd*AU0158 Δ*bcpAIOB*-1 Δ*bcpAIOB*-2 ΔBDAG_03544 | Oates AE, 2021 (*submitted*) |
| AU0158 Δ*bcp*-1 Δ*bcp*-2 Δ*cepR* Kan | Δ*cepR* | *Bd*AU0158 Δ*bcpAIOB*-1 Δ*bcpAIOB*-2 ΔBDAG_03544 *att*Tn7::pUC18Tmini-Tn7-km | Oates AE, 2021 (*submitted*) |
| AU0158 Δ*bcp*-1 Δ*bcp*-2 Δ*cepR* +*cepR* | Δ*cepR* +*cepR* | *Bd*AU0158 Δ*bcpAIOB*-1 Δ*bcpAIOB*-2 ΔBDAG_03544 *att*Tn7::pS12*cepR* | Oates AE, 2021 (*submitted*) |
| AU0158 Δ*bcp*-1 Δ*bcp*-2 +*cepR* | +*cepR* | *Bd*AU0158 Δ*bcpAIOB*-1 Δ*bcpAIOB*-2 *att*Tn7::pS12*cepR* | Oates AE, 2021 (*submitted*) |
| AU0158 Δ*bcp*-1 Δ*bcp*-2 Δ*cspD* | | *Bd*AU0158 Δ*bcpAIOB*-1 Δ*bcpAIOB*-2 ΔBDAG_02644 | Oates AE, 2021 (*submitted*) |
| AU0158 Δ*bcp*-1 Δ*bcp*-2 Δ*hisD* | | *Bd*AU0158 Δ*bcpAIOB*-1 Δ*bcpAIOB*-2 ΔBDAG_02714 | Oates AE, 2021 (*submitted*) |

| | | | |
|---|---|---|---|
| AU0158 Δ*bcp*-1 Δ*bcp*-2 Δ*cspD* Kan | Δ*cspD* | *Bd*AU0158 Δ*bcpAIOB*-1 Δ*bcpAIOB*-2 ΔBDAG_02644 *att*Tn7::pUC18Tmini-Tn7-km | Oates AE, 2021 (*submitted*) |
| AU0158 Δ*bcp*-1Δ*bcp*-2 Δ*hisD* Kan | Δ*hisD* | *Bd*AU0158 Δ*bcpAIOB*-1 Δ*bcpAIOB*-2 ΔBDAG_02714 *att*Tn7::pUC18Tmini-Tn7-km | Oates AE, 2021 (*submitted*) |
| AU0158 Δ*bcp*-1Δ*bcp*-2 Δ*hisD* +*hisD* | Δ*hisD* +*hisD* | *Bd*AU0158 Δ*bcpAIOB*-1 Δ*bcpAIOB*-2 ΔBDAG_02714 *att*Tn7::pS12*hisD* | Oates AE, 2021 (*submitted*) |
| AU0158 Δ*bcp*-1Δ*bcp*-2 +*hisD* | +*hisD* | *Bd*AU0158 Δ*bcpAIOB*-1 Δ*bcpAIOB*-2 *att*Tn7::pS12*hisD* | Oates AE, 2021 (*submitted*) |
| AU0158 Δ*bcp*-1Δ*bcp*-2 Δ*00967* | Δ*00967* | *Bd*AU0158 Δ*bcpAIOB*-1 Δ*bcpAIOB*-2 ΔBDAG_00967 | Oates AE, 2021 (*submitted*) |
| AU0158 Δ*bcp*-1Δ*bcp*-2 Δ*00967* +*gfp* | Δ*00967* +*gfp* | *Bd*AU0158 Δ*bcpAIOB*-1 Δ*bcpAIOB*-2 ΔBDAG_00967 *att*Tn7::pUC18mini-Tn7–kan–*gfp* | Oates AE, 2021 (*submitted*) |
| AU0158 Δ*bcp*-1Δ*bcp*-2 Δ*00967* +*00967* | Δ*00967* +*00967* | *Bd*AU0158 Δ*bcpAIOB*-1 Δ*bcpAIOB*-2 ΔBDAG_00967 *att*Tn7::pS12BDAG_00967km | Oates AE, 2021 (*submitted*) |
| AU0158 Δ*bcp*-1Δ*bcp*-2 Δ*00967* +pD01006 | Δ*00967* +pD01006 | *Bd*AU0158 | Oates AE, 2021 (*submitted*) |
| AU0158 Δ*bcp*-1Δ*bcp*-2 +*00967* | +*00967* | *Bd*AU0158 Δ*bcpAIOB*-1 Δ*bcpAIOB*-2 *att*Tn7::pS12BDAG_00967km | Oates AE, 2021 (*submitted*) |
| AU0158 Δ*bcp*-1Δ*bcp*-2 Kan Tet | Δ*bcp*-1 Δ*bcp*-2 | *Bd*AU0158 Δ*bcpAIOB*-1 Δ*bcpAIOB*-2 *att*Tn7::pUC18Tmini-Tn7-km *att*Tn7::pUC18Tmini-Tn7-tet | Oates AE, 2021 (*submitted*) |
| AU0158 Δ*bcp*-1Δ*bcp*-2 +*bcpI*-1 Tet | Δ*bcp*-1 Δ*bcp*-2 +*bcpI*-1 | *Bd*AU0158 Δ*bcpAIOB*-1 Δ*bcpAIOB*-2 *att*Tn7::pAP3 *att*Tn7::pUC18Tmini-Tn7-tet | Oates AE, 2021 (*submitted*) |

| | | | |
|---|---|---|---|
| AU0158 Δ*bcp*-1Δ*bcp*-2 +*bcpI*-2 Tet | Δ*bcp*-1 Δ*bcp*-2 +*bcpI*-2 | *Bd*AU0158 Δ*bcpAIOB*-1 Δ*bcpAIOB-2 att*Tn7::pAP5 *att*Tn7::pUC18Tmini-Tn7-tet | Oates AE, 2021 (*submitted*) |
| AU0158 Δ*bcp*-1Δ*bcp*-2 *tn*5 1-2 *+00967* | *tn*5 1-2 *+00967* | *Bd*AU0158 Δ*bcpAIOB-1* Δ*bcpAIOB*-2 pUTminiTn5km *att*Tn7::pS12BDAG_00967tet | Oates AE, 2021 (*submitted*) |
| AU0158 Δ*bcp*-1Δ*bcp*-2 *tn*5 1-2 *+00966* | *tn*5 1-2 *+00966* | *Bd*AU0158 Δ*bcpAIOB-1* Δ*bcpAIOB*-2 pUTminiTn5km *att*Tn7::pS12BDAG_00966tet | Oates AE, 2021 (*submitted*) |
| AU0158 Δ*bcp*-1Δ*bcp*-2 *tn*5 1-2 *+00967-66* | *tn*5 1-2 *+00967-66* | Δ *Bd*AU0158 *bcpAIOB-1* Δ*bcpAIOB*-2 pUTminiTn5km *att*Tn7::pS12BDAG_00967-66tet | Oates AE, 2021 (*submitted*) |
| AU0158 Δ*bcp*-1Δ*bcp*-2 *tn*5 1-2 Tet | *tn*5 1-2 | *Bd*AU0158 Δ*bcpAIOB*-1 Δ*bcpAIOB*-2 pUTminiTn5km *att*Tn7::pUC18Tmini-Tn7-tet | Oates AE, 2021 (*submitted*) |
| AU0158 Δ*bcp*-1 Δ*bcp*-2 Δ*00966* | Δ*00966* | *Bd*AU0158 Δ*bcpAIOB*-1 Δ*bcpAIOB*-2 ΔBDAG_00966 | Oates AE, 2021 (*submitted*) |
| AU0158 Δ*bcp*-1 Δ*bcp*-2 Δ*00966* Tet | Δ*00966* | *Bd*AU0158 Δ*bcpAIOB*-1 Δ*bcpAIOB*-2 ΔBDAG_00966 *att*Tn7::pUC18Tmini-Tn7-tet | Oates AE, 2021 (*submitted*) |
| AU0158 Δ*bcp*-1 Δ*bcp*-2 Δ*00966 +00966* | Δ*00966 +00966* | *Bd*AU0158 Δ*bcpAIOB*-1 Δ*bcpAIOB*-2 ΔBDAG_00966 *att*Tn7::pS12BDAG_00966 tet | Oates AE, 2021 (*submitted*) |
| AU0158 Δ*bcp*-1Δ*bcp*-2 *+00966* | *+00966* | *Bd*AU0158 Δ*bcpAIOB*-1 Δ*bcpAIOB*-2 *att*Tn7::pS12BDAG_00966 tet | Oates AE, 2021 (*submitted*) |
| AU0158 Δ*bcp*-1Δ*bcp*-2 +pD01005 | | *Bd*AU0158 Δ*bcp*-1Δ*bcp*-2 BDAG_01005::pD01005 | Oates AE, 2021 (*submitted*) |
| AU0158 Δ*bcp*-1Δ*bcp*-2 +pD01006 | | *Bd*AU0158 Δ*bcp*-1Δ*bcp*-2 BDAG_01006 :: pD01005 | Oates AE, 2021 (*submitted*) |

| | | | |
|---|---|---|---|
| AU0158 △1△2 Tn5 v △1 #1 | tn5 1-1 | *Bd*AU0158 Δ*bcp*-1Δ*bcp*-2 BDAG_01006 ::pD01005 | Oates AE, 2021 (*submitted*) |
| AU0158 △1△2 Tn5 v △1 #2 | tn5 1-2 | *Bd*AU0158 BDAG_00967:: pUT-miniTn5-Km | Oates AE, 2021 (*submitted*) |
| AU0158 △1△2 Tn5 v △1 #4 | tn5 1-4 | *Bd*AU0158 BDAG_00967:: pUT-miniTn5-Km | Oates AE, 2021 (*submitted*) |
| AU0158 △1△2 Tn5 v △1 #6 | tn5 1-6 | *Bd*AU0158 BDAG_00967:: pUT-miniTn5-Km | Oates AE, 2021 (*submitted*) |
| AU0158 △1△2 Tn5 v △1 #8 | tn5 1-8 | *Bd*AU0158 BDAG_00967:: pUT-miniTn5-Km | Oates AE, 2021 (*submitted*) |
| AU0158 △1△2 Tn5 v △2 #2 | tn5 2-2 | *Bd*AU0158 *hisD* Ω::pUT-miniTn5-Km | Oates AE, 2021 (*submitted*) |
| AU0158 △1△2 Tn5 v △2 #3 | tn5 2-3 | *Bd*AU0158 *hisD* ::pUT-miniTn5-Km | Oates AE, 2021 (*submitted*) |
| AU0158 △1△2 Tn5 v △2 #5 | tn5 2-5 | *Bd*AU0158 BDAG_00967:: pUT-miniTn5-Km | Oates AE, 2021 (*submitted*) |
| AU0158 △1△2 Tn5 v △2 #7 | tn5 2-7 | *Bd*AU0158 *cspD* :: pUT-miniTn5-Km | Oates AE, 2021 (*submitted*) |
| AU0158 △1△2 Tn5 v △2 #8 | tn5 2-8 | *Bd*AU0158 *cepR* :: pUT-miniTn5-Km | Oates AE, 2021 (*submitted*) |
| E264 | | *Bt*E264 | Taxonomy ID:271848 |
| E264 Kan | E264 | *Bt*E264 *att*Tn7::pUC18Tmini-Tn7-kan | Anderson MS, 2012 (185) |
| E264::pECG22 | $E264^{ON}$ | *Bt*E264 *bcpAIOB*ΩpECG22 | Anderson MS, 2012 (185) |
| E264 BcpA-EKA | $E264^{Inact.}$ | *Bt*E264 *bcpAIOB* BcpA E3064→A,K3066→A (catalytically inactive mutant) | Anderson MS, 2014 (192) |
| E264 BcpA-EKA Kan | $E264^{Inact.}$ | *Bt*E264 *bcpAIOB* BcpA E3064→A,K3066→A (catalytically inactive mutant) | Anderson MS, (192) |

| | | | |
|---|---|---|---|
| | | *att*Tn7::pUC18Tmini-Tn7-kan | |
| E264 BcpA-EKA::pECG22 | E264$^{Inact.ON}$ | *Bt*E264 *bcpAIOB*ΩpECG22 BcpA E3064→A,K3066→A (catalytically inactive mutant) | Anderson MS, 2014 (192) |
| E264 ΔSS | ΔSecSS | *Bt*E264-WT *bcpA*ΔSecSS | This body of work |
| E264 Δ*bcpAIOB* | *Bt*Δ*bcpAIO* | *Bt*E264 Δ*bcpAIOB* | Anderson MS, 2012 (185) |
| E264 Δ*bcpAIOB* kan | *Bt*Δ*bcpAIO* | *Bt*E264 Δ*bcpAIOB* *att*Tn7::pUC18Tmini-Tn7-kan | Anderson MS, 2012 (185) |
| E264 Δ*bcpA* | *Bt*Δ*bcpA* | *Bt*E264 Δ*bcpA* | Garcia EC, 2016 (210) |
| E264 Δ*bcpA* kan | *Bt*Δ*bcpA* | *Bt*E264 Δ*bcpA* *att*Tn7::pUC18Tmini-Tn7-kan | Garcia EC, 2016 (210) |
| E264 +pECG60 | Bth_I0535-*lacZ* | *Bt*E264-WT Bth_I0535:: pECG60 | Garcia EC, 2016 (210) |
| Δ*bcpAIOB* +pECG60 | Δ*bcp* Bth_I0535-*lacZ* | *Bt*E264 Δ*bcpAIOB* Bth_I0535:: pECG60 | Garcia EC, 2016 (210) |
| E264 +pECG61 | *csuD-lacZ* | *Bt*E264-WT Bth_I2676 (csuD)::pECG61 | Garcia EC, 2016 (210) |
| E264 Δ*bcpAIOB* +pECG61 | Δ*bcp csuD-lacZ* | *Bt*E264 Δ*bcpAIOB* Bth_I2676 (csuD)::pECG61 | Garcia EC, 2016 (210) |
| E264::pECG22 +pECG86 | E264$^{ON}$ +*lexA-lacZ* | *Bt*E264 *bcpAIOB*ΩpECG22 | This body of work |
| E264::pECG22 +pECG87 | E264$^{ON}$ +*uvrA-lacZ* | *Bt*E264 *bcpAIOB*ΩpECG22 | This body of work |
| E264 BcpA-EKA::pECG22 +pECG86 | E264$^{Inact.ON}$ +*lexA-lacZ* | *Bt*E264 *bcpAIOB*ΩpECG22 BcpA E3064→A,K3066→A (catalytically inactive mutant) | This body of work |

| | | | |
|---|---|---|---|
| E264 BcpA-EKA::pECG22 +ECG87 | E264$^{Inact.ON}$ +*uvrA-lacZ* | *Bt*E264 *bcpAIOB*Ωp ECG22 BcpA E3064→A,K3066→A (catalytically inactive mutant) | This body of work |
| E264 +pECG86 | +*lexA-lacZ* | *Bt*E264-WT *att*Tn7:: pECG86 | This body of work |
| E264 +pECG87 | +*uvrA-lacZ* | *Bt*E264-WT *att*Tn7:: pECG87 | This body of work |
| E264 BcpA-EKA +pECG86 | E264$^{Inact.}$ +*lexA-lacZ* | *Bt*E264 BcpA E3064→A,K3066→A (catalytically inactive mutant) *att*Tn7:: pECG86 | This body of work |
| E264 BcpA-EKA +pECG87 | E264$^{Inact.ON}$ | *Bt*E264 BcpA E3064→A,K3066→A (catalytically inactive mutant) *att*Tn7:: pECG87 | This body of work |
| E264 +pUClacZ | Promoterless -*lacZ* | *Bt*E264 WT *att*Tn7::pUClacZ | Anderson MS, (185) |
| E264 +pECG10 | *lacZON* | *Bt*E264-WT *att*Tn7::pECG10 | Anderson MS, 2012 (185) |
| E264Δ*bcpA* +pECG86 | Δ*bcpA* +*lexA-lacZ* | *Bt*E264 Δ*bcpA att*Tn7:: pECG86 | This body of work |
| E264Δ*bcpA* +pECG87 | Δ*bcpA* +*uvrA-lacZ* | *Bt*E264 Δ*bcpA att*Tn7:: pECG87 | This body of work |

(::) Disruption
(Ω) Exchange
(Δ) Deletion

**Appendix C: Plasmids used in this body of work.**

| Plasmids | Backbone | Description | AbR | Reference |
|---|---|---|---|---|
| | | | | |
| pEXKm5 | | Allelic exchange vector | kan | López CM, 2009 (243) |
| pUC18Tmini-Tn7-km | | To deliver kanamycin-resistance cassette to *att*Tn7 site | amp, kan | Choi K-H, 2008 (244) |
| pUC18Tmini-Tn7-tet | pUC18Tmini-Tn7-km | To deliver tetracycline-resistance cassette to *att*Tn7 site | amp, tet | Anderson MS, 2012 (185) |
| pUC18mini-Tn*7*–kan–*gfp* | pUC18Tmini-Tn7-km | To deliver promoterless *gfp* gene cassette to *att*Tn7 site | amp, kan | Norris MH , 2010 (303) |
| pUC18mini-Tn*7*–kan–*rfp* | pUC18Tmini-Tn7-km | To deliver promoterless *rfp* gene cassette to *att*Tn7 site | amp, kan | Anderson MS, 2014 (192) |
| pUCS12km | pUC18Tmini-Tn7-km | To deliver (E264, rpsL gene promoter) S12 -driving cassettes to the *att*Tn7 site | amp, kan | Anderson MS, 2012 (185) |
| pTNS3 | | Helper plasmid to deliver cassettes to *att*Tn7 site | amp | Choi K-H, 2005 (245) |
| pUT-miniTn5-Km | pGP704 derivative | Tn5 transposase (tnp) and mini-Tn5 transposon for mutagenesis | kan | de Lorenzo V, 1990 (249) |
| pAP3 | pUCS12 | To deliver kanamycin-resistance cassette of *bcpI*-1 under the constitutive promoter S12 to the *att*Tn7 site | amp, kan | Perault AI, 2018 (188) |
| pAP5 | pUCS12 | To deliver kanamycin-resistance cassette of *bcpI*-2 under the constitutive promoter S12 to the *att*Tn7 site | amp, kan | Perault AI, 2018 (188) |
| p△*cspD*_overlap | pEXKm5 | To delete AU0158 BDAG_02644 in frame by allelic exchange using first 4 codons and 485bp 5' of the gene and 3 codons and 440bp 3' of the gene | kan | Oates AE, 2021 (*submitted*) |
| p△*hisD*_overlap[a] | pEXKm5 | To delete AU0158 BDAG_02714 inframe by allelic exhange using first 4 | kan | Oates AE, 2021 (*submitted*) |

| | | | | |
|---|---|---|---|---|
| | | codons and 420bp 5' of the gene and 3 codons and 485bp 3' of the gene | | |
| pS12*hisD* | pUCS12 | To deliver kanamycin-resistance cassette of BDAG_02714 under the constitutive promoter S12 to the *att*Tn7 site | amp, kan | Oates AE, 2021 (*submitted*) |
| p△BDAG_00967_overlap[a] | pEXKm5 | To delete AU0158 BDAG_00967 in frame by allelic exchange using 477bp 5' of the gene and 498bp 3' of the gene | kan | Oates AE, 2021 (*submitted*) |
| pS1200967km | pUCS12 | To deliver kanamycin-resistance cassette of BDAG_00967 under the constitutive promoter S12 to the *att*Tn7 site | amp, kan | Oates AE, 2021 (*submitted*) |
| pS1200967tet | pUC18Tmini-Tn7-tet | To deliver tetracycline-resistance cassette of BDAG_00967 under the constitutive promoter S12 to the *att*Tn7 site | amp, tet | Oates AE, 2021 (*submitted*) |
| pS1200966tet | pUC18Tmini-Tn7-tet | To deliver deliver tetracycline-resistance cassette of BDAG_00966 under the constitutive promoter S12 to the *attTn7 site* | amp, tet | Oates AE, 2021 (*submitted*) |
| pS1200967-66tet | pUC18Tmini-Tn7-tet | To deliver tetracycline-resistance cassette of BDAG_00967 through BDAG_00966 under the constitutive promoter S12 to the *att*Tn7 site | amp, tet | Oates AE, 2021 (*submitted*) |
| p△BDAG_966_overlap | pEXKm5 | To delete AU0158 BDAG_00966 in frame by allelic exchange using first 3 codons and 449bp 5' of the gene and 3 codons and 438bp 3' of the gene | kan | Oates AE, 2021 (*submitted*) |
| pECG110 | pEXKm5 | To delete AU0158 BDAG_03544, *cepR*, in frame by allelic exchange | kan | Oates AE, 2021 (*submitted*) |

| | | | | |
|---|---|---|---|---|
| pS12cepR | pUCS12 | To deliver kanamycin-resistance cassette of BDAG_03544 under the constitutive promoter S12 to the *att*Tn7 site | amp, kan | Oates AE, 2021 (*submitted*) |
| pECG113 (pD01005) | pUC18Tmini-Tn7-km | To disrupt BDAG_01005 by cassette of BDAG_01005 3' 158-675bp integration into the chromosomal gene | kan | Oates AE, 2021 (*submitted*) |
| pECG114 (pD01006) | pUC18Tmini-Tn7-km | To disrupt BDAG_01006 by cassette of BDAG_01006 3' 26-573bp integration into the chromosomal gene | kan | Oates AE, 2021 (*submitted*) |
| pAP6S12 | pUCS12 | To integrate (E264, rpsL gene promoter) S12 -driving cassettes 3' of the AU0158 *bcpAIOB-1* locus | kan | This body of work |
| pAP7S12 | pUCS12 | To integrate (E264, rpsL gene promoter) S12 -driving cassettes 3' of the AU0158 *bcpAIOB-2* locus | kan | This body of work |
| pECG22 | pEXKm5 | To integrate (E264, rpsL gene promoter) S12 -driving cassettes 3' of the E264 *bcpAIOB* locus | kan | Anderson MS, 2012 (185) |
| pAEO9 | pEXKm5 | To delete E264 *bcpA* 2439aa-2771aa in frame by allelic exchange | kan | This body of work |
| pAEO12 | pEXKm5 | To delete AU0158 *bcpA-1* 2491-3003aa in frame by allelic exchange | kan | This body of work |
| pAEO14 | pEXKm5 | To delete AU0158 bcpA-1 2805 – 2905aa in frame by allelic exchange using | kan | This body of work |
| pAEO15 | pEXKm5 | To delete AU0158 bcpA-1 2805 – 2855aa in frame by allelic exchange using | kan | This body of work |
| pUClacZ | pUC18Tmini-Tn7-km | To deliver promoterless *lacZ* gene cassette to *att*Tn7 site | kan | Anderson MS, 2012 (185) |
| pECG10 | pUCS12 | To deliver kanamycin-resistance cassette of *lacZ* under the constitutive promoter S12 to the *att*Tn7 site | amp, kan | Anderson MS, 2012 (185) |

| | | | | |
|---|---|---|---|---|
| pEGZH3T | | Tet cloned into BglII site of pEGZH3, disrupting GmR | Amp, Tet | Martuez de Tejada G, 1996 (304) |
| pECG60 | pEGZH3T | To disrupt Bth_I0535 gene with *lacZ* cassette by allelic exchange | Amp, Tet | Garcia EC, 2016 (210) |
| pECG61 | pEGZH3T | To disrupt *csuD* gene with lacZ cassett by allelic exchange | Amp, Tet | Garcia EC, 2016 (210) |
| pECG86 | pECG10 | To deliver kanamycin-resistance cassette of *lexA* promoter to drive *lacZ* expression to the attTn7 site | amp, kan | This body of work |
| pECG87 | pECG10 | To deliver kanamycin-resistance cassette of *uvrA* promoter to drive *lacZ* expression to the attTn7 site | amp, kan | This body of work |

**AbR,** Antibiotic resistance marker
[a] Made using Gibson assembly method

**Appendix D: Experimental replicates of *B. thailandensis* and *B. dolosa* BcpA banding patterns.**

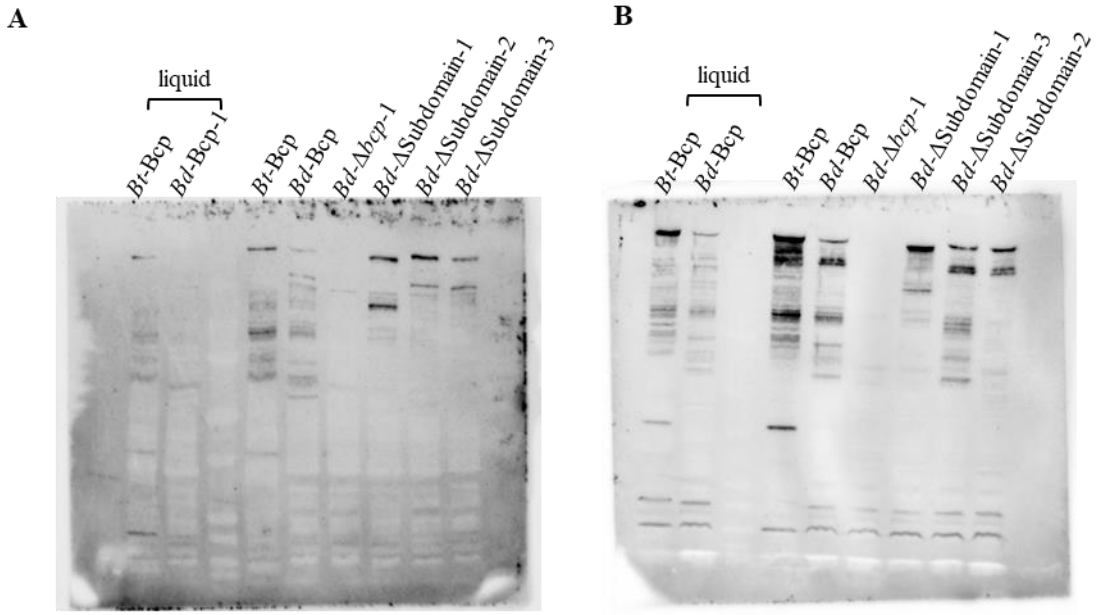


**Appendix Figure 1. Banding patterns between pre-toxin region deletions mutants vary from wild-type BcpA-1.**

**Appendix Figure 1. Banding patterns between pre-toxin region deletions mutants vary from wild-type BcpA-1.**

Western blot assays done **(A)** 09/03/2020 **(B)** 09/07/2020 using whole cell lysate of *B. thailandensis* (E264) and *B. dolosa* (AU0158) constitutively expressing E264 *Bt-bcpAIOB* or AU0158 *Bd-bcpAIOB*-1 locus. Whole cell lysis was collected from either liquid cultures, left, or harvested from plates, right. Constitutive expression of the AU0158 *Bd*-BcpA subdomain-1, subdomain-2, and subdomain-3 deletions were harvested from plates. The deletion of the locus *Bd-bcp*-1 was used as the negative antibody control. Prior to cell lysis, cultures were standardized to the same $OD_{600}$. Membrane probed with αBcpA C-terminal primary antibodies and fluorescent αRabbit secondary antibodies.

**Appendix E: Variations[a] in *B. dolosa* Δ*bcpAIOB-1* Δ*bcpAIOB-2* mutant identified by whole genome re-sequencing.**

| Chr | Position | Variation [b] | Locus tag | Annotation | Seq run #1 [c] | | Seq run #2 [c] | | |
|---|---|---|---|---|---|---|---|---|---|
| | | | | | Cov[d] | Freq (%)[e] | Cov[d] | Freq (%)[e] | Tn? [f] |
| 1 | 1,439,637 | C→G [syn] | AK34_1335 | acetyl-CoA acyl-transferase | 306 | 92 | 38 | 100 | Y |
| 1 | 1,439,658 | C→A [syn] | AK34_1335 | acetyl-CoA acyl-transferase | 339 | 88 | 25 | 100 | Y |
| 1 | 1,778,998 | T→G [V→G] | AK34_1666 | multidrug efflux transporter periplasmic subunit | 294 | 99 | 132 | 100 | Y |
| 1 | 2,565,694 | C→G | intergenic | | ND | ND | 55 | 96 | N |
| 2 | 453,761 | T→G [V→G] | AK34_3567 | enoyl-CoA hydratase | 265 | 100 | 149 | 100 | Y |
| 2 | 612,089 | $(TGGCAA)_{11\rightarrow12}$ | intergenic | | 30 | 100 | 78 | 96 | Y |
| 2 | 614,406 | $(ACTCAGG)_{2\rightarrow1}$ | intergenic | | 25 | 100 | 154 | 99 | Y |
| 2 | 1,386,452 | A→C | intergenic | | 145 | 100 | 96 | 100 | Y |
| 2 | 2,156,583 | T→G | intergenic | | 122 | 100 | 124 | 100 | Y |

Chr, chromosome; Cov, coverage; Freq, frequency; ND, not detected

[a] Variations relative to AU0158 reference genome occurring at >85% frequency in regions having >25 mapped reads

[b] Brackets show amino acid substitution or synonymous change (syn), where applicable.

[c] Control Δ*bcpAIOB-1* Δ*bcpAIOB-2* parent strain was re-sequenced twice, with two batches of transposon mutants. Sequencing run #1 for comparison to transposon mutant Tn1-2 and sequencing run #2 for comparison to transposon mutants Tn2-2, Tn2-7, and Tn2-8.

[d] Number of mapped reads

[e] **%** reads containing indicated mutation

[f] Present (Y) in all re-sequenced transposon mutants. Variation denoted (N) was not detected in Tn1-2 or Tn2-8.

## Appendix F: Influence of *B. thailandensis* BcpA/BcpI complex on SOS response.

*B. thailandensis* E264 has been shown to utilize the CDI system both as a means of competition and as a means of kin-specific interactions. E264 required the BcpAIOB proteins when mediating biofilm formation and is associated with additional phenotypes including pigmentation and Congo-Red binding. These community behaviors were dependent on the function of BcpA. Loss or initialization on of BcpA C-terminal toxin (E3064A to K3066A substitution - EKA) was defective in the above described cooperative behaviors (209, 210). RNA sequencing identified various genes associated with BcpA induces global gene expression changes, including expression of *csuD* and Bth_I0535. This CDI system-mediated intercellular communication was termed contact-dependent signaling (CDS) (210).

*B. thailandensis* E264 has been shown to utilize the CDI system both as a means of competition and as a means of kin-specific interactions. E264 required the BcpAIOB proteins when mediating biofilm formation and is associated with additional phenotypes including pigmentation and Congo-Red binding. These community behaviors were dependent on the function of BcpA. Loss or initialization on of BcpA C-terminal toxin (E3064A to K3066A substitution - EKA) was defective in the above described cooperative behaviors (209, 210). RNA sequencing identified various genes associated with BcpA induces global gene expression changes, including expression of *csuD* and Bth_I0535. This CDI system-mediated intercellular communication was termed contact-dependent signaling (CDS) (210).

At the time of these experiments, the understanding of contact-dependent growth signaling (CDS) was limited to kin-restriction based on the catalytically active BcpA C-

terminus *B. thailandensis*, BcpA-CT, binds to its cognate immunity protein, BcpI, of the recipient cell upon toxin translocation. *B. thailandensis* BcpA-CT is predicted to be a DNase, both having predicted secondary structure to Holliday junction reductase and purified BcpA-CT degrading DNA of *E. coli* plasmid (185, 200). The proposed hypothesis of these experiments was that the formation of the *B. thailandensis* BcpA-CT/BcpI toxin-immunity complex may cause DNA damage in the recipient cell, inducing an 'SOS' response. However, the current understanding is that CDS in *B. thailandensis* is associated with a large mobile genetic element termed 'mega circle' that contain the *bcpAIOB* locus of *B. thailandensis.* The mega-circle was shown to be induced by the catalytically active BcpA-CT (196). Similar mechanisms have not been observed for other *Burkholderia* CDI systems (188, 193).

At the time of these experiments, the understanding of contact-dependent growth signaling (CDs) was limited to kin-restriction based on the catalytically active BcpA C-terminus *B. thailandensis*, BcpA-CT, binds to its cognate immunity protein, BcpI, of the recipient cell upon toxin translocation. *B. thilandensis* BcpA-CT is predicted to be a DNase, both having predicted secondary structure to Holliday junction reductase and purified BcpA-CT degrading DNA of *E. coli* plasmid (185)(Anderson 2012, Ruhe et al., 2013). The proposed hypothesis of these experiments was that the formation of the *B. thailandensis* BcpA-CT/BcpI toxin-immunity complex may cause DNA damage in the recipient cell, inducing an 'SOS' response. However, the current understanding is that CDS in *B. thailandensis* is associated with a large mobile genetic element termed 'mega circle' that contain the *bcpAIOB* locus of *B. thailandensis.* The mega-circle was shown to

be induced by the catalytically active BcpA-CT (196). Similar mechanisms have not been observed for other *Burkholderia* CDI systems (188, 193).

The bacterial SOS response is the result of environmental stress-induced DNA damage, and thus SOS genes are associated with DNA repair. Two such SOS genes are *LexA* and *csuD.* (252). Expression of *uvrA* is negatively regulated by *lexA*; when LexA proteins are active, expression of *uvaR* is upregulated. The UvrA proteins the respond to the SOS signal, and repair DNA damage (Appendix Figure 2A) (252).

The bacterial SOS response is the result of environmental stress-induced DNA damage, and thus SOS genes are associated with DNA repair. Two such SOS genes are *LexA* and *csuD*. Expression of *uvrA* is negatively regulated by *lexA*; when LexA proteins are active, expression of *uvaR* is upregulated. The UvrA proteins the respond to the SOS signal, and repair DNA damage (Appendix Figure 2A) (252).

These studies sought to determine whether the formation of the BcpA-CT/BcpI toxin-immunity complex led to an SOS response, inducing CDS associated global gene expression changes.

Donor bacteria were either expressing wild-type *bcpA*, or the inactive *bcpA*-EKA and co-cultures on X-gal plates with *lacZ* expressing CDS genes, *csuD-lacZ* and Bth_I0535-*lacZ,* or SOS genes; *lexA-lacZ* and *uvrA-lacZ.* The production of β-galactosidase assay (encoded by *lacZ*), visualized as blue when cultured on X-gal plates, is representative of the expression of the associated genes. As shown in the initial CDS findings, co-culturing either CDS *lacZ* expressing CDS genes, *csuD-lacZ* and Bth_I0535-*lacZ,* had increased levels of blue compared to the recipient alone or co-cultured with the inactive *bcpA* expressing donor cells. These results support that active BcpA intoxication

is driving increased expression of *csuD* and Bth_I0535 (210). Similar results were seen with active BcpA donor cells co-cultured with *uvrA-lacZ* recipient cells, indicating that BcpA maybe driving expression of *uvrA.* However, there was no change in the amount of blue produced in *lexA-lacZ* expressing recipient cells, regardless of the donor bacteria cultured with (Appendix Figure 2B).

To determine the correlation with generic DNA damage and expression of either the SOS genes or CDS genes, cultures were supplemented with Mitomycin C (MMC) and β-galactosidase assays performed. MMC induces various types of DNA damage, and at high enough levels is cytotoxic to the cells. β-galactosidase assays measure, indirectly, measure the promoter or gene driving expression of *lacZ* though a color metric assay ##.(252). The *lacZ* associated gene mutants were compared to with or without MMC to determine change in *lacZ* expression, and none were found to have significant differences, including the SOS gene mutants *lexA-lacZ* and *uvrA-lacZ.*

Measuring only the *lacZ* expression from the SOS genes, the *csuD-lacZ* and *lexA-lacZ* cassettes were mated and inserted into the chromosome of *bcpA* mutants. The *bcpA* mutants were either wild-type ($bcpA^{WT}$), constitutively expressing the *bcpAIOB* locus ($bcpA^{ON}$), inactive *bcpA* ($bcpA^{inact.}$), or constitutively expressing the inactivated *bcpAIOB* locus ($bcpA^{inact.ON}$). Similar to the MMC induced DNA damage β-galactosidase assays, there was no significant difference in expression of *csuD-lacZ* or *lexA* regardless of the *bcpA* mutant background (Appendix Figure 2 D). However, the average β-galactosidase levels indicate that the *lexA* promoter may naturally be more active than the *uvrA* promoter (Appendix Figure 2 C,D) .

Altogether, these results indicate that neither BcpA-CT/BcpI complex nor DNA damage drive expression of the CDS genes, Bth_I0535 or *csuD*. Although, the current understanding of CDS gene regulation is due to production of the mega-circle, as to how BcpA/BcpI triggers the mobile element is still unknown.

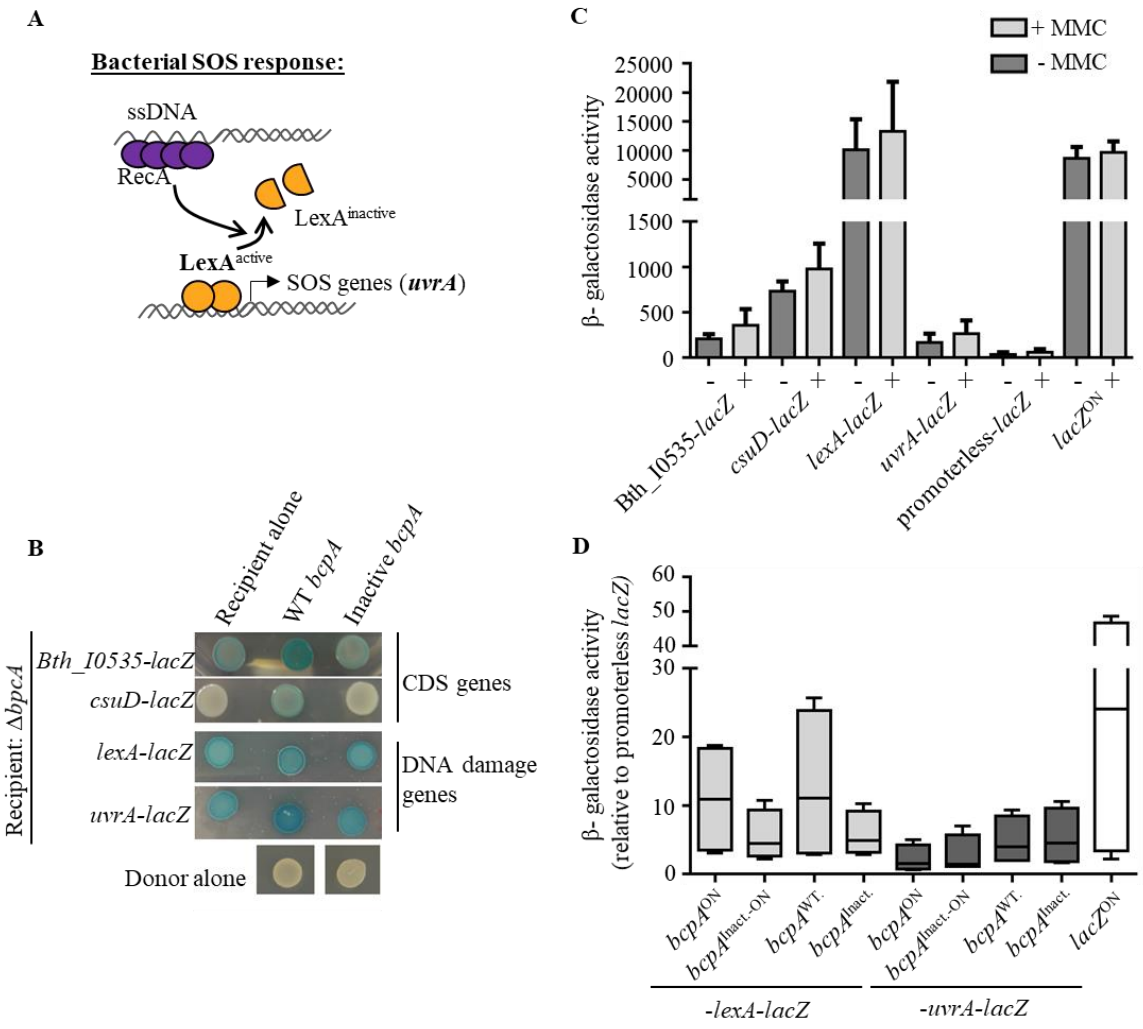


**Appendix Figure 2. Measuring DNA damage in *B. thailandensis* E264 bacteria.**

**Appendix Figure 2. Measuring DNA damage in *B. thailandensis* E264 bacteria.**

**(A)** Diagram of the SOS DNA damage response in bacteria. Upon DNA damage, RecA will bind to single stranded DNA (ssDNA). This initiates an enzymatic response that will cleave LexA. LexA is a negative regulator of the SOS locus and binds to the SOS locus promoter. Once cleaved then transcription of the SOS locus genes, such as UvrA, will occur. **B)** Co-culture (1:1) on Xgal agar of *B. thailandensis* Δ*bcpA* recipient bacteria carrying CDS-responsive reporters (rows 1,2) Bth_I0535-*lacZ* or *csuD-lacZ*, and SOS response reporters (rows 3,4) *lexA-lacZ* or *uvrA-lacZ* with donor bacteria producing WT *(bcpA*$^{WT}$*)* or catalytically inactive BcpA (*bcpA*$^{Inact.}$). **C)** β-galactosidase activity assay for DNA damage. Reporter mutants were split into two conditions: treated and untreated. Treated grouped were incubated with 5X the minimum inhibitory concentration of mitomycin C (-/+ MMC). **D)** β-galactosidase activity assay for DNA damage associated with BcpA toxicity. Reporter strains were made with *lacZ* under the promoters of SOS related genes, *lexA* and *uvrA*. Contact dependent signaling (CDS) *lacZ* reporter strains were made with *lacZ* under the promoters of CDS related genes, *csuD* and Bth_I0535. Parental background strains include overexpression via constitutive promoter of either *bcpA (bcpA*$^{ON}$*).* Inactivated BcpA strains (*bcpA*$^{Inact.-ON}$) are set as the catalytic control for BcpA-BcpI complex. B-galactosidase assay controls are promoterless *lacZ* and *lacZ* under a constitutive promoter *(lacZ*$^{ON}$*).* Panels **C** show results from three biological replicates, and **D)** show results from four biological replicates. Student T-tests were performed and found no significant differences. Student T-tests were performed and found no significant differences. **A)** Figure adapted from Ulrich et al., 2013 (252)

**Appendix G: Polymicrobial biofilm formation of *B. dolosa* CDI mutants.**

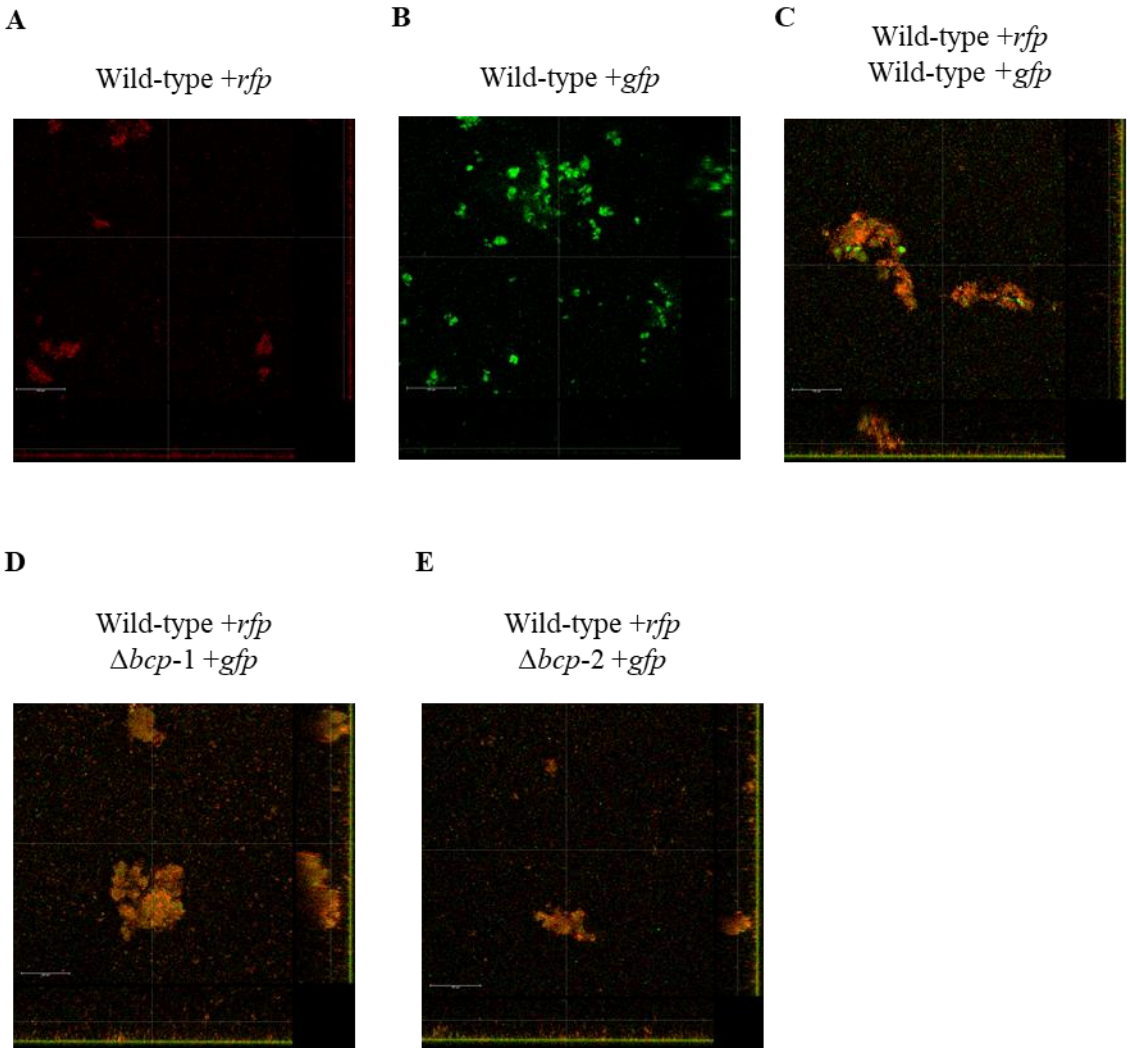


**Appendix Figure 3. Confocal co-culture B. dolosa CDI mutant biofilms.**

**Appendix Figure 3. Confocal co-culture *B. dolosa* CDI mutant biofilms**.

Confocal laser scanning microscopy of Biofilm formation in chambered well by either constitutively expressing *gfp* strains, +*gfp*, or constitutively expressed *rfp* strains, +*rfp*. Single bacterial strain **A)** wild-type +*gfp*, or **B)** wild-type +*rfp* static grown biofilms. Co-culture biofilms starting at 1:1 ratio of wild-type AU0158 +*rfp* and **C)** wild-type AU0158 +*gfp*, **D)** Δ*bcpAIOB-1 +gfp*, or **E)** Δ*bcpAIOB-2 +gfp*. Bacteria were grown for 48h in TSB+1% glucose cultures grown in three biological replicate and bars show the mean (*n*=3). In Z stack renderings (48 h), cross-sections through the plane parallel to the coverslip (shown by large center image). Scale bars represent 100 μm. Images are representative.

## Appendix H: Contributions

This body of work was supported by grants from the National Institutes of Health (K22AI118949 and R01AI150767 awarded to Dr. E.C. Garcia) and start-up funding from the University of Kentucky. Dr. E. C. Garcia performed bacterial competition assay experiments in Figure 5.5. T. Myers-Morales performed LPS visualization assays used in Figure 5.11. B. Shaw aided in the creation of phisD_overlap plasmid used for *hisD* gene deletion. Divya Sunderam, high school research program, carried out experiments in Appendix F.1BC under the direction of Dr. E. C. Garcia's and myself. Zaria Elery aided in technical assistance along with other members from the E. C. Garcia laboratory.

## Vita

### Education

2016 - 2021: University of Kentucky – Lexington, KY
Microbiology, Immunology and Molecular Genetics Discipline

2012 - 2016: Illinois State University –Bloomington-Normal, IL
Bachelor of Science Molecular and Cellular Biology, and Chemistry Minors

### Professional Positions

2016 – 2021: Graduate Research Assistant, E.C. Garcia Lab.
University of Kentucky – Lexington, KY

2021: Science Policy Fellow
Virtual, Federation of American Societies for Experimental Biology headquarters – Rockville, MD

2018-2020: External Writer for *Cancer Policy Monitor*,
Virtual, American Association For Cancer Research Headquarters – Washington D.C.

2016: Summer Research Intern, N.T. Mortimer Lab
Illinois State University – Bloomington-Normal, IL

2014 – 2016: Undergraduate Research Assistant, W. Nicholas Lab
Illinois State University - Bloomington-Normal, IL

### Leadership Positions

2019 – 2021: Young Ambassador for State Of Kentucky, American Society For Microbiology
2019 – 2021: President and Founder, American Society for Microbiology Chapter At The University Of Kentucky
2020 – 2021: Secretary, Kentucky Advocates for Science Policy And Research
2019 – 2020: Special Assistant for Legislative Event, National Association Of Graduate And Professional Students

### Scholastic Awards

2021: Pillar Award for Academic Success, University of Kentucky Graduate Student Congress
2020: Above and Beyond Award, National Association For Graduate And Professional Students
2020: Women in Medicine and Science Rising Star Award Nominee, Women In Medicine And Science Organization

2019: Infectious Disease Day 3-Minute Thesis Competition, 1st Place
2018: Infectious Disease Day 3-Minute Thesis Competition, 3rd Place
2018: College of Medicine Student Travel Award, Kentucky Office of Biomedical Education

**Publications**

**Oates, A.E.,** Myers-Morales, T., Elery Z., and Garcia, E.C. 2021. Identification of recipient cell factors that affect *Burkholderia dolosa* competitive fitness during contact-dependent growth inhibition. *J. Bacteriol. Submitted*

Myers-Morales, T., **Oates, A.E.,** Byrd, M.S., and Garcia, E.C. 2019. *Burkholderia cepacia* complex contact-dependent growth inhibition systems mediate interbacterial competition. *J. Bacteriol.* 113(29): 8296-301.

Alvarado, G., Holland, S.R., DePerez-Rasmussen, J., Jarvis, BA., Telander, T., Wagner, N., Anast, A.A., Davis, A.B., Frank, A., Genenbacher, K., Larson, J., Mathis, C., **Oates, A.E.**, Rhoades, N.A., Scott, L., Young, and Mortimer, N.T. 2020. Bioinformatic analysis reveals mechanisms underlying parasitoid venom evolution and function. *Genomics*. 112(2), 1096-1104